UNIVERSITY OF SOUTHAMPTON

FACULTY OF ENGINEERING, SCIENCE AND MATHEMATICS

SCHOOL OF OCEAN AND EARTH SCIENCE

DEVELOPMENT OF MICROFLUIDIC TECHNOLOGY FOR IN-SITU DETERMINATION OF IRON AND MANGANESE IN NATURAL AQUATIC SYSTEMS

by

Ambra Milani

Thesis for the degree of Doctor of Philosophy

October 2013

Graduate School
of the
National Oceanography Centre, Southampton

This PhD dissertation by Ambra Milani has been produced under the supervision of:

Supervisors

Prof. Peter J. Statham
Dr. Matt Mowlem
Dr. Doug Connelly
Dr. Cedric Floquet

Chair of Advisory Panel

Dr. John Allen

UNIVERSITY OF SOUTHAMPTON

ABSTRACT

FACULTY OF ENGINEERING, SCIENCE AND MATHEMATICS
SCHOOL OF OCEAN AND EARTH SCIENCE

Doctor of Philosophy

DEVELOPMENT OF MICROFLUIDIC TECHNOLOGY FOR IN-SITU DETERMINATION OF IRON AND MANGANESE IN NATURAL AQUATIC SYSTEMS

by Ambra Milani

In-situ sensors are crucially important for understanding the physico-chemical processes that occur in natural water environments. Manual sampling with laboratory analysis cannot provide the temporal and spatial resolution required to characterize marine and fresh water ecosystems, and this approach is both expensive and time consuming, and may also be affected by artefacts during handling and storage. In-situ sensors minimize these drawbacks and provide a tool to obtain long-term data banks which will allow a more synoptic interpretation of the biogeochemical cycles of key elements in water systems. The trace metals iron and manganese are examples of key elements that shape the biogeochemistry of aquatic systems. Processes influenced by them include phytoplankton growth, deep-sea vent chemistry and redox equilibria in environments with strong oxygen concentration gradients.

This thesis describes the development, optimisation and application in environment of two sequential prototypes of a Lab-On-A-Chip microfluidic autonomous analyser for the in-situ determination iron and manganese in aquatic environments. A first prototype (Prototype 1,P1) of the device existed at the beginning of this project. It was lab-tested and deployed at depth in the Lucky Strike Vents Field (Mid Atlantic Ridge) for the determination of Fe(II). An operative fault during the deployment triggered a trouble shooting process which highlighted some weak points in the device. Those weaknesses were addressed and solved in a second version of the device (Prototype 2, P2) whose novel feature was the in-line mixing by diffusion of reagents and samples. Total Fe, Fe(II) and Mn could be measured with a frequency of up to 12 and 6 samples per hour respectively, with limits of detection of 35 nM and 27 nM for Total Fe and Fe(II) and 28 nM for Mn.

The robustness and reliability of P2 was tested in the laboratory and in the environment in both marine (Baltic Sea) and fresh (Beaulieu River) waters. The results of these deployments are presented and directions for further developments of the technology are proposed.

Declaration of authorship

I, Ambra Milani, declare that this thesis entitled “Development of microfluidic technology for in-situ determination of iron and manganese in natural aquatic systems” and the work presented in it are my own, and have been generated by me as the result of my own original research.

I confirm that:

1. This work was done wholly or mainly while in candidature for a research degree at this University;

2. Where any part of this thesis has previously been submitted for a degree or any other qualification at this University or any other institution, this has been clearly stated;

3. Where I have consulted the published work of others, this is always clearly attributed;

4. Where I have quoted from the work of others, the source is always given. With the exception of such quotations, this thesis is entirely my own work;

5. I have acknowledged all main sources of help;

6. Where the thesis is based on work done by myself jointly with others, I have made clear exactly what was done by others and what I have contributed myself.

Signed: .....

Date: .....

Contents

Contributions to the work

Dr. Cedric Floquet **Sensors Group, NOC, Southampton**	Tinted PMMA substrate choice Prototype 1 concept, design and first manufacture Post-MoMAR-D deployment pressure and temperature tests
Dr. Ed Waugh **Sensors Group, NOC, Southampton**	Syringe pump concept and design, V1 and V2 Electronics package concept and manufacture Analyser software interface (ASM)
James Wyatt **Sensors Group, NOC, Southampton**	Prototype 2 housing design
Dr. Samer A. Beyh **Sensors Group, NOC, Southampton**	Pre-MoMAR-D deployment pressure test

Acknowledgments

This work was supported by SENSEnet, a Marie Curie Initial Training Network (ITN) funded by the European Commission Seventh Framework Programme, Contract Number PITN-GA-2009-237868.

I would like to thank my supervisors Prof. Peter Statham, Dr. Matt Mowlem and Dr. Doug Connelly for the incredible opportunity they gave me and for their support throughout this project.

A special thank you to Peter, whose constant guidance and patience have made this thesis possible.

Thank you to Dr. Cedric Floquet for letting me sharing his project and eventually passing it to me.

Through the SENSEnet project, Dr. Doug Connelly provided me with the opportunity of meeting scientists from across Europe and oversea and share knowledge and ideas. Dr. Carla Sands guided me securely through the EU bureaucracy and made sense of my Italian messiness.

Thank you to the crew of the *Pourquoi-pas?* who helped us deploy our system on the Mid Atlantic Ridge.

A special appreciation for the Elizabeth Mann-Borgese crew, from the IOW, Warnemünde. In particular to Dr. Olaf Dellwig (cruise PI) and Dr. Ralf Prien who invited us to participate to the expedition, helped us with the logistics and shared their knowledge of the Baltic Sea with us; Dr. Siegfried Krüger, who provided us with power and communication between P2 and the pump-CTD; Dr. Johann Ruickoldt, who gave us access to the CTD profiles.

Many thanks to the Sensors Group, NOC, Southampton. Beyond the specific contribution of individuals, I could always count on the support of the group, and this project could not have happened without it.

Finally, thank you to all the friends who shared the rollercoaster with me. You know who you are. Hard times come and go, but you are always there.

List of Figures

List of Tables

Chapter 1

Introduction

1.1 Biogeochemical background

Micronutrients hold a paramount role in the global oceanic cycle of elements. The trace metals iron and manganese, in particular, have received great attention in the last two decades since they have been recognised to have an essential role and partly control the growth of phytoplanktonic organisms and thus the cycling of macronutrients (Brand et al. 1983, HELCOM 2009, Landing and Bruland 1987, Morel and Price 2003). In addition, dissolved Fe and Mn are important indicators of redox processes in aquatic environments, and in hydrothermal systems they can act as tracers of vent fluids and biogeochemical processes.

1.1.1 Iron in natural waters

Iron is an essential element for phytoplankton organisms, and it is perhaps the most important of all the bioactive trace metals (Bruland et al. 1991). Iron plays a preeminent physiological role being a component of electron carrier proteins involved in photosynthetic and respiratory electron transport, nitrate and nitrite reduction, N_2 fixation and sulphate reduction. The availability of iron controls phytoplankton growth, species composition and trophic structure in vast areas of the ocean (Shaked and Lis 2012, Sunda 2001, Watson 2001).

The crucial role played by iron in phytoplankton growth leads directly to the influence that this metal has in the global carbon cycle. By enhancing phytoplankton productivity Fe increases carbon fixation in the surface waters (Coale 2001, Martin 1990) which is one of the processes by which atmospheric CO_2 can be removed and transferred to the deep ocean, where it is sequestered for long periods of time (Street and Paytan 2005).

Consequently, iron fluxes to the ocean and the carbon dioxide uptake by the ocean have been linked to climate change (Barbante and Cairns 2002, Breitbarth et al. , Henderson et al. 2007).

Despite being a vital component in aquatic plants and being the fourth most abundant element in the Earth's crust, iron is present at very low concentrations in the open ocean (0.05-2.0 nM) (Boyd and Ellwood 2010), with the lowest values being typical of HNLC (high nutrient low chlorophyll) areas (Bruland and Rue 2001, Coale 2001) .

In the early '90s iron's peculiar role within marine trace metals was defined by the work of Martin (1990) who put forward *the iron hypothesis*: the "productivity in today's southern ocean is limited by iron deficiency, and hence the phytoplankton are unable to take advantage of the excess surface nitrate/phosphate" (Martin 1990). In the last two decades Martin's arguments have been confirmed by iron enrichment experiments throughout the major HNLC (high-nutrients low-chlorophyll) areas of the world's oceans (Boyd et al. 2007). Both bottle enrichment experiments and mesoscale in-situ fertilisation experiments such as IRONEX I-II (carried out in the eastern equatorial Pacific) and SOIREE (Southern Ocean Iron Release Experiment) have successfully supported the iron hypothesis (Boyd et al. 2007, Boyd et al. 2000, Martin et al. 1994, Watson et al. 2000).

The main sources of Fe to the oceans are: atmospheric (aeolian) deposition; rivers discharge; release from sediments; deep-sea inputs from hydrothermal processes. The removal mechanisms for this element are scavenging and adsorption into particulate matter, incorporation into sediments and uptake by planktonic organisms (de Baar and de Jong 2001).

A typical dissolved Fe profile in the open ocean is shown in Figure 1-1. With concentrations depleted at the surface and enriched at depth, dissolved Fe has a nutrient-like distribution rather than that of a scavenged element.

Iron's counterintuitive distribution pattern is explained by its chemical properties and behaviour.

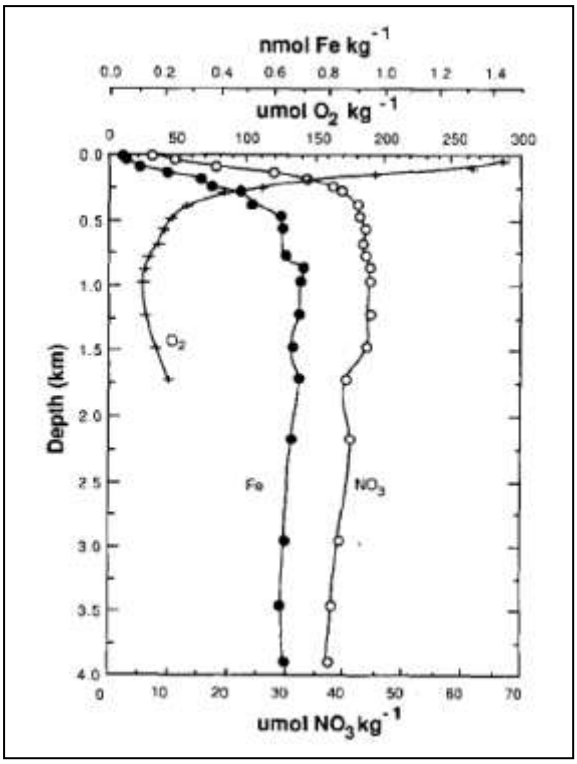

Figure 1-1 – Example of a typical profile of dissolved Fe. Distribution of Fe, nitrate and oxygen along the water column at Ocean Station Papa (50°N, 145°W), after Martin et al. (Martin et al. 1989).

Iron has two oxidation states of importance for natural water biogeochemistry: Fe(II) and Fe(III). These two species can inter-convert depending on the redox conditions in the systems where they are present. Under reducing conditions Fe(II) is largely dissolved.

The Fe(III) oxidation state predominates in well oxygenated waters, where it is expected to form primarily insoluble oxyhydroxides and colloids. However, most of the dissolved Fe(III) present in seawater is now known to be complexed with strong organic ligands which prevent it from forming insoluble oxyhydroxides, limiting both its precipitation and scavenging into particulate phases (Gledhill and Vandenberg 1994, Hunter and Boyd 2007, Kuma et al. 1996, Liu and Millero 2002, Millero 1998, Rue and Bruland 1995). The nature of these ligands is not yet fully understood, but they are presumed to be similar in composition to the bacterially produced siderophores (Bergquist et al. 2007, Hunter and Boyd 2007, Johnson et al. 1997, Rue and Bruland 1995, Toner et al. 2009, Ussher et al. 2005, Van den Berg 1995), although recent work has suggested humic substances may also be an important complexing group (Laglera and van den Berg 2009, Laglera et al. 2011) .

In oxic marine conditions Fe(II) is thermodynamically unstable and is readily oxidised to Fe(III). Despite this, low dissolved Fe(II) concentrations have been found in sunlit surface

oxic waters, where photoreduction maintains the presence of Fe(II) (Gammons et al. 2008, Miller et al. 1995, Willey et al. 2005). Substantial concentrations of Fe(II) are found in anoxic water basins, where the lack of oxygen prevents its oxidation to Fe(III) (Dellwig et al. 2010, Konovalov et al. 2004, Kremling 1983, Yakushev et al. 2007) and in hydrothermal vent fluids emitted from the seafloor at these reductive sites (Von Damm 2000).

In river waters Fe concentration can be in the range of several hundreds of nanomoles/L (Martin and Windom 1991). However, in low salinity estuarine regions, riverine dissolved Fe can be rapidly converted to particulate phases through colloidal Fe flocculation due to the major change in pH and ionic strength (Krachler et al. 2005). These processes limit the river inputs of bioavailable Fe to the oceans (de Baar and de Jong 2001), resulting in a net dissolved Fe flux from rivers of ~0.1 x 10^{12}g per year (Martin and Windom 1991) with globally on the order of 90% of the riverine Fe being removed.

1.1.2 Manganese in natural waters

As for iron, the distribution of manganese in the ocean is defined by the interplay of sources and sinks as well as water masses circulation and physical mechanisms. Riverine load and long-range atmospheric transport through aeolian dust represent the major source of manganese to the ocean, but hydrothermal inputs have been recognised to have an important role in the cycle of this element in seawater (Burton and Statham 1988, Klinkhammer et al. 1977).

From a thermodynamic point of view, dissolved manganese is present at extremely low concentration in the open ocean (lower than nM) and particulate forms as MnO_x are expected to form. However, low oxygen concentration and low pH values increase Mn solubility (Landing and Bruland 1987, Stumm and Morgan 1995) and since the re-oxidation of MnII is a slow process, inputs of reduced manganese in the ocean can persist for long periods of time and thus be used as tracers (Burton and Statham 1988, Klinkhammer et al. 1977, Mallini and Shiller 1993). In particular manganese is an excellent indicator of hydrothermal activity (Chin et al. 1992, Vondamm 1990).

Moreover, manganese is an essential element in the growth of phytoplankton organisms: it acts as a cofactor for many proteins and enzymes serving a variety of physiological functions (Roitz et al. 2002). Given its low concentration in oceanic waters (normally between 0.1 and 3 nM (Bruland et al. 1991)) manganese has been identified as another potentially limiting or co-limiting factor for primary productivity (Brand et al. 1983).

1.2 Conventional measurements of Fe and Mn in natural waters

The determination of Fe and Mn concentrations and their speciation in natural waters requires sensitive and accurate measurement techniques in order to provide high quality data. Not until very recently have analytical techniques reached a level of accuracy and precision that allows us to improve our understanding of Fe and Mn biogeochemical cycles. Before the 90s contamination was a major issue and resulted in poor quality measurements. Since then an increased understanding of contamination sources has allowed the collection of more accurate data.

The main analytical techniques used for the determination of Fe and Mn in aqueous systems are spectrophotometry, atomic spectrometry, stripping voltammetry and chemiluminescence. While these techniques could be performed also on ships, others like graphite furnace atomic absorption spectrometry (GFAAS) or inductively coupled plasma mass spectrometry (ICPMS) are limited to land based laboratories.

1.2.1 Limitations of conventional measurements of water samples

The methods mentioned in paragraph 1.2 are laboratory based techniques which imply sample storage after sampling and prior to analysis, unless the analysis can be carried out on the research vessel. These storage approaches (e.g. acidification) often fail in preserving the original state of the water samples, introducing errors in the analysis itself (Buffle and Horvai 2000). This is even more likely to happen in the case of Fe determination, given the potential changes of the metal oxidation state in the samples (Pehkonen 1995). Moreover, manual water sampling and the following analytical procedures carried out in the laboratory must be performed by highly qualified staff, are time consuming and thus very expensive.

In order to gain a clear understanding of ocean biogeochemistry, chemical data collection over broad time and space scales (Figure 1-2) are needed (Daly et al. 2004, Prien 2007, Tokar and Dickey 2000). Therefore current laboratory measurement techniques cannot provide the temporal and spatial resolution necessary to properly describe the biogeochemistry of the oceans from a chemical perspective.

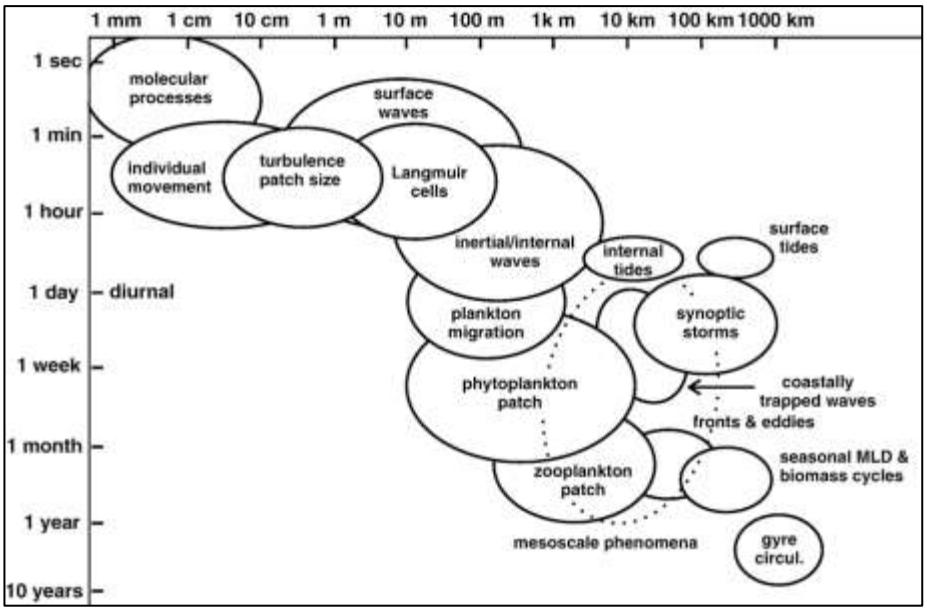

Figure 1-2 – Spatial and temporal scales of physical and biological processes affecting the ocean biogeochemistry (from Prien, 2007).

1.3 In-situ technology

In contrast to the methodologies mentioned above, more and more attention has recently been drawn towards in-situ technology for water monitoring (Buffle and Horvai 2000, Daly et al. 2004, Gallager and Whelan 2004, Johnson et al. 2007, Moore et al. 2009, Prien 2007, Tokar and Dickey 2000). In-situ sensors are built to perform their measurements directly at the location of interest, partially or completely immersed in the water body, thus avoiding sample handling and storage (Vuillemin et al. 2009). Some of the advantages of using in-situ analytical systems rather than laboratory or on site techniques are:

- the elimination of many of the artefacts due to sample handling and storage;
- the minimization of the cost of sample collection;
- the possibility of real-time analysis, allowing the rapid detection of pollutant inputs;
- the ability to accumulate detailed spatial and temporal data sets;
- the possibility to perform measurements in locations which are difficult to access;
- the possibility of measuring concentration gradients and fluxes at environmental interfaces (Buffle and Horvai 2000, Laes et al. 2005).

Along with these benefits come the challenges that in-situ sensors have to face to perform their tasks. These sensors have to work in very hostile environments, characterized by high pressures, steep gradients of temperature, pH and salinity, as well as high biological

activity (which eventually results in biofouling) (Mowlem et al. 2008, Prien 2007). Moreover, the compounds they aim to detect are often present at very low concentrations in highly complex natural matrices (Johnson et al. 2007) and this poses an issue for the detection techniques with regards to the specificity of the analytical method and the limit of detection of the instrument itself.

In the last tens of years many groups working in water analysis have turned to the development of in-situ sensors for chemical measurements. The existing systems for the in-situ detection of dissolved Fe and Mn are reviewed in the next paragraph and a summary of their main features can be found in Table 1-1.

1.3.1 State of the art: in-situ Fe and Mn analysers for aquatic systems

1.3.1.1 SCANNER

The first in-situ system for the detection of iron and manganese in seawater was the submersible chemical analyser SCANNER developed by Johnson and co-workers in 1986 (Johnson et al. 1986a). The SCANNER was an in-situ analyser based on the unsegmented continuous flow of sample mixed with reagent for online spectrophotometric determination. The system was at first configured for the detection of silica and sulfide in a deep-sea hydrothermal vent field, but was built with the possibility of being adapted to a variety of chemical procedures. It was later used by Johnson et al. (Johnson et al. 1986b) to detect nitrite and nitrate and finally by Coale and colleagues (Chin et al. 1992, Chin et al. 1994, Coale et al. 1991) for the determination of iron and manganese in-situ during the VENTS '89 cruise on the Juan de Fuca Ridge.

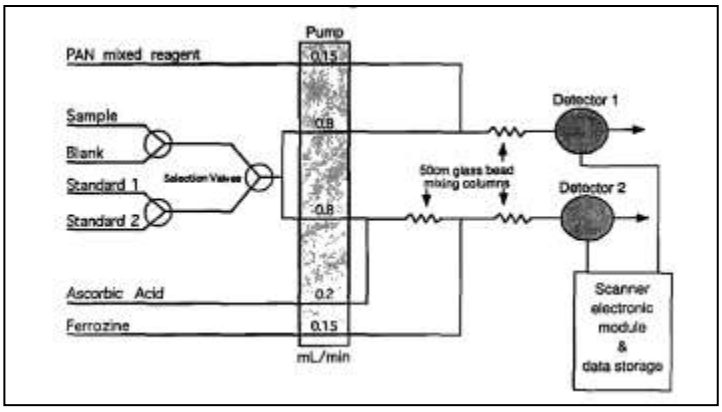

Figure 1-3 – SCANNER manifold configuration for the determination of dissolved Mn and total dissolved Fe in-situ. From (Chin et al. 1994).

SCANNER had an electronics module, which contained the valve selection circuitry and the signal processing and data storage units; a chemistry module that housed the pump, the

selection valves, the detectors and the reagents; and a battery pack (Figure 1-3). It was able to determine dissolved Mn and total dissolved Fe (Fe(II) + Fe(III)) at the same time through continuous measurements recorded every 5 seconds. The two methods of analysis were based on the PAN (1-(2-pyridylazo)-2-naphthol) assay for the manganese determination (Betteridge et al. 1963, Chin et al. 1992) and on the colorimetric detection of iron complexed with Ferrozine (Stookey 1970) after reduction of Fe(III) to Fe(II) with ascorbic acid for total iron. Configured as described in Figure 1-3 SCANNER was able to collect more than 3700 sets of analysis for both Mn and Fe during vertical casts and 'tow-yos', working at depths ranging from 1700m to 2300m. It performed in-situ calibrations at pre-programmed intervals before each cast and achieved a detection limit of 22 nM for manganese and 25 nM for total iron. The authors claimed good agreement between data collected by the SCANNER and measurements of Fe and Mn obtained by column extraction-GFAAS (graphite furnace atomic absorption spectrometry) analysis performed in the laboratory on discrete samples and the limit of detection for both analyses seemed good enough for many environmental applications of the technology (see paragraph 1.3.2).

1.3.1.2 SUAVE

Following the prototype of the SCANNER, a second generation submersible chemical analyser was developed by Massoth and colleagues (Massoth et al. 1991, Massoth et al. 1995) to perform in-situ measurements of iron and manganese. The Submersible System Used to Assess Vented Emissions (SUAVE) employed a manifold similar to the one used by the original SCANNER based on flow analyses and colorimetric detection for the simultaneous selective determination of free dissolved Mn(II) and Fe(II) plus Fe(III) (Massoth et al. 1998). The system reached quoted limits of detection of less than 10 nM for Mn and less than 5 nM for total Fe. The chemical techniques used were the kinetic catalytic oxidation of leucomalachite green catalyzed by Mn (Resing and Mottl 1992) and the oxidation of DPD (N-N-dimethyl-p-phenylenediamine) catalyzed by Fe (Measures et al. 1995). The analyser was calibrated by comparison to discrete samples or by the injection of reference fluids in-situ, depending on the deployment setting ('tow-yos' and vertical casts or deployment within fluids issuing directly from the seafloor).

1.3.1.3 ZAPS

The College of Oceanic and Atmospheric Sciences (Oregon, US) developed an in-situ analyser for dissolved manganese based on a fiber optic spectrometer: the zero angle photon spectrometer or ZAPS (Klinkhammer 1994).

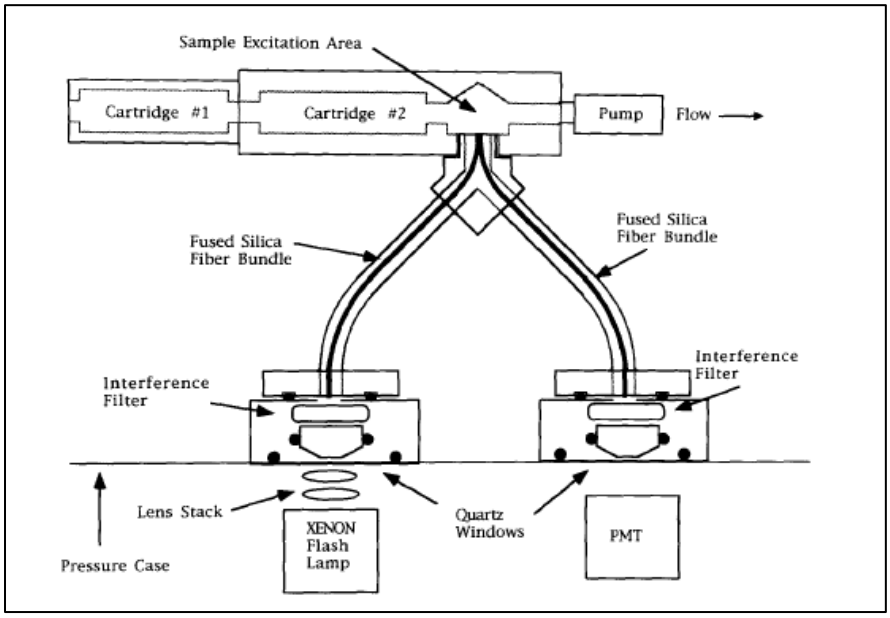

Figure 1-4 – Schematic of the ZAPS fiber optic spectrometer. From (Klinkhammer 1994)

The ZAPS combined solid-state chemistry with photomultiplier fluorometric detection to make flow-through measurement in-situ. The basic configuration of the system consisted of a Xenon flash lamp housed in a pressure case connected via optical fibres to a flow-cell and to the cartridges containing the reagents, which were linked to the PMT (photomultiplier tubes) detector via other optical fibres (see Figure 1-4). The chemical method on which the ZAPS is based is the catalytic effect of reduced manganese on the oxidative coupling of the fluorophor DEA (N,N',diethylaniline) forming a non-fluorescent product. Thus Mn concentration is inversely, linearly related to the amount of fluorescence seen by the PMT. Since only reduced manganese is capable of the oxidative coupling with DEA, this technique is selective for Mn(II). The method allowed subnanomolar measurements of Mn(II) and proved useful for Mn profiles in the North Pacific and for detection of hydrothermal emissions from mid ocean ridges (Gorda Ridge off the coast of Oregon). The system performed simple calibrations in the field but further adjustments of these values were required once the instrument returned to the laboratory.

1.3.1.4 GAMOS

Another flow-through chemical analyser for in-situ determination of manganese was developed by Okamura et al. (Okamura et al. 2001). The Geochemical Anomalies MOnitoring System (GAMOS) measured concentrations of dissolved manganese using the luminol-hydrogenperoxide chemiluminescence method (Okamura et al. 1998).

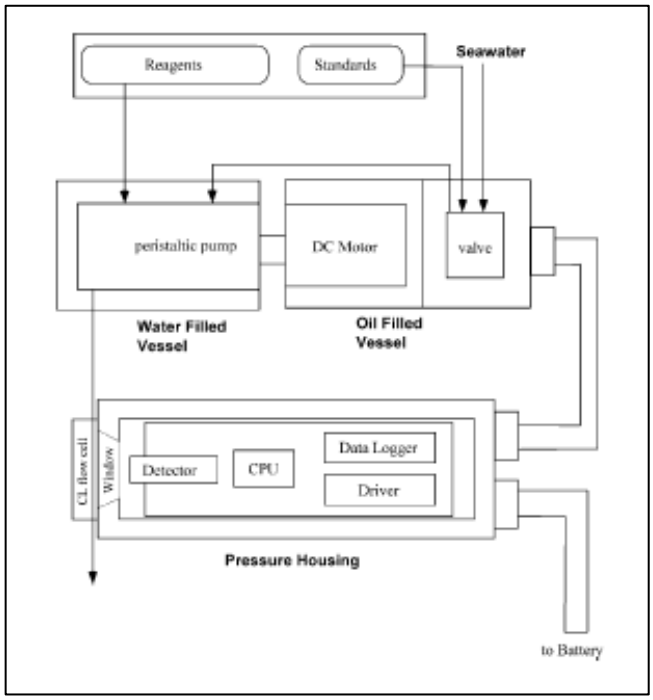

Figure 1-5 – Schematic of GAMOS Mn analyser. From (Okamura et al. 2001).

GAMOS, as shown in Figure 1-5, was composed of four modules: an acrylic, oil- and water-filled, pressure compensated vessel containing a flow through system; an aluminium pressure housing containing the electronic modules; an acrylic cylinder which held the flexible plastic bags filled with analytical reagents; and a battery for the power supply (Okamura et al. 2001). The analyser allowed in-situ calibrations with three standard solutions prepared in seawater and had a range of detection between 0.23 nM and 2μM for Mn(II). GAMOS was a stand-alone system which could be deployed both during submersible vehicle operations and on 'tow-yo' surveys from a surface ship and was deployed at depths up to 3647 m. In 2004 the configuration of the analyser was updated by Okamura and co-workers (Okamura et al. 2004) who replaced the peristaltic pump with a micro-diaphragm pump system which reduced the power and reagents consumption but did not improve the analytical performance of the system.

1.3.1.5 Fe-Osmo analyser

More recently Chapin and co-workers adapted a submersible, osmotically pumped analyser for continuous in-situ determination of nitrate developed by Jannasch et al. (Jannasch et al. 1994) to the determination of iron in seawater (Chapin et al. 2002). The Fe-Osmo analyser was based on the principle of continuous flow analysis, but the flow through the device was produced by diffusion of water through a rigid semi-permeable membrane from lower to higher osmolality. The use of this technique enabled the saving of electrical power because the osmotically driven flow could be used to squeeze the flexible reagents bags, to create a reagent delivery pump or to deliver sample to the manifold. The device was composed of 4 main parts (see Figure 1-6): osmotic sample and reagent pumps; standard and blank pumps; reaction manifold and detector; electronics. As with the SCANNER, the Fe-Osmo analyser was based on the colorimetric detection of total Fe after reduction of Fe(III) to Fe(II) with ascorbic acid and complexation of the product with Ferrozine, but in this system the reagents were kept under vacuum to prevent degradation.

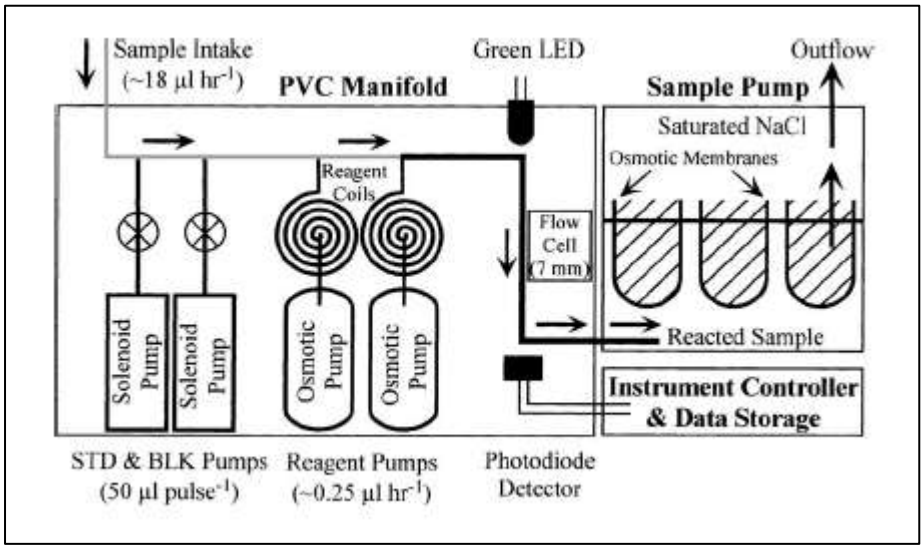

Figure 1-6 – Schematic of Fe-Osmo analyser. From (Chapin et al. 2002).

The Fe-Osmo analyser was deployed over low temperature hydrothermal vents (<3°C) at 1100m depth (Loihi seamount, off the coast of Hawaii) for 10 months and at 1500m depth (Axial volcano, Juan de Fuca Ridge) for 1 year, collecting data every 15 minutes. The drift of the instrument was tested by in-situ standards and blank injections. This analyser achieved a detection limit of 100 nM Fe for a 0.7cm pathlength cell and obtained a linear response up to 50 µM.

1.3.1.6 ALCHIMIST

The submersible chemical analyser ALCHIMIST (AnaLyseur CHIMique In-SiTu) (Figure 1-7) was adapted for iron determination by Sarradin and colleagues (Sarradin et al. 2005) from the original design of Le Bris et al. (Le Bris et al. 2000) who configured the instrument for in-situ measurements of nitrate and sulphide over hydrothermal vents' biological communities.

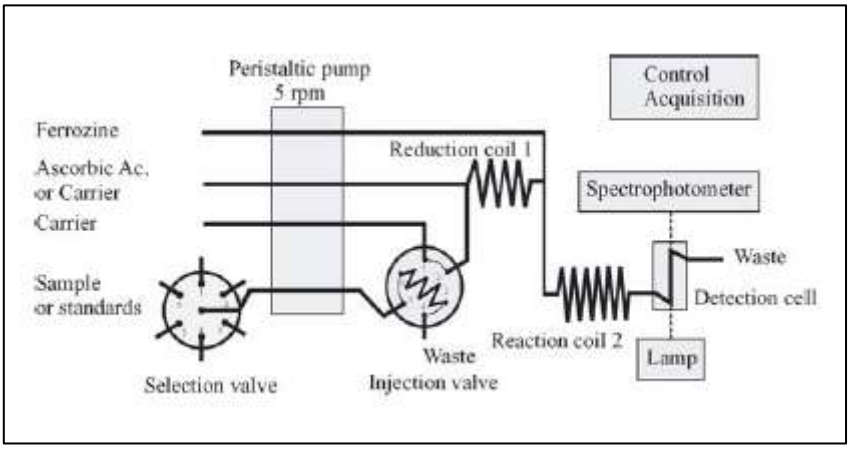

Figure 1-7 – Schematic of ALCHIMIST Fe analyser. From (Sarradin et al. 2005).

The device had three main modules: an hydraulic element housing pumps, valves and reagent bags; a spectrophotometric module containing 2 custom made PMMA (poly(methyl methacrylate)) flow measurement cells with 2 dual wavelength spectrophotometric detection units; an electronics component which included a battery and the elements for communication with the other modules. As the scheme in Figure 1-7 shows, Fe(II) was determined via colorimetric analysis after complexation with Ferrozine. The reducing agent (ascorbic acid) extended the method to total Fe (Fe(II) + Fe(III)). Sarradin et al. (Sarradin et al. 2005) adapted the FIA (flow injection analysis) method developed by Chin et al. (Chin et al. 1994) to reduce the limit of detection (eventually resulting in 600 nM for ΣFe) and to widen the measurement range up to 100 μM, thus making ALCHIMIST able to deal with wide chemical gradients. The ALCHIMIST permitted in-situ calibrations and was successfully tested in the laboratory for pressures equivalent to ~3000 m; it worked in-situ to a depth of 1650 m performing 22 analyses per hour (Le Bris et al. 2000).

1.3.1.7 ISMAN

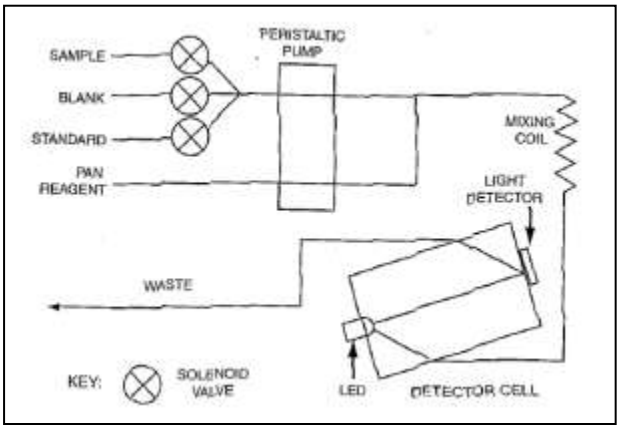

Figure 1-8 – Schematic of Statham et al. in-situ Mn analyser manifold. From Statham et al. (2003).

In 2000 Statham and co-workers developed the first in-situ metal analyser system to be used in combination with an autonomous underwater vehicle (AUV) (Statham et al. 2003), the ISMAN (In-Situ Manganese Analyser). The device performed the spectrophotometric detection of the PAN-manganese complex at 560 nm in a continuous flow stream as previously described by Chin et al. (Chin et al. 1992). Figure 1-8 shows a schematic of the system. The optical detection system of the analyser consisted of a block of opaque PVC (polyvinyl chloride) with a 2mm diameter central hole (5cm in length) passing through it. At the two ends of the channel were placed a green LED (light emitting diode) (as light source) and a combined silicon photodiode-CMOS (complementary metal oxide semiconductor) amplifier. The physical isolation of the manifold, pump and associated components from seawater was achieved by immersing the elements in silicone oil held within an acrylic tube. The analyser was able to perform in-situ calibrations and averaged data each 10 seconds, returning a spatial resolution of about 10m. It worked in the Loch Etive survey (Statham et al. 2005) either at constant depth above the bottom (135m) or at set depths below the surface, allowing a three dimensional assessment of the environment. It achieved a detection limit of 25 nM.

1.3.1.8 CHEMINI

The IFREMER Centre of Brest developed the CHEMINI (CHEmical MINIaturized analyser) system (Vuillemin et al. 2009). It is a modular device which allows the independent but contemporary measurement of different parameters. It has two main parts (see Figure 1-9): a hydraulic module containing the manifold based around a two-layer engraved circuit in PMMA; and a detection module housing the electronic board and the colorimeter.

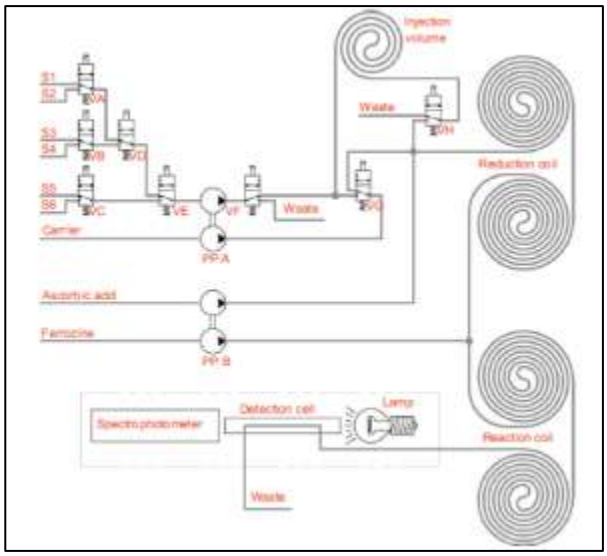

a

b

Figure 1-9 – a. Schematic of CHEMINI manifold. b. Integrated system ready for deployment. From (Vuillemin et al. 2009).

The whole instrument weighs 12.6 Kg without reagents. The analyser was used to detect total Fe on the active hydrothermal vent field Lucky Strike in 2006 at a depth of about 1650 m and at temperatures ranging from 4°C to 14.2°C. Calibrations were performed in-situ using 4 standards. The chemical method used to determine Fe(II) (or total Fe if needed) was the colorimetric detection after complexation with Ferrozine (Chapin et al. 2002). It achieved a detection limit of 300 nM Fe and could be extended to 2 mM if the conditions of the deployment required it. After a first environmental test on the Lucky Strike vent site where the CHEMINI was implemented on the ROV Victor 6000, the analyser was included in the TEMPO monitoring station (a long-term imaging module) and deployed near a mussel assemblage on the same hydrothermal site (Colaco et al. 2011).

1.3.1.9 IISA-Mn

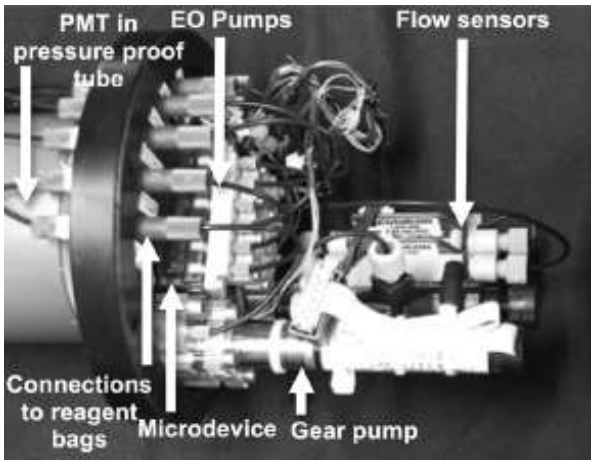

Figure 1-10 – IISA-Mn setup on ROV. (Provin et al. 2013)

More recently the Institute of Industrial Science in Tokyo developed and tested an integrated microfluidic system for the detection of manganese based on chemiluminescence (Provin et al. 2013), the IISA-Mn (Integrated In-Situ Analyser for Mn; Figure 1-10). With a polydimethylsiloxane (PDMS) microdevice at its core, the analyser is composed of a fluidic module, an electronics module attached to the ROV power supply and reagents bags. It detects MnII using its chemiluminescent reaction with luminol reaching a limit of detection of 280 nM. Possible interactions of Fe with the chemical method are thought to be limited by the presence of sodium citrate and triethanolamine (TEA) among the reagents. In 2010, the system was deployed in the Okinawa Trough, on an ROV at depths up to 1400 m for up to 8 hours at a time. The in-situ calibrations were unreliable, nonetheless the analyser helped to discover new active hydrothermal sites by tracing their Mn signals.

Name of analyser	Year	Parameters	Chemical method	Samp freq	Reagents consump	Power consump	Injection method	Detection method	LOD	ROD	depth	Depl time	On-board calibr	Size	Ref
SCANNER	1986	dMn Fe(II) Fe(III)	PAN/FZ; ascorbic acid	5 sec	PAN 150 µL/min FZ 150 µL/min a.a. 200 µL/min	10 V-50 mA average 24 V-500mA	peristaltic pump	Spec.	TFe 25 nM Mn 22 nM	n.p.	2300 m in-situ	ROV dive time	possible	electronics package: 15.2 cm i.d. x 63 cm	(Chin et al. 1994, Coale et al. 1991, Johnson et al. 1986a)
SUAVE	1991	dMn Fe(II) Fe(III)	leucomalachite green DPD oxidation	45 sec	0.12-1.5 mL/min	18-30 V - 0.25-0.60 A	peristaltic pump	Spec.	TFe < 5 nM Mn < 10 nM	n.p.	3000 m in-situ	several days	no	78 x 40 x 30 cm frame	(Massoth et al. 1998)
ZAPS	1994	dMn	catalytic oxidation of DEA fluorofor	30 sec	35 mL/min	15 V	Sea Bird pump	PMT	< 0.1 nM	n.p.	6000 m by design 3325 m in-situ	n.p.	need lab correct.	n.p.	(Klinkhammer 1994)
GAMOS	2001	dMn	MnII catalysed luminol CL with H2O2	n.p.	1.8 mL/min	24 V	peristaltic pump	PTM	0.23 nM	.23 nM 2 µM	3647 m	CTD casts	yes	4 parts ~ 37 x 80 cm	(Okamura et al. 2004)
Fe-Osmo Analyser	2002	Fe(II) Fe(III)	FZ; ascorbic acid	15 mins	0.25 µL/h	15 V plus 3 V over a year time	osmotically driven flow	Spec.	100 nM	0 - 50 µM	1500 m	1 year	blanks	n.p.	(Chapin et al. 2002)

Name of analyser	Year	Parameters	Chemical method	Samp freq	Reagents consump	Power consump	Injection method	Detection method	LOD	ROD	depth	Depl time	On-board calibr	Size	Ref
ALCHIMIST	2005	Fe(II) Fe(III)	DPD oxidation	< 3 mins	0.4 mL/min	n.p.	peristaltic pump	Spec.	600 nM	.6-100 µM	in-situ n.p. in lab tested to 400 bar	ROV dive	yes	maximum length 66 cm, total width > 50 cm	(Laes et al. 2005, Sarradin et al. 2005)
In-situ Mn analyser	2003	dMn	PAN	10 sec	1.6 mL/min	n.p.	peristaltic pump	Spec.	25 nM	25 nM-1000 nM (at least)	135 m in-situ	AUV dive	yes	n.p.	(Statham et al. 2003)
CHEMINI	2009	Fe(II) Fe(III)	FZ; ascorbic acid	n.p.	0.44 mL/min	12 V - 20 mA per meas.	peristaltic pump	Spec.	300 nM	300 nM - 2000 nM	1640 m in-situ	> 1 year	yes	148 x 120 x 250 mm plus electronics module	(Vuillemin et al. 2009)
IISA-Mn	2013	dMn	MnII catalysed luminol CL with IO_4^-	n.p.	88 µL/min	24 V – 300 mA	dc motor-driven pump	PMT	280 nM	n.p.	~ 1400 m	ROV dive (8 hours)	no	12 x 50 cm	(Provin et al. 2013)

Table 1-1 – Features of existing in-situ chemical analysers for dissolved Mn and Fe. n.p., non published; LOD, limit of detection; ROD, range of detection; Spec.: spectrophotometry; dMn: dissolved manganese.

1.3.2 The limitations of current in-situ systems

As the examples listed above demonstrate, in the last tens of years there have been several attempts to construct in-situ Fe and Mn sensors. Most of the in-situ devices described in the literature demonstrated their applicability in the field, but they did not possess all the main features required in an in-situ measuring system. These features are commonly understood to be:

- low cost (< 5000£ per unit);
- low power consumption (average < 4 W);
- low reagent consumption (tens of µl per sample);
- portability;
- selectivity for the analyte;
- applicable to a wide range of environmental concentrations (nM to µM);
- fast response to environmental changes (10-30 samples per hour);
- high tolerance to harsh ambient conditions (T and P resistant);
- high precision and accuracy (±3%);
- good detection limits (tens of nM);
- stability for long-term deployments (days to months);
- minimum direct operator intervention;
- usable by non-experts

(Johnson et al. 2007, Moore et al. 2009, Mowlem et al. 2008).

Many of the Fe-Mn in-situ analysers developed up to the present time use high volumes of reagents compared to the smaller volumes needed for long term deployments and low cost of maintenance (SCANNER, SUAVE, In-Situ Mn analyser, ZAPS, GAMOS). Power consumption is an issue for several of these devices as is the size of the analyser itself (ALCHIMIST, GAMOS, Fe-Osmo Analyser): the presence of separate modules containing the electronics, the manifold or the detection elements of the device limited the portability of the systems and made the devices less suitable for use by non-experts. Even more importantly, most of the devices had trouble with on-board calibrations (CHEMINI, IISA-Mn, ZAPS, SUAVE, Fe-Osmo Analyser) or with accuracy and sensitivity in relation to the changing environmental conditions met during the deployments (SCANNER, GAMOS, Fe-Osmo Analyser, CHEMINI, IISA-Mn). Stability issues will make the devices unreliable and although sometimes this problem can be resolved by pre/post deployment calibration, once again they make the devices less user-friendly and less ready for routine use. The sample frequency was yet another drawback of some of these earlier systems as many of

them required a long time to get ready to measure the targeted analyte and could also fail to register quick changes or temporary phenomena (Fe-Osmo analyser).

The above mentioned systems claimed limits of detection that would allow their use in many natural water environments; nonetheless no data resulting from their routine use in water systems could be found in the literature. This suggests that some of the systems described might still require further development and optimisation before being used as reliable tools for water monitoring, while some others might have been abandoned to pursue more promising technology or to return to traditional sampling and laboratory analysis.

1.4 Microfluidic technology

Microfluidics involves the manipulation of small volumes of fluid within devices whose features (e.g. channel widths) measure from tens of nanometers to several hundred micrometers. Typically, microfluidic devices feature:

- small volumes (μL, nL, pL, fL);
- small size;
- low energy consumption;
- effects in the micro domain.

Hence, microfluidic technology can offer an answer to the requirements listed in paragraph 1.3.2 for in-situ measuring systems.

Miniaturisation of the components of a laboratory system requires simplification of the analytical processes as well as their automation (Brett 2007): all these features perfectly align with the description of the ideal in-situ system, thus making miniaturisation a useful starting point for the development of future sensors (Marle and Greenway 2005).

The concept of " a 'total chemical analysis system' (TAS), which periodically transforms chemical information into electronic information" was developed in the '90s by Manz et al. (Manz et al. 1990), and was soon tied to Lab-on-a-chip (LOC) technology, where all the steps commonly performed in a laboratory are transferred onto portable, cheap, miniaturised devices.

Microsystems operate on a scale between a few millimetres and 50 μm (Rios et al. 2006), and thus using microfluidics takes advantage of the scaling down in size at all levels: from the limited sample and reagent consumption to the presence of laminar flows (Janasek et

al. 2006). Thus, microfluidic technologies can successfully answer the challenges of size and power consumption associated with macro-sized chemical analysers.

LOC systems are already widely used in the bio-medical field (Huikko et al. 2003, Ohno et al. 2008, Ong et al. 2008, Prien 2007, van den Berg and Lammerink 1998, Xu et al. 2009), while their application in the environment is still limited. Nevertheless the need for microsystems for monitoring in-situ environmental variables is growing stronger within the scientific and government sectors, both for ground and freshwater analysis and for oceanographic applications (Brett 2007, Crevillen et al. 2007).

1.5 Aims and structure of the work

The aim of this project was the delivery of an in-situ, autonomous, portable and cost effective device for the determination of dissolved Fe and Mn in natural aquatic systems.

The starting point of the work was a microfluidic system designed by Dr Cedric Floquet for the determination of Fe(II). The system was based on devices for the determination of nutrients in seawater (Beaton et al. 2012, Legiret et al. 2013, Sieben et al. 2010) already under development within the Sensors Group at NOC, Southampton.

The final expected outcome of the project was a device which could operate at depths up to 3000 m; with a working period without maintenance of at least 2 weeks; a detection limit below 10 nM for both Fe and Mn; a concentration working range between the LOD and 10 μM for both Fe and Mn; accuracy and precision of ±3%; using low volumes of reagents consumption (< 500 μL per sample); with high sample throughput (> 5 samples per hour); highly portable and user-friendly.

To move towards this target a series of objectives were identified and are described in the following chapters as outlined below:

1. identify chemistry (Chapter 2);
2. fabricate prototype chips (Chapter 2);
3. test and characterise prototype device (Chapter 3);
4. deploy prototype (Chapter 3);
5. analyse performance in deployment (Chapter 3);
6. redesign system for a second improved prototype (Chapter 4);
7. manufacture prototype version 2 (Chapter 4);
8. deploy in a range of operational settings (Chapter 5);

Finally, Chapter 6 provides conclusions about the project, analyses which targets have been met and suggests directions for future work.

Chapter 2

Methods

This chapter presents the chemical methods and the manufacturing techniques used for the development of the Fe and Mn analyser in the course of the whole project.

2.1 Chemical methods

The available wet chemical methods for detecting Fe and Mn in water solutions were considered, and the benefits and drawbacks of each one of them with regards to their implementation on a portable, in-situ device were compared. With the objective of producing a device which could work for both Fe and Mn, colorimetry was chosen as the technique to pursue.

2.1.1 Colorimetry

The colorimetric method is based on the use of reagents that form a coloured compound with the analyte once it is added to the water sample. The intensity of the produced colour reflects the concentration of the analyte, which can then be quantitatively determined by measuring the absorbance of the solution at specific wavelengths. Absorbance is a measure of the quantity of light absorbed by a sample. Concentration and absorbance are directly related via the Beer-Lambert Law:

$$A = \varepsilon L c$$

where A is the absorbance, ε ($M^{-1}cm^{-1}$) is the absorptivity coefficient of the solution, L (cm) is the length of the optical path and c (M) is the concentration of the absorbing compound. A and ε are functions of the wavelength.

Absorbance is related to the transmission of light through the solution according to the equation:

$$T = \frac{I}{I_0}$$

where T is the experimental measurement of the light transmittance, I_0 is the measured intensity in the absence of the absorbing species (i.e. the blank measurement) and I is the intensity measurement of the light that emerges from the absorbing medium (i.e. the sample measurement).

Absorbance is then calculated as the negative base-ten logarithm of the transmittance using:

$$A = -\log_{10} \frac{I}{I_0}$$

In practice, the analyte concentration in the sample is calculated based on the measurement of the optical absorption of the coloured compound formed after the reaction with a reagent. This is normally achieved comparing the absorbance measured for the unknown sample to that of a known standard solution.

2.1.2 Iron assay

The colorimetric assay used for the determination of Fe(II) was the method developed by Stookey (Stookey 1970). It has very good sensitivity thanks to the high molar absorptivity coefficient (ε = 27900 $M^{-1}cm^{-1}$) and the specificity of the bond between Ferrozine (disodium salt of 3-(2-pyridyl)-5,6-bis(4-phenylsulfonic acid)-1,2,4-triazine), the ligand, and reduced iron.

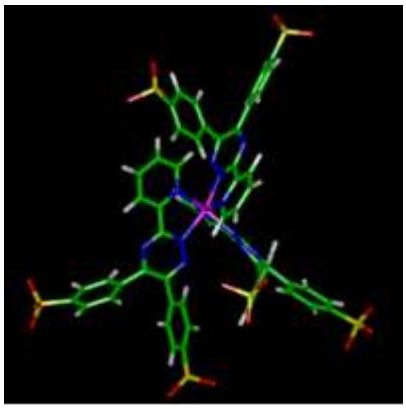

Figure 2-1 - Stick representation of the Iron-Ferrozine complex, $FeFz_3$: Fe(II) is complexed with three Ferrozine molecules. Figure from RasMol (Sayle and Milnerwhite 1995).

Ferrozine is highly soluble in water, has a low cost per gram and can be produced at a high purity level (Gibbs 1976). The method works between pH values of 4 and 9 and the Ferrozine (FZ) reagent can be buffered in advance and kept for months without showing signs of degradation (see below). The complexation kinetics is very fast (order of milliseconds) and the $FeFZ_3$ complex has a maximum absorbance at 562 nm. The above features contribute in making Ferrozine the ideal reagent for the determination of Fe(II) in natural waters.

2.1.2.1 Ferrozine reagent preparation

A 0.01 M Ferrozine reagent solution was used for the determination of Fe(II). It was prepared by dissolving 1.25 g of FZ (Ferrozine for spectrophotometric determination of Fe, ≥97.0%, Sigma-Aldrich) in 100 mL of 2 M acetate buffer. The buffer was made by adding 6.4 mL acetic acid (Acetic acid TraceSELECT® Ultra, ≥99.0%, Sigma Aldrich) and 155.3 g sodium acetate (Sodium acetate BioXtra, ≥99.0%, Sigma Aldrich) to 1000 mL of Milli-Q water (Ultra pure water, 18.2 MOhm.cm, Millipore). The resulting solution had a pH of ~6.

A long-term storage experiment was set up to check the stability of this reagent. A batch of fresh FZ solution was prepared and divided into Teflon bottles, which were kept at different temperatures (4°C, 25°C, 40°C) for 10 weeks. The stability of the solution was checked against a freshly prepared FZ solution on a weekly basis on newly prepared Fe(II) standards. For each temperature, 3 replicates measurements were taken and each measurement was repeated with both an Ocean Optics HR4000 Spectrometer and a HITACHI U-2800 Spectrometer. Less than 1% difference was observed in the results obtained in week 0 and week 10, increasing the confidence in the use of FZ as a long-lasting colorimetric reagent.

2.1.2.2 Iron standards

The Fe(II) standards were prepared by dilution from a stock solution of 1 mM ammonium iron II sulfate hexahydrate (99.997% trace metal basis, Sigma-Aldrich); the pH of the standards was kept below a pH of 2 by the addition of ascorbic acid (TraceSELECT®, ≥99.9998%, metals basis, Fluka) to give a final ascorbic acid concentration in solution of 0.01 M.

The standards were used for up to one week after preparation. During laboratory work they were preserved in PTFE bottles, while during deployments gas impermeable Flexboy bags (ethylene-vinyl-acetate/ethylene-vinyl-alcohol, Sartorius, UK) were used as storage

reservoirs. To increase the longevity of the reduced iron standards the Flexboy bags were degassed with the aid of a vacuum pump.

Fe(III) standards were prepared by dilution of a stock solution of 1000 mg/L Iron Standard for AAS (TraceCERT®, in nitric acid, Sigma Aldrich) and preserved as described for the Fe(II) standards, without the addition of ascorbic acid.

2.1.2.3 Total Iron measurements: reduction step

In order to perform measurements of total Fe in natural waters, a reduction step had to be implemented on the device.

The choice of the reducing agent had to take into account the chemical resistance of the components of the integrated analyser (see paragraph 2.3.1 and following chapters) given the final purpose was to develop a long-term, fast-response device. For these reasons, the pH of the final sample-reagents solution had to be between 4 and 9 pH units (which is the working range of ferrozine) and the reduction reaction had to be fast, on the order of minutes or less.

The literature was scrutinized in order to find the most common procedures for iron reduction on bench-top systems. A summary of the main methods used is shown in Table 2-1.

Sodium sulfite		
Author	**Method used**	**Reduction time**
(Ussher et al. 2009)	FIA-CL	4 hours
(Osullivan et al. 1995)	CL	
Ascorbic acid		
Author	**Method used**	**Reduction time**
(Huang et al. 2009)	reverse FIA with FZ	10 min
(Pascoa et al. 2009)	SIA-LWCC	immediate
(Sarradin et al. 2005)	FIA / spectrophotometry with FZ	
(Pullin and Cabaniss 2001)	FIA / spectrophotometry with FZ	70 sec
(Zhang et al. 2001)	Gas-segmented CFA with LWCC	60 sec
(PascualReguera et al. 1997)	FIA / reverse FIA / spectrophotometry with FZ	72 sec
(Blain and Treguer 1995)	FIA with FZ	2 min at 60˚C
(Elrod et al. 1991)	FIA-CL	5 min
Hydroxylamine hydrochloride		
Author	**Method used**	**Reduction time**
(Viollier et al. 2000)	spectrophotometry with FZ	10 min
Statham, 2010	spectrophotometry	2 hours

Table 2-1 – Summary of common bench-top procedures for iron reduction. FIA: flow injection analysis; CL: chemiluminescence; FZ: ferrozine; SIA: segmented injection analysis; LWCC: liquid waveguide capillary cell; CFA: continuous flow analysis.

Ascorbic acid was chosen as reductant because, according to previous successful work (in particular (Pullin and Cabaniss 2001) and (Sarradin et al. 2005), it reacts quickly with Fe(III), and the reaction has a high Fe(II) recovery rate. The reaction does not need heating at room temperature and the ascorbic acid can be added to the ferrozine reagent and stored in the same reservoir, provided it has been degassed.

2.1.3 Mn assay

As for iron, colorimetric methods are the simplest procedures to determine manganese. Among the few colorimetric methods developed for Mn(II) detection (Chiswell and Ohalloran 1991), the PAN (1-(2-pyridylazo)-2-naphtol) assay provides a high molar absorpitivy coefficient (44000 M^{-1} cm^{-1}) and is thus potentially the most sensitive. PAN was first used in solvent extraction procedures by Betteridge et al. (1963) while its use for spectrophotometric measurements was defined by Goto et al. (1977). This latter work solved the issue related to the reagent's poor solubility in water by adding a surfactant, Triton X-100, to the solution.

However, PAN is not highly selective towards manganese and measurements in aqueous systems can be affected by interferences from zinc, nickel, cobalt, copper and iron. Although the other metals compromise the reaction only when present at concentrations much higher than those usually found in seawaters, iron interference might be significant, especially in systems such as hydrothermal vent fields where the amount of iron injected into the water is often much higher than the manganese. To compensate for this potential interference , (Chin et al. 1992) added an iron masking agent, Desferrioxamine B.

2.1.3.1 PAN preparation

The procedure described by Chin et al. (1992) was followed to prepare a 0.8 mM PAN solution. To make 250 mL of PAN reagent, 0.05 g of PAN (PAN for spectrophotometric determination of metal ions, ≥97.0%, Sigma Aldrich) and, because PAN has limited solubility in water, 5 mL of Triton-X100 surfactant (laboratory grade, Sigma Aldrich) were added to 50 mL of Milli-Q water. This was then heated on a stirring hot plate for 3-4 hours, or until PAN was completely dissolved. To enhance PAN's solubility in water, the amount of Triton-X100 could be increased to up to 15 mL, but the resulting solution would be very foamy and difficult to handle. While this was cooling, a borate buffer solution was made up from 0.618 g of Boric acid (Boric acid, 99.999% trace metal basis, Sigma Aldrich) dissolved in 100 mL of 0.1 M NaOH solution (made up from sodium hydroxide pellets, 99.995% trace metal basis, Sigma-Aldrich). The buffer was then added to the PAN-surfactant solution and brought up to a total volume of 250 mL with Milli-Q water. At this point 400 µL of the Fe masking agent Desferrioxamine B powder (Desferal® (deferoxamine mesylate), 500 mg vials for injection – a prescription drug usually used to chelate the excess of Fe in the human body), dissolved in 3.05 mL of Milli-Q water, could be added to make the reagent ready for Mn determination. The final reagent had a pH of 9.

2.1.3.2 Mn standards

The Mn standards were prepared by dilution of 1000 mg/L Mn AAS standard (TraceCERT®, Fluka) and were stable for at least one week. They were stored as described for the Fe standards for both the laboratory and in-situ deployments.

2.1.3.3 Desferrioxamine B lifetime experiment

In (Chin et al. 1992) the longevity of the PAN reagent after the addition of Desferrioxamine B was estimated to be circa 1.5 days. Since one of the aims of the project was to develop a long-term device for the detection of manganese, an experiment was set up to test the stability of the reagent over a longer period of time. This test would provide information on whether the PAN assay was fit for the purpose of the project.

PAN reagent and Mn standards (0 µM, 1 µM, 2 µM) were prepared as described in the above paragraphs in volumes big enough to allow triplicate measurements of absorbance over 9 days.

On day 0,1,4,7 and 9 the standards were mixed with the PAN-Desferrioxamine reagent and the absorbance of the solutions were measured with an HR 4000 Ocean Optics spectrometer.

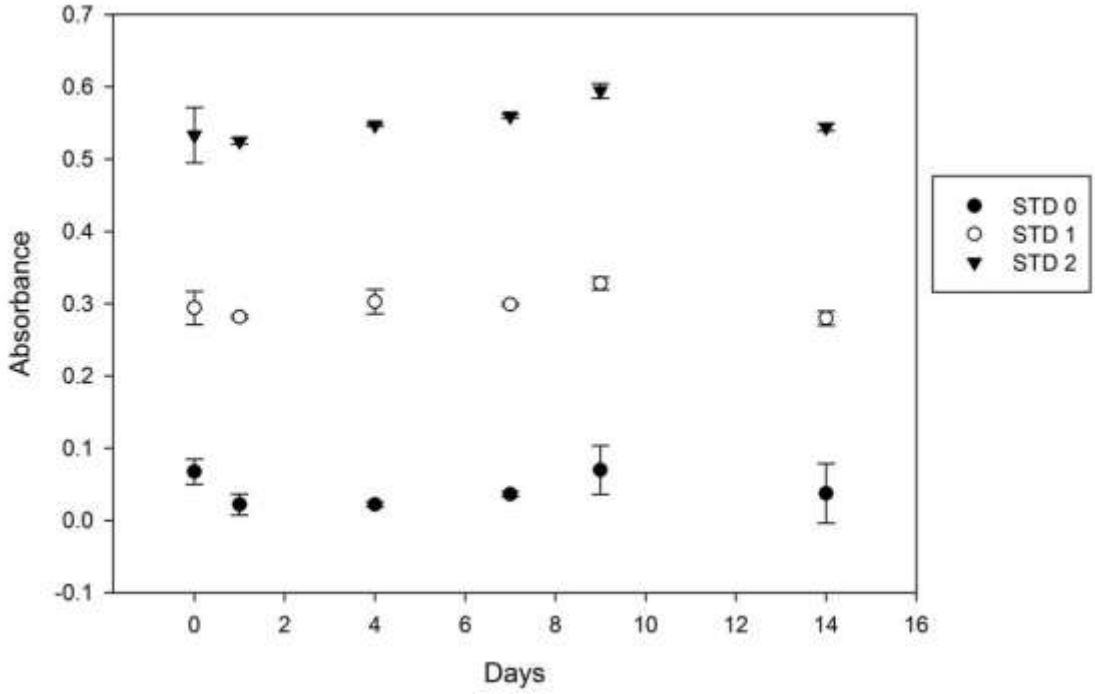

Figure 2-2 - Long-term experiment to test the stability of the PAN-Desferrioxamine reagent over time. STD 0: 0 µM Mn; STD 1: 1 µM Mn; STD 2: 2 µM Mn.

The results showed a slight increase in the absorbances of standards 1 and 2 (standard 0 being a blank sample) around day 9 (Figure 2-2). The increase in absorbance was expected as the Desferrioxamine loses its power to chelate any iron possibly present and releases it into solution, where it forms a complex with PAN. However the increase in the absorbance values over time was almost negligible, and 6 days was decided as a safe time limit for the use of the PAN-Desferrioxamine reagent.

2.2 Laboratory and shipboard procedures

2.2.1 Laboratory procedures

Previous to any laboratory analysis of both standards and samples, all glassware and plastic-ware was firstly cleaned with Decon detergent (if new), then soaked overnight in 10% hydrochloric acid and finally rinsed three times with Milli-Q water. It was then stored in double re-sealable plastic bags.

For all the laboratory measurements, samples were added to the reagents in 30 mL plastic (Sterilin) tubes, in a ratio of 10:1. The solutions were then immediately analysed with both an Ocean Optics HR4000 Spectrometer and an HITACHI U-2800 Spectrometer. The results were compared to check the accuracy of the measurements.

2.2.2 Sampling during the EMB cruise – Baltic Sea

In August 2012 the second prototype of the Fe(II)-Mn analyser (paragraph 5.1) was taken to sea during the Elisabeth Mann-Borgese (EMB) cruise (06EZ1215) on the Baltic Sea in collaboration with the Leibniz Institute for Baltic Sea Research (IOW, Warnemünde, Germany). Over 16 days in the Baltic proper, ten successful deployments of the analyser attached to a custom-made CTD carousel were done. To check the accuracy of the analyser, at most stations water sampling bottles on the CTD-rosette carousel were fired at depths corresponding to the in-situ measurements. Water sub-samples were collected from the water samplers into 30 mL vials pre-charged with FZ for Fe(II) determination and with PAN for manganese determination. Fe samples were not filtered and were directly added to the vials in order to limit as much as possible the oxidation of the Fe(II) in solution prior to the reaction with the reagent. For dissolved Mn, where oxidation is much slower than for Fe(II), there was time to filter the samples with polyethersulfonate MILLEX filter units (0.45 μm, Millipore, Germany) prior to analysis in the ship laboratory. On board a Shimadzu UV-mini 1240 bench top spectrometer was used to measure the concentration of metals in the water samples. A 10 cm path-length cell was used for the Fe(II) samples and a 2 cm cell for the Mn samples (whose expected concentrations were on the order of several μM and use of a 10 cm long cell would have potentially led to absorbances beyond the linear calibration range).

2.3 Chip fabrication methods

The fabrication techniques explained below were used to manufacture chips for both Prototype 1 and Prototype 2 devices. The details of each of these prototypes and of their integration into the analyzing system are given in Chapter 3 and Chapter 4.

The core of the system developed is a microfluidic device in which the samples and reagents are injected, mixed and finally analysed. This device is a chip manufactured in PMMA (poly(methyl methacrylate) in which opto-fluidic cells and a mixer have been machined by micro-milling (Figure 2-3).

2.3.1 Substrate choice

Before integrating the PMMA chip into a detecting system, the basics of the technology were explored. The effectiveness of the use of tinted (dark grey) PMMA to build micro-fluidic optical cells has been studied by Dr C.F.A. Floquet and the Sensors Group team at the National Oceanography Centre (NOC, Southampton). This study validated a low-cost manufacturing technique for the production of high-performance opto-fluidic devices in tinted PMMA and confirmed that the use of this substrate reduces stray light from the LED light source reaching the detector, thus improving the LOD (limit of detection) of the system (Floquet et al. 2011).

2.3.2 Micro-milling technology

The microfluidic device was created by machining micro-channels, optics and detectors recesses, valve inlets and mounts, and a pump footprint into a 8.0 mm thick tinted PMMA (PLEXIGLAS® GS, Grey 7C83 GT, Röhm, Darmstadt, Germany) substrate (chip body) using an LPKF Protomat S100 micromill. A matching lid was cut in a thinner (3.0 mm thick) sheet of the same substrate. The design of the chip was drawn in a 2D drawing software, DraftSight (Solidworks), and it was then converted as a tool path with the CircuitCam software (LPKF laser and electronics AG, Garbsen, Germany) for use on the LPKF Protomat S100 micromill.

2.3.3 Bonding

The matching lid was bonded to the chip body by exposure to chloroform vapour prior to pressure being applied. The exposure to the solvent also reduced the surface roughness of channels thus enhancing the optical efficiency of the cells as described in Ogilvie et al. 2010 (Ogilvie et al. 2010).

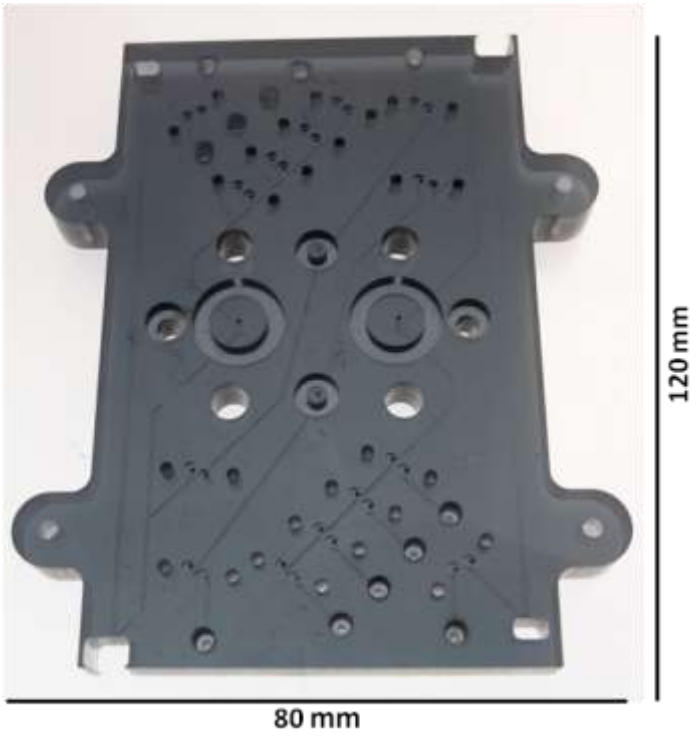

Figure 2-3 - A bonded chip in which optical channels have been machined (chip made by A. Milani).

2.3.4 Optics alignment

The light sources for the detection cell were super green light emitting diodes (LEDs, B5b-433-20, Roithner Laser Technik, Austria) with output centered on 572 nm with a full width half maximum (FWHM) of ~30 nm. They were chosen because in Milli-Q water the $FeFZ_3$ complex absorbs at 562 nm with a FWHM of ~100 nm and the PAN-Mn complex absorbs at 560 nm with a FWHM of ~50 nm. To measure the light that reached the end of the opto-fluidic cells photodiode detectors with internal amplification and the ability to produce a voltage output that was directly proportional to incoming radiation (TSL257, TAOS Inc., USA) were used.

In order to align the optical elements, the microfluidic chip was secured to a multi-axis platform for micro-positioning (a combination of linear manual translational stages from Thoralabs, USA) and the LED and photodiode were placed in the recesses at the extremes of the optical absorption cell. An optical adhesive (NOA 68, Norland, USA) was then gently added into the recesses so to separately cover the LED and the photodiode. These were then carefully aligned to maximise the output signal from the photodiode. Once this was achieved, the optical adhesive was cured with ultraviolet (UV) light to fix the optics in place. The objective of this operation was to obtain a signal output as close as possible to the photodiode's saturation (5 V) in order to provide the maximum dynamic range for the absorbance measurements.

2.4 Summary

This chapter described the chemical and fabrication methods used for the development of the Fe(II) and Mn microfluidic analyser. Those techniques were applied along the course of the whole project and were common to the development and optimisation process of both Prototype 1 and Prototype 2 devices.

Colorimetry was chosen as the determination technique for Fe(II) and Mn and the Ferrozine and PAN method were used respectively. Standards and reagents were stored in gas-tight nutrition bags and their shelf life was determined and resulted suitable for long-term (several weeks) deployments for Fe(II), and medium-term (6 days) deployments for Mn.

PMMA microfluidic chips were at the core of the analyser under development. The manufacturing techniques included micro-milling the microfluidic manifold in a tinted plastic substrate (chip body); bonding of the chip body to a lid via exposure to solvent vapours; alignment of the optical components (LEDs and photodiodes) to the opto-fluidic measuring cell.

The integration of the chips with the mechanical and electronic components of the analyser is detailed in Chapter 3 for Prototype 1 and in Chapter 4 for Prototype 2.

Chapter 3
Microfluidic Analyser
Prototype 1 (P1)

The core of the system is a microfluidic chip in which the samples and reagents are injected, mixed and finally analysed. The production techniques for this chip are described in Chapter 2.

At the beginning of this work, a first prototype of the device existed. It had been designed by Dr. Cedric Floquet (Sensors Group, NOC), to participate to the MoMAR-D (Monitoring the Mid-Atlantic Ridge Demonstration) mission (see paragraph 3.2). Prototype 1 (P1) also used aspects of other devices already under development within the Group, such as the nitrite analyser designed by Dr. Vincent Sieben (Sieben et al. 2010). The use of tinted PMMA as the device substrate is discussed in paragraph 2.3.1 (Floquet et al. 2011).

P1 was developed firstly for the detection of Fe(II) in seawater. Its use as a Mn analyser was considered a secondary target, and hence most efforts were focused on optimizing the device for Fe(II) measurements. The results of this optimization process are described here.

3.1 Prototype 1 description

In overview, solutions were moved through the chip channels by a syringe pump with 2 barrels (one for standards and sample, the second for the reagent) that was operated by a screw drive stepper motor. The solution (sample, standard or blank) injected into the manifold could be chosen through use of the valves. The injected solution was then mixed with the Ferrozine reagent in the serpentine mixer, and the resulting color measured in the optical cell. The pump, valves, light sources and detectors were controlled by a custom made electronics package. Details of each analyser's component are given below.

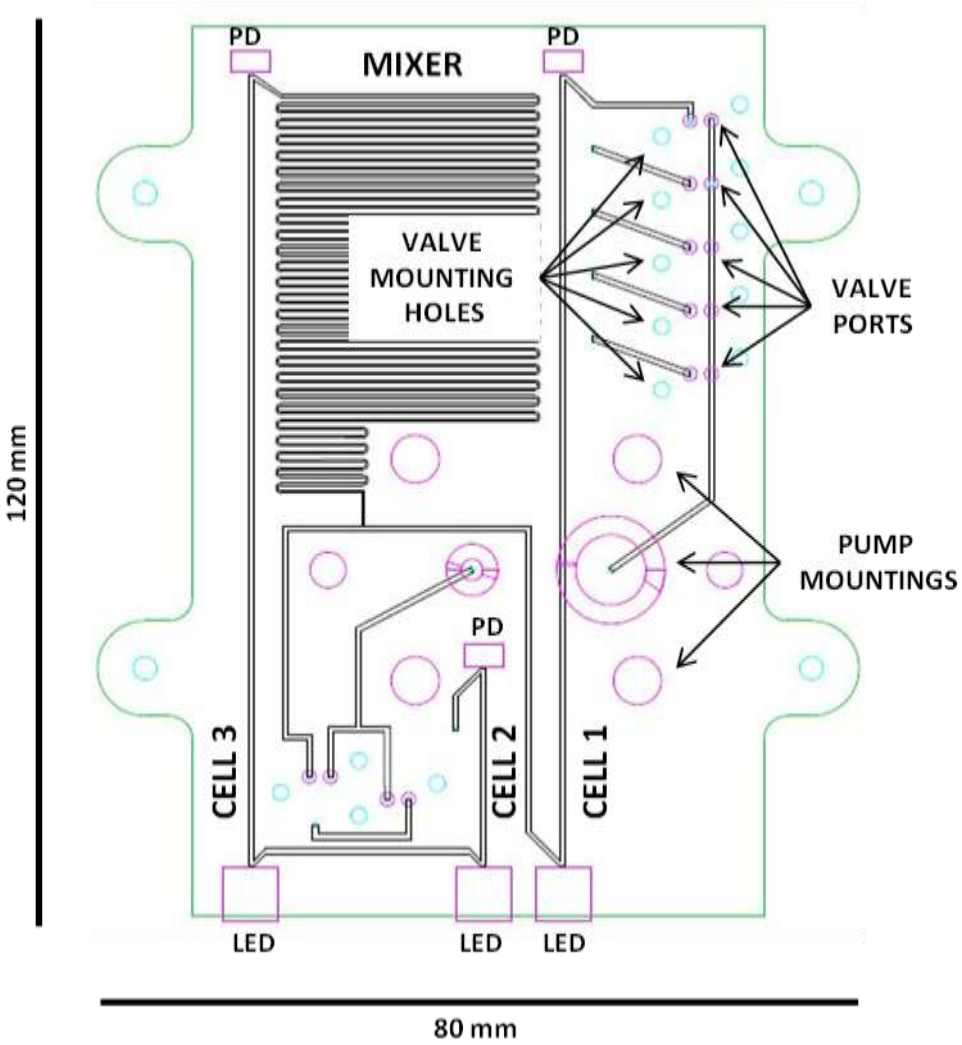

Figure 3-1 - CAD drawing of the microfluidic chip showing external shape (green), location of LEDs (large pink squares), photodiodes (PD) (small pink rectangles), recesses for pump mountings (pink doughnuts and big circles), microfluidic channels (black), valve ports (pink small circles), and valves mounting holes (turquoise circles). All channels are 400 µm by 300 µm except the optical cells which are 700 µm by 300 µm. The serpentine mixer is 1.4 m long, 250 µm wide, 300 µm deep.

Figure 3-1 shows the CAD drawing of the PMMA chip developed for P1. It was a 120 mm x 80 mm x 11 mm device in which opto-fluidic cells, pump and valve mounting indents, and LEDs and photodiodes recesses had been micromilled (see paragraph 2.3.2).

P1 was originally conceived to be used under continuous flow conditions and its design elements reflected that target.

3.1.1 Optofluidic Cells

Three opto-fluidic cells were milled in the PMMA substrate. All three cells were 700 µm wide and 300 µm deep. This cross section was chosen as a compromise between minimising the internal volume of the channels and maximising the area of the detector

(positioned at one end of the cell) that could be illuminated by the light source (fixed at the opposite end; see optics alignment, paragraph 2.3.4).

As can be seen Figure 3-1, the cells are of different lengths. Cell number 1 was 100 mm long. It received the sample/standard but not the reagent. This feature was implemented in order to associate each measurement with a measurement of the background signal due to the sample's matrix contribution.

The second and third cells received sample mixed with the reagent. The second long cell (Cell 3) was 100 mm in length and it allowed measurements of concentrations of Fe(II) up to ~3.50 μM, at higher concentrations the absorbance would exceed 1 resulting in non-linearity. The short cell (Cell 2) was 25 mm long, thus allowing measurement of concentrations of Fe(II) up to ~14 μM, with A <1. The presence of these two different absorption cells were intended to extend the top limit of the range of detection of the system and to make the analyser suitable to be used in Fe enriched environments.

3.1.2 Mixing

Microfluidic systems operate with laminar flows (Reynolds numbers < 2300). This implies that mixing processes in microfluidic devices are driven by diffusion rather than by turbulence. In the specific case of the reaction between Ferrozine and Fe(II), although the complexation happens almost instantaneously, if a continuous flow set up is chosen, a long mixing coil is required to make sure that the desired level of mixing via diffusion is achieved. Other mixing options could be investigated (see section 6.1.4.1 in Ogilvie (2012)) , but at the time of the development of P1 chip design the priority was to have a reliable mixer, easy to manufacture with the tools present in the group.

To calculate the ideal length of the serpentine (coil) mixer, the time (diffusion time, t) needed by the molecule of Ferrozine to diffuse across the channel must be determined. It is calculated as follows:

$$t = \frac{w^2}{D}$$

where w is the width of the channel and D the diffusivity of the diffusing molecule.

In the microfluidic chip the width of the mixing coil was 250 μm. Although a narrower channel would shorten the diffusion time, this width was initially chosen because of the limits of the fabrication technique (no tools able to cut a channel smaller than 250 μm were available).

The diffusivity, D, of the Ferrozine molecule is calculated with the Einstein-Stokes equation for diffusion of spherical particles through liquids with low Reynolds numbers:

$$D = \frac{k_B \cdot T}{6\pi\eta R}$$

where

- k_B is the Boltzmann constant;
- T is the absolute temperature;
- η is the viscosity of the fluid through which the molecule diffuses;
- R is the radius of the diffusing molecule.

Ferrozine is assumed to be spherical and its radius is calculated as the average of the lengths of the longest and shortest chains of the molecule (maximum length 14.70 Å, minimum length 8.88 Å).

Diffusivity varies with temperature. Table 3-1 summarizes Ferrozine's diffusion coefficient at different temperatures and the related diffusion times for the flow rate chosen at the time, 810 µl/min.

Once the diffusion time t is obtained, the ideal length of the mixing coil is calculated as the overall flow rate of the flow in the microfluidic chip (µl/s) multiplied by t. As Table 3-1 shows, the ideal lengths calculated are much longer than that allowed by the space and volume constraints of the chip surface area (120 mm x 80 mm).

Temperature	**2˚C**	**10˚C**	**20˚C**
Diffusivity of Ferrozine, D_{Fz}	2.04 x 10^2 µm^2/s	2.69 x 10^2 µm^2/s	3.64 x 10^2 µm^2/s
Diffusion time, $t = w^2/D$	305.91 s	232.27 s	171.80 s
Calculated length	55.06 m	41.81 m	30.92 m

Table 3-1 - Diffusivity, diffusion times of Ferrozine and ideal length of the mixing coil at different temperatures. Width of the channel: w = 250 µm.

Another parameter had to be taken into account while designing the serpentine mixer: the backpressure tolerated by the valves in use in the system. For the device under development this figure could not exceed 2 bars.

The maximum length of the mixing coil is then calculated from the Darcy-Weisbach equation which expresses the pressure drop, Δp, along a pipe of given length:

$$\Delta p = f \cdot \frac{L}{D} \cdot \frac{\rho \cdot V^2}{2}$$

where

- f is the Darcy friction factor, a dimensionless number which for flows at low Reynolds numbers has been empirically defined as: $f = 64/Re$;
- L is the length of the channel;
- D is the hydraulic diameter of the channel;
- ρ is the density of the fluid at a given temperature;
- V is the average velocity of the fluid.

Considering a maximum pressure drop of 2 bar, and a fluid of temperature T = 2 ˚C flowing through the chip, the maximum length of the channel is 1543 mm for a flow rate of 810 µl/min.

Having taken into account the space and volume constrains of the microfluidic chip and not wanting to push the valves to the limit of their pressure tolerance, the serpentine mixer was designed with a length of 1400 mm.

The mixer was validated by comparing the absorption of samples mixed off-line and then injected into the system to the absorption of samples mixed on-line (in the chip mixing coil). As Figure 3-2 and Table 3-2 show, the values obtained agreed greatly.

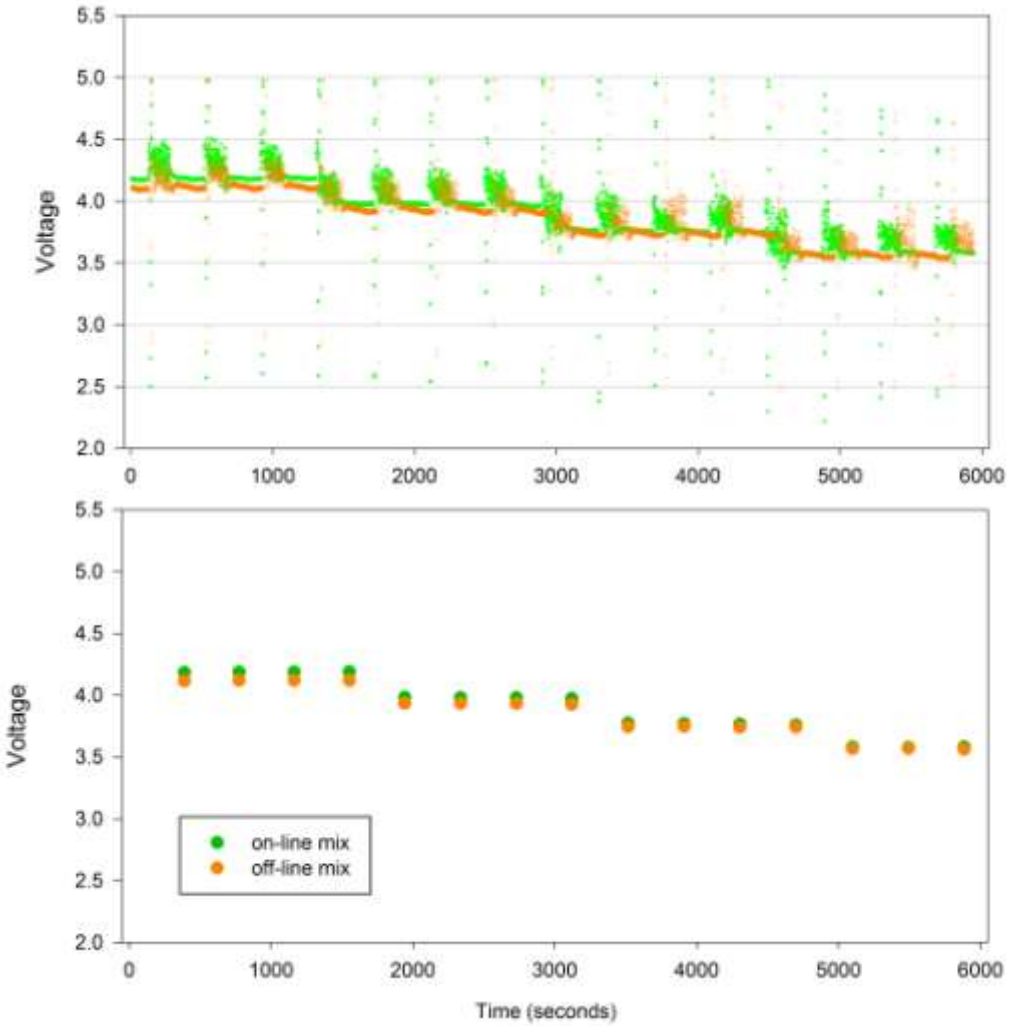

Figure 3-2 – Raw voltage output of the Fe(II) analyser for 0 nM, 100 nM, 250 nM, 500 nM Fe(II) Standards..

Comparison of samples mixed off-line and on-line with Ferrozine reagent.

	Replicate	on-line	off-line
STD 1	1	4.183	4.115
	2	4.187	4.120
	3	4.187	4.119
	4	4.189	4.118
	average	4.187	4.118
	stdev	0.002	0.003
	%RSD	0.060	0.062

	Replicate	on-line	off-line
STD 3	1	3.774	3.744
	2	3.770	3.748
	3	3.765	3.741
	4	3.760	3.743
	average	3.767	3.744
	stdev	0.006	0.003
	%RSD	0.163	0.080

STD 2	1	3.984	3.935
	2	3.980	3.934
	3	3.980	3.933
	4	3.973	3.925
	average	3.979	3.932
	stdev	0.004	0.004
	%RSD	0.111	0.111

STD 4	1	3.580	3.567
	2	3.577	3.570
	3	3.582	3.562
	4	3.581	3.567
	average	3.580	3.567
	stdev	0.002	0.003
	%RSD	0.063	0.090

Table 3-2 – Raw voltage output data from Figure 3-2.

3.1.3 Electronic components

A light source and a detector were placed at the two ends of each opto-fluidic cell. The light sources used in the system were super green light emitting, while the light detectors were photodiodes, see paragraph 2.3.4.

Two Hall-effect sensors were mounted on a custom-made pump. These transducers vary their output voltage in response to a magnetic field. They were used to accurately identify the position of the syringe pump and thus the volume of sample and reagent withdrawn/injected.

The sensor was controlled by a custom-designed stand-alone electronics package (5 x 6.2 x 4 cm). It included: eight 18-bit analogue-to-digital inputs (for Hall-effect sensors and photodiodes), three constant current source LED drivers, a stepper motor driver for the pump, a temperature sensor, a real time clock, and 8 spike and hold circuits for powering the valves. A micro-controller (PIC18F87J11, Microchip, USA) performed all low-level operations, and a 2 GB flash memory card stored the final data (filtered to 1 Hz); it could record about 3.7 million readings, which equates to circa 1.2 years of continuous use). A fault tolerant file system ensured data were not corrupted in the event of power loss.

The sensor package was operated through a programmable Autonomous State Machine (ASM), which controlled the operations performed by the analyser at any given time and associated them with a time stamp in the final data file. The ASM was modified according to what the measurement routine required. A user-friendly interface allowed for quick access to the sensor's operations script Screenshot in Figure 3-2).

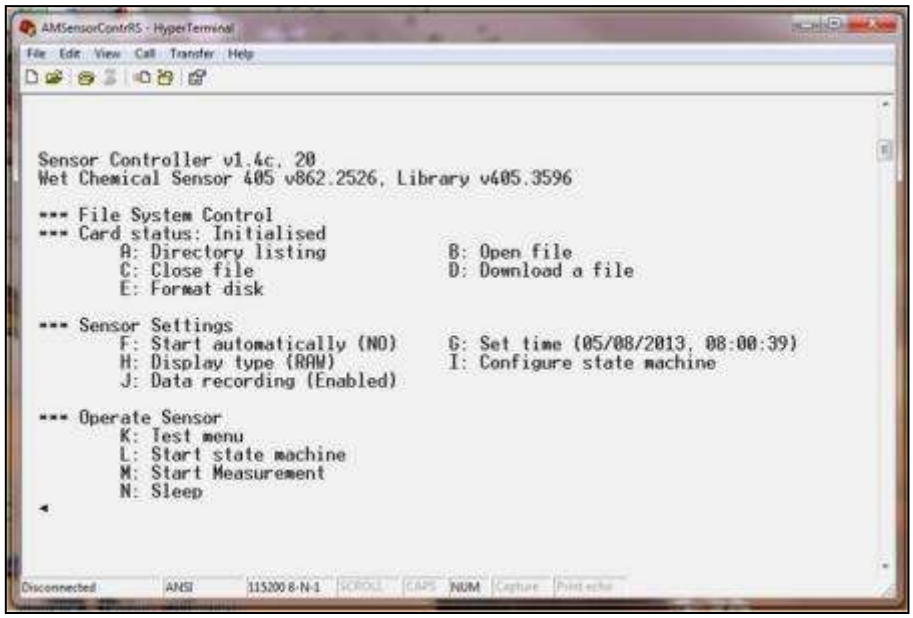

Figure 3-3 – Screen-shot of the user-sensor interface used to control the sensor's operations.

3.1.4 Mechanical components

A custom-designed syringe pump was used for sample, standard, blank and reagent withdraw from their reservoirs and injection into the manifold. The pump was a modification of the one designed for nutrient sensors under development in the Sensors Group, NOCS, where one large and one small plunger were used, rather than 4 small ones. This modification was necessary because of the different ratio of sample to reagent used in the Fe(II)-Ferrozine method (10:1).

The pump was mounted directly on the PMMA chip to minimize dead volumes. The pump footprint was milled into the top of the chip to a depth of 2 mm, and the supporting rods were inserted through the body of the chip and secured to a platform on the bottom of it. The titanium syringe plungers were moved up and down by a sliding plate driven by a stepper motor, while the barrels were inserted into the top of the chip.

Viton quad-rings (Polymax Ltd., UK) were fitted to the small and big plungers to seal the fluid compartment of the syringes.

The pump allowed a maximum withdrawal of 987 µl of sample and of 102 µl of reagent. It drew a peak current of 360 mA when in operation (withdrawing or injecting).

Details of the pump design can be seen in Figure 3-4.

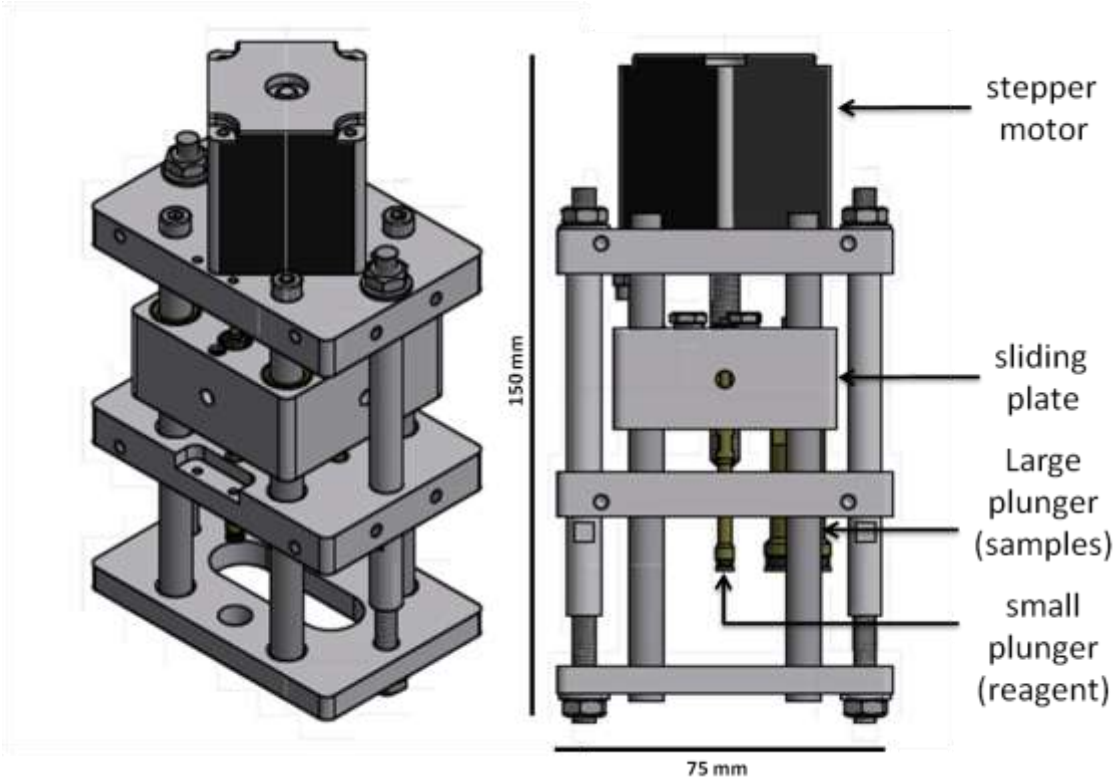

Figure 3-4 – CAD drawing of the custom-made syringe pump. Top and side view. In the picture can be seen the stepper motor driving the sliding plate and the two (small and large) plungers. The barrels covering the plungers are not shown. Idea and drawings by Dr. Ed Waugh, Sensors Group, NOC, Southampton.

Lee Products 300 Series Solenoid Valves were used to guide the fluid through the microfluidic chip for different measurement steps. They were connected to the chip by mounting holes and valve ports milled into the top of the chip. They were operated according to a *spike-and-hold* power waveform design to minimize the power consumption. The *spike* voltage was 12 V that dropped to the *hold* voltage of 6 V after 5 seconds. They operated up to a maximum back pressure of 2.0 bars.

PTFE tubing (0.8 mm internal diameter) was used to introduce the samples/standards and reagent into the manifold. These tubes were connected to the chip by fluidic connectors (MINSTAC, Lee Company, USA) that consisted of a plastic nipple, a steel compressor ring and a plastic nut.

The reagent and standard lines were connected to storage reservoirs (gas-tight nutrition bags, see paragraph 2.1.2.2). During deployments, to avoid clogging of the microfluidic manifold by particles present in the water samples, the sample inlet was connected to polyethersulfonate MILLEX filter units (0.45 µm, Millipore, Germany; dead volume <100 µL).

The microfluidic chip, the pump, the valves and the electronic elements were fitted into a 15 cm (external diameter) x 40 cm clear cylindrical PMMA housing when deployed in water. This housing was filled with mineral oil and hermetically closed to avoid any contact between the analyser and the water it was immerged in. The cylinder was pressure compensated with a bladder that accommodated changes in the oil volume with temperature and depth during deep water deployments. On the top Delrin endcap were fitted 6 connectors for the fluidic tubing coming out of the chip, a bulk head connector (Subconn microseries, 8 contacts, MCBH8M) for power supply to and communication with the sensor, and 2 oil filling caps.

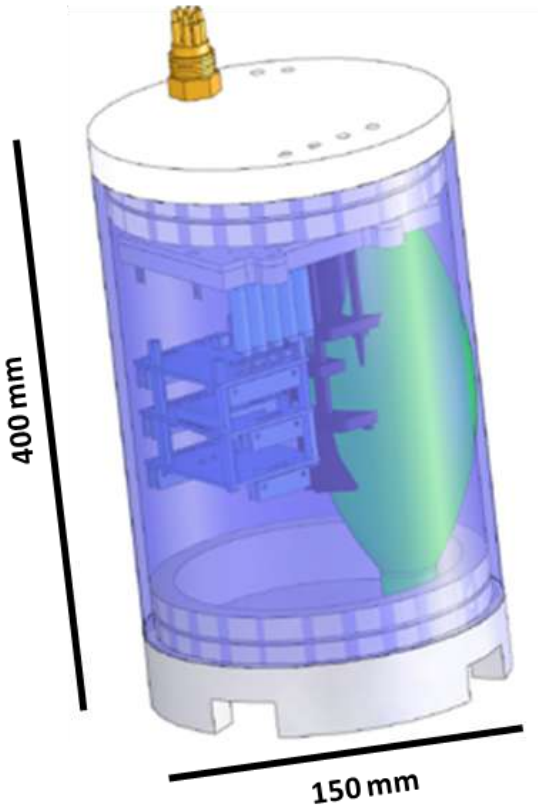

Figure 3-5 – The analyser enclosed in the clear plastic cylindrical housing. In green is the pressure compensating bladder, over-expanded. On the top end cap are the the bulk head connectors. Fluidic connectors are not shown. Idea and CAD drawing by Dr. C.F.A. Floquet.

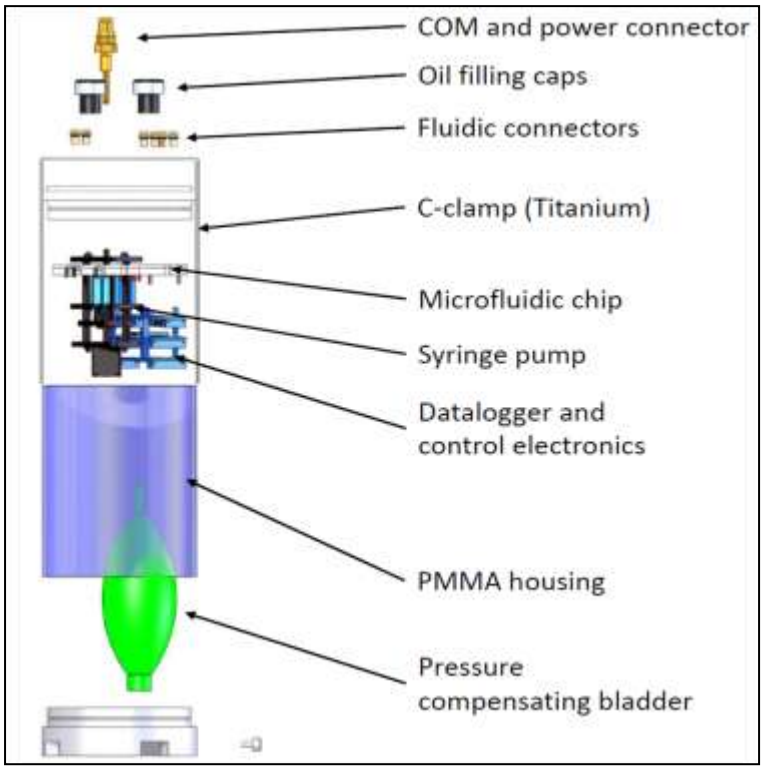

Figure 3-6 – Exploded view of the analyser in the pressure compensated housing. CAD drawing by Dr. C.F.A. Floquet.

Figure 3-7 – Photographs of assembled analyser outside and inside the pressure compensated housing.

3.2 MoMAR-D mission

In 2008 the Sensors Group, NOC, committed to participation in the MoMAR-D (Monitoring the Mid-Atlantic Ridge Demonstration) mission which was part of the ESONET (European Seas Observatory NETwork) project. ESONET aimed to implement and manage a network of long-term multidisciplinary ocean observatories (nodes) in deep waters around Europe. Within this wider project, MoMAR focussed on the hydrothermal vent sites in the Azores region and in particular the MoMAR-D demonstration mission targeted the Lucky Strike vent field. MoMAR-D planned to implement the Azores ESONET's node through a one year deployment of a multidisciplinary observing system with satellite connection to shore. The deployment of two stations with connection based on the SEAMON technology developed by Blandin and Rolin (Blandin and Rolin 2005) would allow the interaction of several different sensors split between the platforms according to their target measurements. One SEAMON was to host geophysical instruments ("geophysical node", SEAMON OUEST) while the other one would focus on fluid chemistry and ecology ("Tour Eiffel node", SEAMON-EST). The platforms would be acoustically linked to a surface buoy for satellite communication to an onshore station based at Ifremer, France (see Figure 3-8).

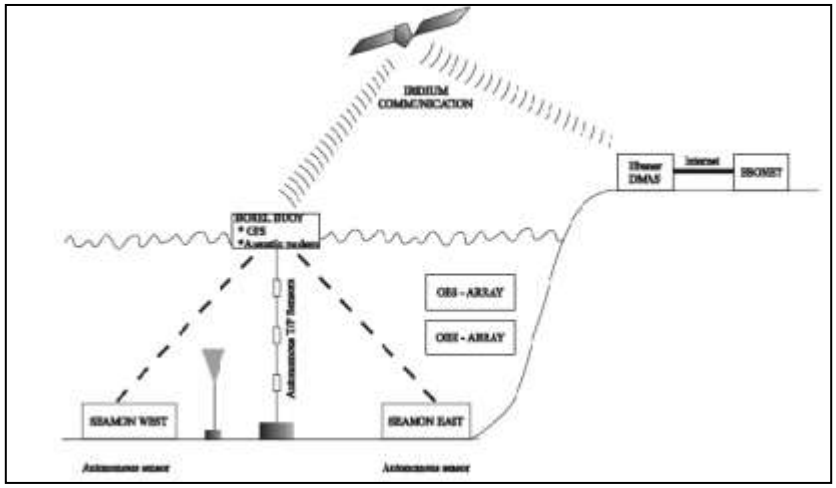

Figure 3-8 – Sketch of the MoMAR-D experiment. From the "ESONET – WP4 – Call for Demonstration Mission", Ifremer, France.

For the MoMARSAT2010 cruise the NOC Sensors Group had to provide two analysers for the detection of Fe(II). They were intended to be connected to the SEAMON-EST platform and deployed on a diffuse emission site next to the *Tour Eiffel* hydrothermal edifice.

The MoMAR-D project started in October 2010. The French vessel *Pourquoi pas?* set sail from Horta (Fajal, Azores Islands) with 37 researchers and the ROV (Remote Operated Vehicle) Victor 6000 (Ifremer, France) on board.

3.2.1 Pre-deployment tests

Before leaving for the cruise, a fully assembled iron analyser was tested in a temperature controlled chamber at 4°C and, separately, in a pressure pot at pressures up to 200 bars at ambient temperature (20°C) for 4 hours by Dr. C.F.A. Floquet and Dr. K.S. A. Beyh. No calibrations or long cycle measurements could be run on the analyser during these tests because of time constraints; the main aim of the tests was to assess the tolerance of the device's mechanical and electronic elements to harsh, real-environment conditions. While the analyser performance was not affected by temperature, during the pressure test the pump stopped. An increase in the supplied current from 200 mA to 400 mA was enough to restart the motor. This could be done remotely as the pressure pot connections allowed communication from and to the analyser.

Three identical analysers with pressure compensated housings were prepared for the cruise (two were meant to be deployed and one was prepared as a backup).

On the ship, overnight tests were run on each analyser and a calibration curve was obtained on the bench for each system before moving two of them to the SEAMON-EST station. An example of the raw voltage outputs of the analysers during two calibration cycles is shown in Figure 3-9: two measurement loops with the repeated injection of 3 Fe(II) standards were performed in the 3 cells of each chip. The decrease in the voltage output from standard 1 (0 nM or blank) to standard 3 (200 nM) corresponds to the increasing absorbance of the solutions with concentration.

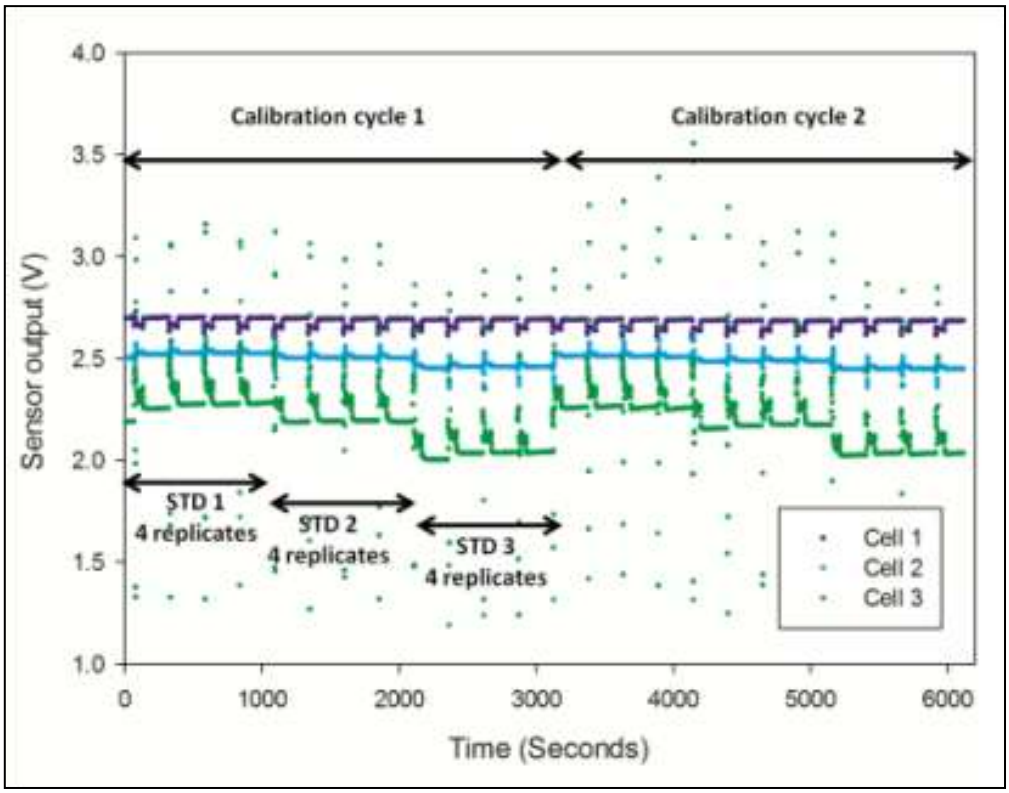

Figure 3-9 – Raw voltage output of the Fe(II) analyser during 2 calibration cycles.

		STD1			STD2			STD3		
	CELLS	**no reagen**	**2.5 cm**	**10 cm**	**no reagen**	**2.5 cm**	**10 cm**	**no reagent**	**2.5 cm**	**10 cm**
REPLICATES	**1**	2.658	2.526	2.318	2.653	2.514	2.269	2.648	2.465	2.084
	2	2.658	2.536	2.351	2.650	2.516	2.282	2.659	2.470	2.110
	3	2.656	2.535	2.353	2.649	2.515	2.284	2.650	2.469	2.109
	4	2.654	2.534	2.350	2.648	2.514	2.283	2.648	2.466	2.102
	average Cal 1	2.657	2.533	2.343	2.650	2.515	2.280	2.651	2.468	2.101
	Stdev	0.002	0.004	0.017	0.002	0.001	0.007	0.005	0.002	0.012
	%RSD	0.077	0.173	0.717	0.074	0.036	0.319	0.200	0.094	0.571
REPLICATES	**1**	2.646	2.518	2.325	2.641	2.497	2.249	2.643	2.452	2.072
	2	2.644	2.520	2.336	2.639	2.500	2.261	2.642	2.458	2.100
	3	2.642	2.519	2.338	2.640	2.499	2.260	2.642	2.458	2.100
	4	2.641	2.518	2.336	2.639	2.499	2.261	-	-	-
	average Cal 2	2.643	2.519	2.334	2.640	2.498	2.258	2.642	2.456	2.091
	Stdev	0.002	0.001	0.006	0.001	0.001	0.006	0.001	0.003	0.016
	%RSD	0.08	0.04	0.25	0.04	0.05	0.28	0.02	0.14	0.77
	overall average	2.650	2.526	2.339	2.645	2.507	2.269	2.647	2.463	2.097
	Stdev	0.007	0.008	0.013	0.006	0.009	0.013	0.006	0.007	0.014
	%RSD	0.27	0.31	0.54	0.22	0.35	0.58	0.24	0.27	0.66

Table 3-3 – Data from calibration in Figure 3–9. Average, standard deviation and % RSD of two calibration cycles.

3.2.2 Lucky Strike deployment

The settings used during deployment of the two analysers are detailed in Table 3-2. The systems were programmed to start a three point (blank, 100 nM Fe(II), 200 nM Fe(II)) calibration cycle as their first task once they had landed on the seafloor. This was meant to validate the reliability of the measurements in case the instruments had suffered any damage during the descent that would afterwards make the analysis drift.

N. of measuring days	60	**N. of standards for calibration**	3
Sleeping (no activity) time between each measurement	3600 s	**Pump current**	360 mA
N. of measurements before next calibration cycle	24	**Pump time out (time to wait before sending an error message in case the pump got stuck)**	120 s
N. of flushes after each injection	4	**N. of pump timeouts allowed before putting the sensor to sleep**	5

Table 3-4 - Deployment settings of the 2 Fe(II) analysers for the MoMAR-D mission.

Deploying two identical systems for the determination of Fe(II) was an opportunity for the inter-comparison of the system itself, and allowed to increase the time resolution of the analysis. The two analysers were in fact programmed for sampling every four hours, with an offset of two hours between the systems, for 60 days (the maximum amount of measurements allowed by the power allocated to the module from the SEAMON-ESTplatform).

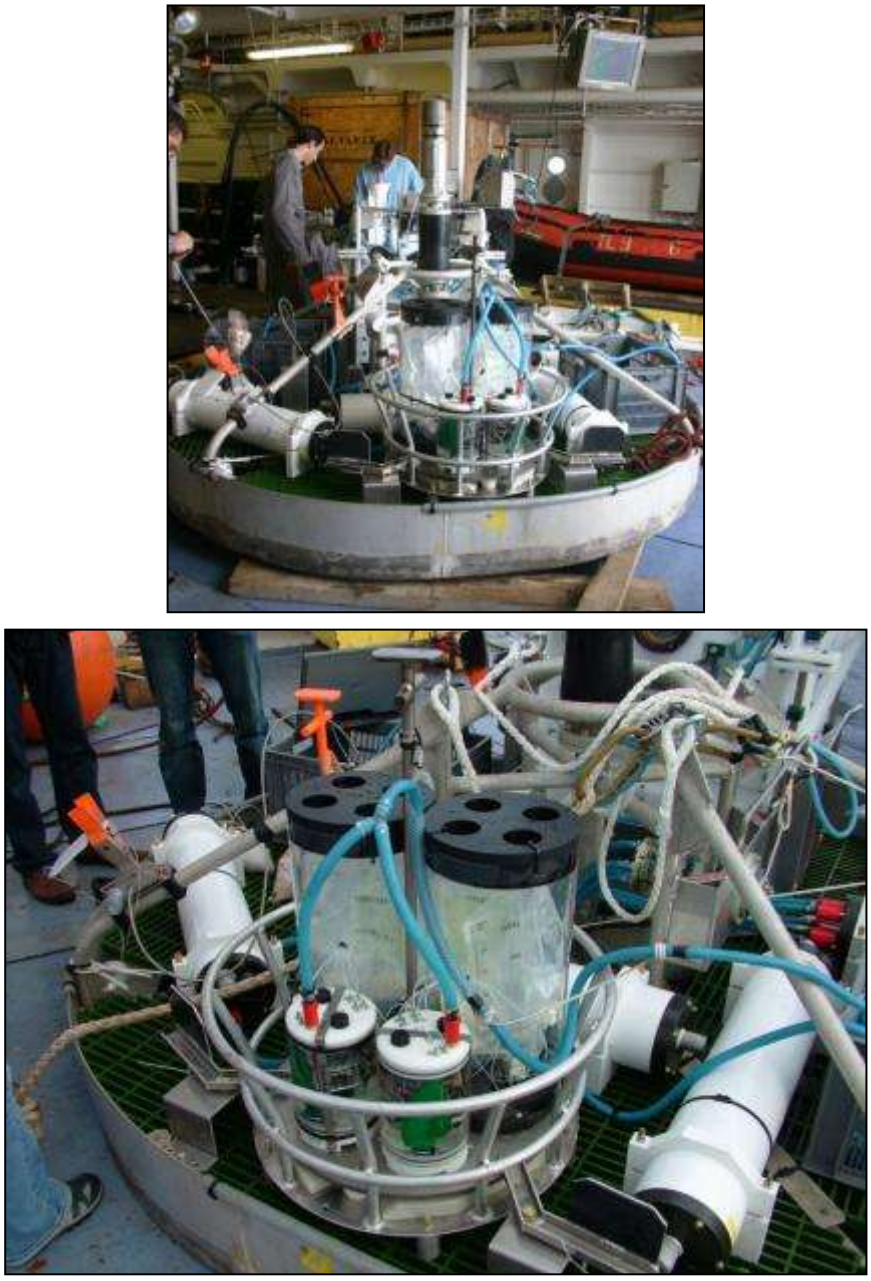

Figure 3-10 – Iron analysers on SEAMON-EST platform. Deployment set up. *Pourquoi Pas?* main deck.

The analysers were securely attached to a custom-built titanium platform for the deployment (Figure 3-10). The platform also accommodated two bigger cylindrical containers (800 mm x 250 mm), which housed the gas-tight nutrition bags for reagents and standards and a bag for the collection of the waste from the analyser.

Right before deploying the SEAMON-EST platform, mechanical and communication tests were performed on the analysers on the ship deck: they did not highlight any issues with the systems and the pumps operated smoothly at the set current of 360 mA. The platform descended to the seafloor at about 1700 m depth without major problems and when the analysers were interrogated from the ship they proved to have survived the deployment

and to be in good working condition. However, the connection between the SEAMON-EST platform and the ship control station did not allow access to the sensors' Autonomous State Machine script, hence there was no option of changing the analysers' settings once deployed.

The ROV VICTOR 6000 positioned the analysers' module on a suitable site previously identified on the Lucky Strike Vent Field (Figure 3-11). Temperature measurements (~15 deg C) and local biology indicated the presence of diffuse vent fluids which were expected to have concentrations of Fe(II) well above the detection limit of the analysers.

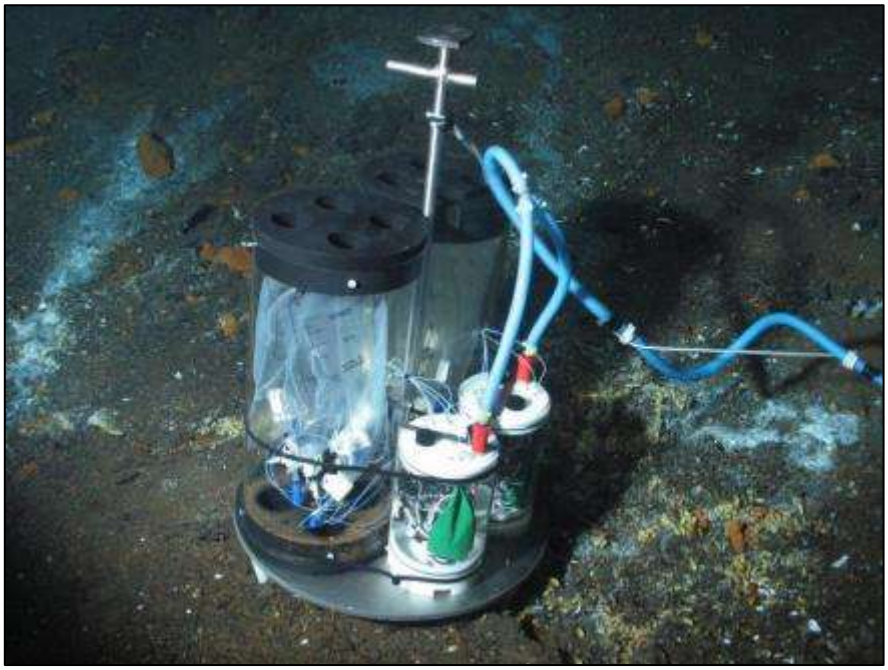

Figure 3-11 - Module of two Fe(II) analysers positioned on a diffuse flow vent site. Two small cylinders (400 mm x 150 mm): chemical analysers. Two big cylinders (800 mm x 250 mm): plastic housings for reagents/standards and waste storage bags. The cable for power and communication connection to SEAMON-EST is also visible. Photo: Victor 6000, Ifremer, France.

Unfortunately, once the platform received power, both analysers went into sleep mode as soon as the calibration process was started. Both instruments sent an error code associated with a pump failure. The analysers were rebooted from the ship remote control station, but the same error message was sent back right after the pump withdraw started. A mechanical problem with the pump was evident and the power supply from the platform to the analysers was cut in order to redistribute the energy to the other modules attached to SEAMON-EST.

The module with the analysers remained in the same position until it was recovered during the MoMARSAT2011 cruise in July 2011 by the Ifremer team.

A fault-finding process immediately began with the third, spare analyser in order to find the cause of the pump failure.

3.3 Post MoMAR-D deployment tests

The spare analyser brought back from the cruise was an identical copy of the two systems deployed next to the Tour Eiffel hydrothermal edifice. It was thus an ideal system to try to understand what had failed during the deployment. The approach to identifying the problem was to simplify the variables of the system by testing the most relevant ones in order to identify the cause of the failure. Once the origin of the fault had been indentified and possibly corrected, the following step would be a deployment in less rigorous conditions to test the robustness and reliability of the analyser.

3.3.1 Bench optimisation and calibration at different temperatures

At first the sensor was run on the bench with just MQ water and rinsed with 10% HCl solution, so that the fluidic circuit and the pump and valves dead volumes could be flushed from any impurities that might have entered and settled into the channels. This was a standard procedure for cleaning the PMMA chip and the attached tubing in case of trouble shooting or changing reagents.

Once this basic condition was restored, Fe(II) standards of different concentrations (0 nM, 100 nM, 250 nM, 500 nM) were prepared in MQ water and they were put into tight nutrition bags connected to the inlets of the system.

Since the module deployed at 1700 m had to face a great temperature gradient, the first variable tested was temperature. A range of temperatures that would include not only the values met during the MoMAR-D deployment, but also the ones most likely to be encountered in oceanic environments was chosen and a set of experiments was arranged in a temperature controlled environmental chamber. The sensor was tested at the temperatures of 4 °C, 10 °C and 20 °C. Good linear calibration curves were obtained for both the long (100 mm) and the short (25 mm) cells. The blank, standards and the Ferrozine reagent were prepared in MQ water. The first important observation was that the system worked with no error message sent.

The limits of detection of the system were calculated as three times the standard deviation of the blank value, which in these experiment was the 0 nM Fe(II) standard. The LOD obtained are detailed in Table 3-5. Lower limits of detection would be expected for the

longer channel (Ch 2) than for the shorter channel (Ch 1); and the LOD should decrease with temperature. However, these patterns are not represented by the test results shown in Tab 3-5. The higher LODs found in Channel 2 at 10°C and 20°C are most likely to be attributed to the diminished light reaching the detector, due to the cell length and the optics alignment difficulties. The reasons for the further discrepancies from the expected pattern were not found.

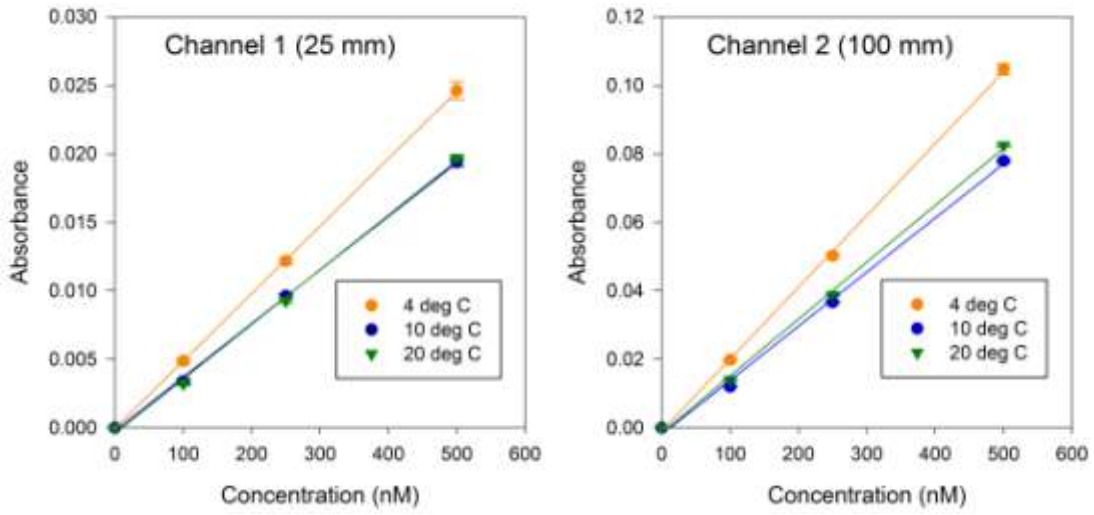

Figure3-12– Calibration at different temperatures, Channel 1 (25 mm) and Channel 2 (100 mm) results shown separately.

	Ch1			Ch2		
deg C	**4**	**10**	**20**	**4**	**10**	**20**
slope	4.92E-05	3.91E-05	4.0E-05	2.10E-04	1.58E-04	0.000166
intercept	-4.79E-05	-2.23E-04	-0.00041	-9.04E-04	-1.98E-03	-0.00151
StDev of Blanks	0.000835	0.00040	0.00040	0.001256	0.00188	0.002297
3* StDev Bl	0.002506	0.00121	0.00121	0.003767	0.00564	0.00689
LOD	**51.89**	**36.60**	**40.70**	**22.27**	**48.16**	**50.51**

Table 3-5 – LOD of the Fe(II) analyser at different temperatures.

3.3.2 Calibration at high pressure and low temperature

Once the system had been shown to be reliable in response to temperature variations, a set of higher complexity experiments that could mimic the conditions of the MoMAR-D deployment was planned.

A calibration of the analyser in a temperature and pressure controlled pot was planned. The test facility was not available within the premises of NOC, so the tests were carried out at the Ifremer institute in Brest (France).

The chemicals used for the calibration were prepared in MQ water at the NOC and then transported via ferry, together with the analyser, to the test site. No issues of reagent and standards degradation arose given the short time delay between the preparation of the chemicals and the analysis. A set of standards ranging from 0 nM Fe(II) to 2000 nM Fe(II) was prepared; the set was meant to be divided in two batches (0 nM to 500 nM and 750 nM to 2000 nM) in order to obtain two calibration curves that would cover the whole detection range of the analyser.

The settings of the system for this test were the same as those used to perform the temperature tests on the bench, which in turn did not change from the deployment settings summarised in Table 3-2. The analyser communicated with and was controlled by the user via the Autonomous State Machine interface and data were recorded on a data logger as in previous experiments.

The sensor was put in a conditioned chamber that could reach the target temperature of 4 °C and the pressure of 170 bar in less than three hours. The environmental parameters were chosen as such in order to mimic a deep-water deployment, which is the worst scenario the sensor could be expected to face.

Once the chosen temperature and pressure conditions were reached in the testing pot, the analyser was started and immediately the fault that happened during the MoMAR-D deployment was reproduced: the pump could not start withdrawing as the pistons were stuck in the bottom position. An increase in the supplied current from 360 mA to 500 mA solved the problem and allowed the pump to run correctly again.

With this new parameter, a calibration curve was obtained from the less concentrated set of standards; it is shown in

Figure 3-13. The second set of standards could not be measured because of time constraints. However, considering the usual concentration of Fe(II) in the ocean (paragraph 1.1.1), this calibration was enough to prove that the analyser could be applied in most marine environments where measurements of Fe(II) are relevant.

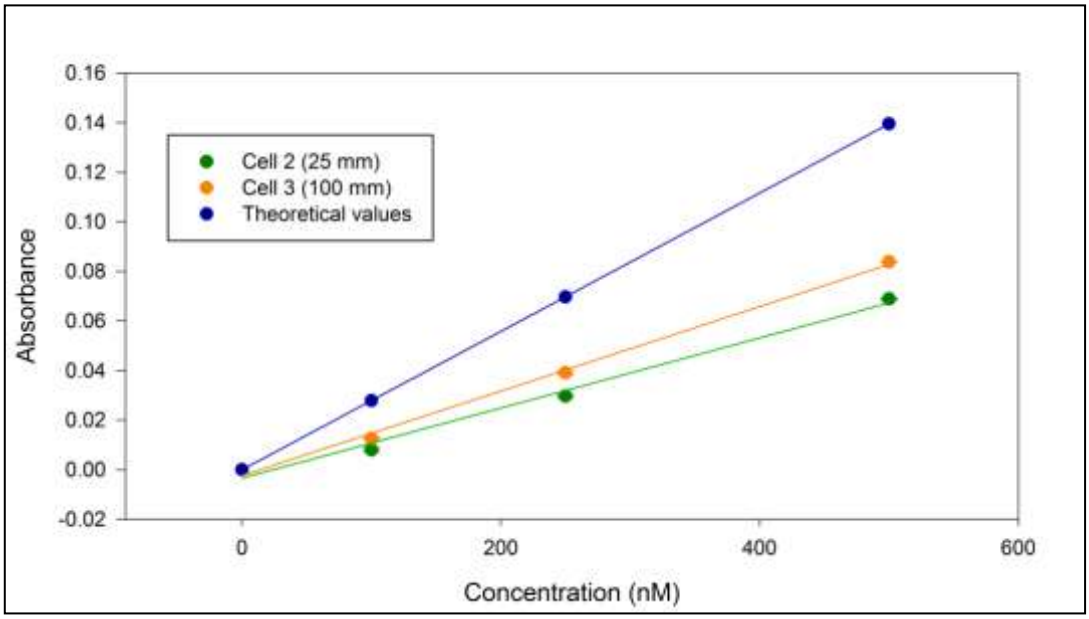

	CELL 2 (25 mm) x 4		CELL 3 (100 mm)	
Conc (nM)	**av**	**std**	**av**	**std**
0	0	0	0	0
100	0.0080	0.0007	0.0126	0.0003
250	0.0297	0.0006	0.0391	0.0009
500	0.0689	0.0003	0.0838	0.0001
Rsqr	0.990		0.997	

Figure 3-13 - Concentration vs absorbance plot of calibration curve obtained with 0 nM, 100 nM, 250 nM, 500 nM Fe(II) standards in a temperature and pressure controlled pot (4 °C, 170 bar) at Ifremer, Brest (France). Data from cell 2 (25 mm) have been multiplied by 4 to make them comparable to the cell 3 (100 mm) values. 3 replicates per standard. Errorbars on graph; data summarized in table.

A complete calibration cycle – including 4 rinses per standard - would last about an hour. The limits of detection were calculated as in the temperature dependent experiments (paragraph 3.3.1) and resulted to be much higher than expected: 170 nM for the short channel (25 mm) and 450 nM for the long channel (100 mm). The values of absorbance, much lower than the theoretical ones, and the low sensitivity suggested incomplete mixing of the standards and reagents in the serpentine mixer.

3.3.3 Results of post-deployment tests

The tests performed at NOC and at Ifremer highlighted a pump problem related to the increase of external ambient pressure. This issue did not show when the pump was tested on its own for pressure resistance, it only arose when the pump was integrated with the chip and immersed in mineral oil. This last issue was then thought to be responsible for

the pump-fault as its viscosity could have increased with pressure and reduced temperature, and the added viscosity exercised a too high resistance on the pump movement. However, calculations made by Dr. Ed Waugh (Sensors Group, NOC) on the predicted viscosity of the mineral oil used with increasing pressure showed that no major changes in the oil's physical properties would have occurred over the range of pressure and temperature at which the sensors were deployed.

The reason behind the MoMAR-D deployment fault thus remained not fully defined, but the pump current was increased to at least 500 mA for any following tests.

3.4 Problems related to P1 design and mechanics

Although the issue relating to the pump current had been resolved, further use of the analyser on the bench and in simpler deployments in the NOC dock waters highlighted additional problems related to the first prototype of the Fe(II) analyser that are reported and explained below.

3.4.1 Flushing and reagent volumes

The complexity of the manifold of P1's chip, with the 3 absorption cells and the long serpentine mixer, resulted in high dead volumes, which proved extremely difficult to flush. This might not have been such a problem in the case of sampling in slow changing environments, but in environments with steep Fe(II) concentration gradients, or rapidly changing concentrations, it would have invalidated any measurements. Poor flushing also slowed down calibrations greatly, as it would take several flushes before switching safely from a higher to a lower concentration standard in repeated cycles.

The possibility of calculating the carry-over from one sample to the other was explored, but a high number of flushes remained the most effective option. The number of flushes was conservatively fixed at 4 before any measurement could be taken. This meant that 4 full withdraws of the Ferrozine reagent, or 4 x 102 µl, were necessary for every measurement. Figure 3-14 and Table 3-6 show the raw voltage data obtained from running a set of MQ - 1000 nM Fe(II) standard - MQ on the analyser. Starting from a clean channel, MQ water was injected in the manifold 4 times, followed by 8 injections of the standard and 8 more injections of MQ. We calculated how many flushes were needed to achieve a precision of < 3% and obtained a figure to 4.

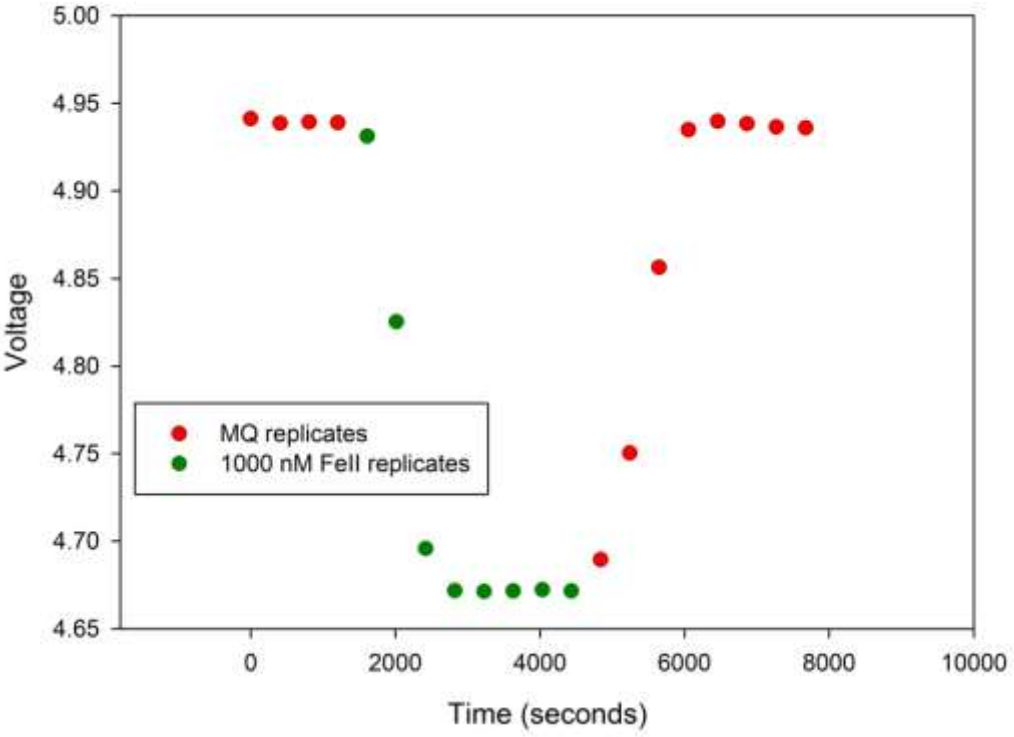

Figure 3-14 – Flushing test. Raw voltage data.

TIME	REPLICATE	SAMPLE	RAW DATA (Volts)	
0	1	MQ	4.9412	
407	2		4.9386	
808	3		4.9393	% RSD
1205	4		4.9389	0.023492
1610	1	1000 nM	4.9312	
2014	2		4.8253	
2419	3		4.6958	% RSD
2822	4		4.6718	2.524531
3228	5		4.6713	
3631	6		4.6716	
4034	7		4.6723	% RSD
4436	8		4.6716	0.007899
4841	1	MQ	4.6894	
5244	2		4.7503	
5650	3		4.8563	% RSD
6055	4		4.9349	2.272478
6460	5		4.9397	
6865	6		4.9383	
7270	7		4.9364	% RSD
7675	8		4.9359	0.039266

Table 3-6 – Flushing test. Raw voltage data output. RSD calculated across first 4 replicates and last 4 replicates.

The complexity of the manifold also made it very difficult to release any trapped air bubbles during tests on the bench.

3.4.2 Pump longevity

Related to the flushing time issue was the pump longevity. The high number of pump actuations needed to flush the manifold led to the fast decay of the Viton quad-rings used as seals on the syringes' plungers. An issue with the alignment of pump components resulted in the continuous rubbing of the plungers' seals against the walls of the barrels. The friction meant rapid wear of the rubber, which was then released in the chip manifold in the form of small particles. This debris contaminated the fluidic paths, and eventually blocked the chip's micro-channels.

Figure 3-15 – Picture of worn out pump's Viton quad-rings. a) Quad-ring on small syringe plunger. Plunge size: 3.30 mm x 12.4 mm (maximum stroke). b) Quad-ring on big syringe plunger. Plunger size: 9.69 mm x 12.4 mm (maximum stroke). c) Drawing of the original shape of the quad-rings.

Figure 3-15 shows two pictures of the Viton quad-rings after circa 1500 pump actuations. The wearing of the seals is very visible, as are the small particles of rubber attached to the sides of the plungers, for both the small and the large units. When compared to the original shape of the quad-rings, the damage undergone by the seals is even more evident. As a consequence of the shape loss, contamination of the fluids derived not only from the debris, but potentially also from bad sealing.

In response to this issue it was decided to limit the pump's use to 7000 actuations before maintenance. With the P1 prototype this figure would translate to about 1750 measurements.

3.4.3 Redundancy of optofluidic cell 1

The 100 mm optofluidic cell which did not receive any reagent was initially conceived and implemented in the microfluidic chip manifold under the assumption that the sample matrix could provide some contribution to the measurement of Fe(II). However, given the high selectivity of Ferrozine for Fe(II) and the use of a filter attached to the analyser's sample line the potential for a contribution from the sea water or a fresh water sample matrix was negligible. Cell 1 thus resulted in a design feature which increased the internal volume of the chip manifold and complicated the overall device set-up without any material advantage.

3.4.4 Incomplete mixing at pressure

The calibration experiments carried out at Ifremer highlighted a potential mixing problem when the sensor was exposed to high pressures.

3.4.5 Cross talk between LEDs and photodiodes

The closeness of the three opto-fluidic cells in the P1 microfluidic chip resulted in cross-talk between the LEDs and the photodiodes (TAOS) positioned at the ends of each cell. The contribution of the light emitted by each LED to the measurements of the other cells' photodiodes was calculated and taken into account when processing measurement data. However, this was considered a drawback in the microfluidic chip design.

3.4.6 Contamination from non-plastic connectors

The MINSTAC fluidic connectors used for interfacing the reagent and samples tubing to the PMMA chip contained a stainless steel component. This part was not supposed to ever get in contact with the fluid. Nonetheless this possibility could not be completely discarded, because in the case of a slight misalignment of the connector's parts a small

volume of fluid could come into contact with the steel ring, thus leading to contamination of the measurements.

3.4.7 Conclusions on use of the P1 flow-through microfluidic device

P1 was never used as a continuous-flow analyser even though it had been conceived to work in this way. A waiting time after the injection of a sample proved to be necessary for the stabilization of the output signal, making the device a stop-flow one. As such, the long mixing coil was no longer needed and different mixing options needed to be explored in order to simplify the whole system.

3.5 Summary

This chapter described the individual elements of the Fe(II) analyser Prototype 1 and how they were integrated in the system. P1 was originally thought as a flow-through device and the design choices made reflected this purpose. In particular, a long serpentine channel was chosen as the mixer for samples/standards and the Ferrozine reagent.

Two identical analysers were deployed on the Lucky Strike hydrothermal vent field as part of the MoMAR-D mission, October 2010. The deployment was unsuccessful because of issues with the pump mounted on the system. These problems were later investigated with tests on the bench and in environmental conditioning chambers.

While performing the tests, additional issues arose such as length of flushing time, wear of the pump seals, cross-talk between detectors and light sources, redundancy of the first optical cell and others. All the above in combination with the incomplete mixing at pressure indicated that a new version of the microfluidic chip was needed.

Changes in the design and the mechanical elements of the system were incorporated in device Prototype 2, which is described in details in Chapter 4.

Chapter 4
Microfluidic Analyser
Prototype 2 (P2)

Given the issues found on device Prototype 1, a simplification of the system design was thought to be the way forward. Re-thinking the manifold design led to other major changes in the device components. The pump, the number of valves, the fluidic connectors and consequently the housing were affected by the modifications of the manifold. The result of these changes was a new prototype (P2) of the system, which was optimised for the measurement of reduced iron, manganese and total iron. Its development and testing are described below.

4.1 Description of P2 microfluidic chip

In order to simplify the manifold design, the key elements of the system were revised and re-arranged into a chip of the same size (120 mm x 80 mm x 11 mm) and shape as P1.

4.1.1 Optofluidic cell

P1 had 3 optofluidic cells: one for the measurement of the background signal due to the sample matrix (Cell 1); one for high concentrations of Fe(II) (Cell 2); and one for low concentrations of Fe(II) (Cell 3) (see paragraph 3.1.1).

Cell 1 (100 mm long) was found to be redundant as the measurement it was designed to provide did not add any meaningful information to the overall analysis (paragraph 3.3.3). It was thus decided to remove Cell 1 from the manifold of the chip as a step towards a more general simplification of the design.

Cell 2 (25 mm long) was included in P1 in order to measure higher Fe(II) concentrations. However, such high concentrations were not expected in most marine systems and the calibrations of the long (100 mm) optofluidic cell (Cell 2 in P1) demonstrated the potential use of the device to up to micromolar concentrations.

These two factors, together with the aim of limiting as much as possible the internal volume of the manifold, led to the removal of Cell 2. The new P2 manifold included just one 100 mm long optofluidic cell, which received both the sample or standard and the reagent injected by the pump.

4.1.2 Diffusive mixing

As mentioned in paragraph 3.1.2, microfluidic systems operate under laminar flow regimes, where viscous forces prevail over turbulent ones and mixing happens by diffusion rather than by turbulence. In the case of a flow-through device, a prolonged contact between reagent and the analyser solutions injected in the channels is needed for mixing to happen. A long serpentine mixer (as used in P1) is a possible solution to provide a long surface of contact. However, this feature is only needed if the flow through the system is continuous. On the contrary, if a stop-flow routine is implemented, the diffusion can happen within the channels, where the reagent and analyte molecules, once in contact, will diffuse across the width of the cell. The length of the stop-flow step varies according to the chemistry, as larger molecules will take longer to diffuse (Tabeling 2010) and more viscous solutions will increase the diffusion time.

P1 was designed as a flow-through device, but could not be used as such (paragraph 3.4.7). Changes to mixing in the chip were necessary to simplify the system and limit flushing times, and thus the long serpentine mixer was removed in favour of a simpler in-cell mixing process. The rationale behind this choice was that a long enough waiting-time (stop-flow routine) with the sample and reagent solutions in contact in the cell, would allow for complete mixing by diffusion. Without the long serpentine the manifold internal volumes would be reduced and the dead volumes limited, thus decreasing flushing times.

The calculations made from the diffusion time equation (paragraph 3.1.2) did not take into account the diffusion of both the analyte and the reagent across the channel, but just that of the reagent; hence they probably overestimated the diffusion time. For this reason and because no value for the diffusivity coefficient of PAN could be found, the optimal times for the complete diffusion of the Fe(II)-FZ and Mn-PAN across the cell in P2 were estimated through mixing tests.

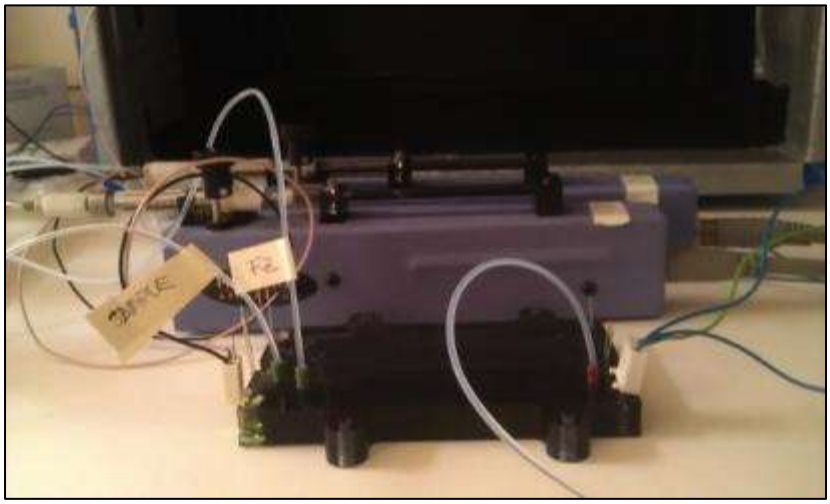

Figure 4-1- Diffusion time tests set up. For this test a new purpose built chip was used. The test-chip is shown attached to the syringe pumps for the injection of sample and reagent.

The Fe(II)-Fz diffusion time was determined through tests carried out at room temperature on a test chip whose manifold contained three 100 mm cells of different widths (400 µm, 600 µm, 700 µm) and 300 µm deep, sample and reagent inlets connected to the cells, and waste outlets (Figure 4-1). Two syringe pumps (Nanomite, Harvard Apparatus, UK) were used to push the standards and reagent through the manifold, in sequence. The overall flow rate was 940 µl/min and the pumps were stopped after 20 seconds. The 400 µm cell could not be tested because of a flaw in the manufacturing of the chip; the results of tests carried out with both 600 µm cell and 700 µm cell are shown in Figure 4-2.

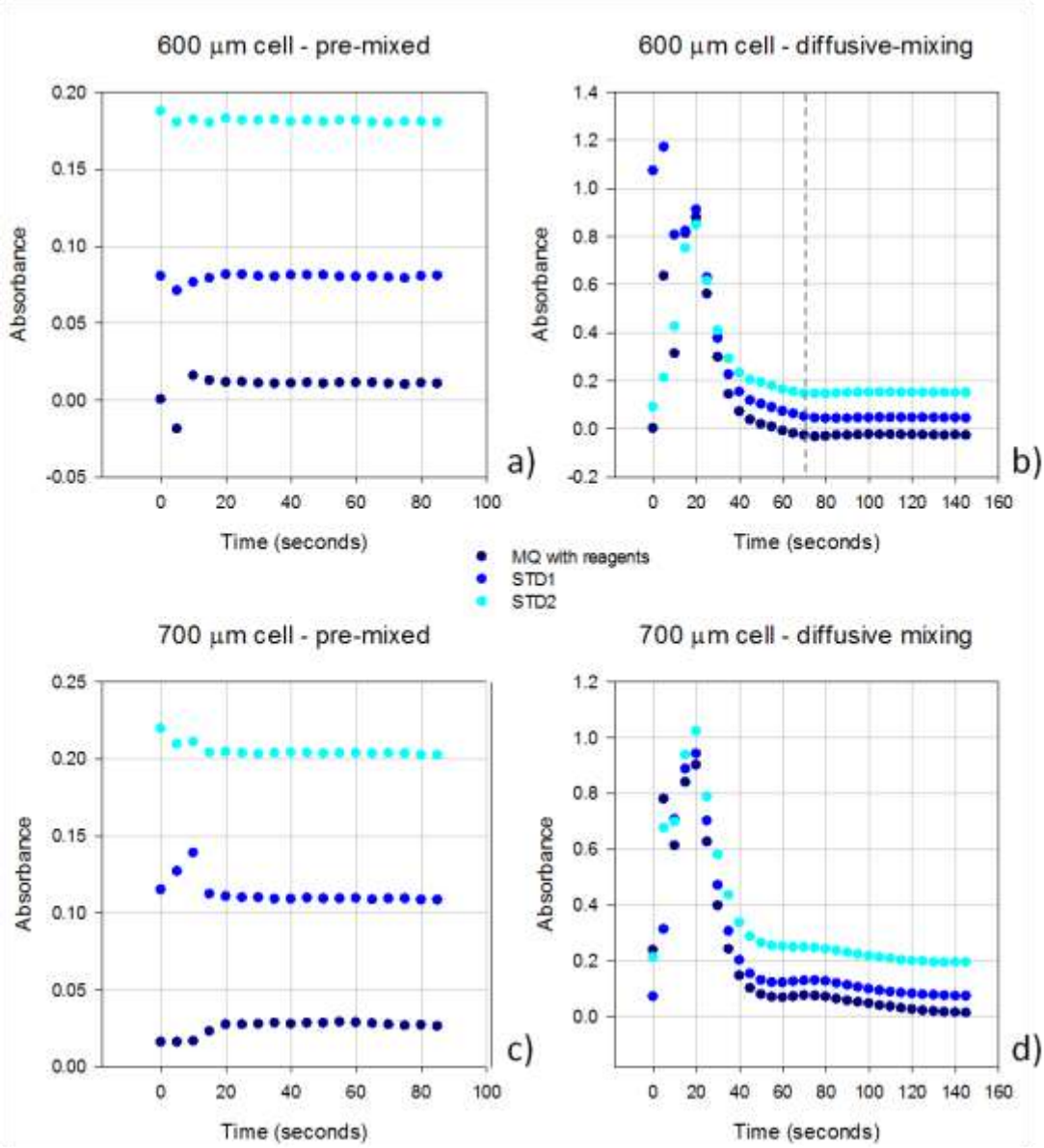

Figure 4-2 - Fe(II) and FZ diffusion time tests for mixing across a 600 µm and a 700 µm wide x 100 mm long cells under no-flow conditions. Temperature 20°C. Standards prepared in Milli-Q water matrix. The dashed grey line in plot b) indicates when the analyte and reagent solutions are fully mixed and reacted. Standards 0.5 µM, 1.0 µM.

Plots a) and c) show the absorbance of pre-mixed standards (full colour development was achieved by turbulent mixing, outside the chip manifold, before injection) measured in the 600 µm and 700 µm wide cells. These were the reference values for the diffusive mixing tests that were needed to confirm that full colour development had been achieved in the optofluidic cell. Plots b) and d) show the results of diffusive mixing tests. The first part of both plots shows noise probably caused by a combination of the fluidic movement and the pressure of the liquid against the optical window due to the fluids being injected in the cell by the pumps. Once the fluid is still, the noise disappears. In the 600 µm wide cell the

mixing and reaction is achieved after 75 s from the start of the injection: the absorbances of standards reach a plateau, confirming full mixing and thus full colour development in the cell. (The complexation reaction happens within milliseconds of the analyte and reagent molecules being in contact and thus does not contribute to the total mixing time).

The plateau was achieved when the %RDS of the following replicate measurements dropped below 3%. In the 600 μm mixing test, the %RSD of replicate measurements after 75 seconds of run was 1.33 (n = 16). This guaranteed the precision of the technique. In the 700 μm wide cell the plateau was not completely reached even after 2 minutes waiting time (stop-flow step) (%RSD = 8.69, n = 16). The absorbance signal appears to be decreasing even after it apparently started stabilizing around t = 80. No evident reason was found for this behaviour; however, it could be attributed to a range of mechanical imperfections associated with the channel (e.g. pressure loss due to poor gluing, imperfect LED functioning). These issues were not investigated further because of time constrains and because of the satisfactory results obtained from the narrower cell.

Hence the 600 μm cell was chosen to be included in the new chip design. The stop-flow step for the Fe(II)-Fz colour development was set to 3 minutes (180 s), to ensure all colour had developed.

Similar tests were carried out to assess the diffusive mixing time of Mn and PAN. Figure 4-3 shows the result of on-line mixing tests performed in a 600 μm wide cell. Unlike the data in Figure 4-2, the plot does not show any noise due to fluidic movement, because the tests were performed directly on the new Prototype 2 chip, whose elements limited any disturbance to the output signal. The diffusion time is 480 s (time after which the signal reaches a plateau). As expected, the mixing time is much longer for the Mn-PAN than for Fe(II)-Fz; this is due to the higher viscosity of the PAN reagent after the addition of the surfactant Triton-X100 (see paragraph 2.1.3.1). In the case of the Mn determination, the stop-flow step was set to 10 minutes (600 seconds) to ensure full colour development.

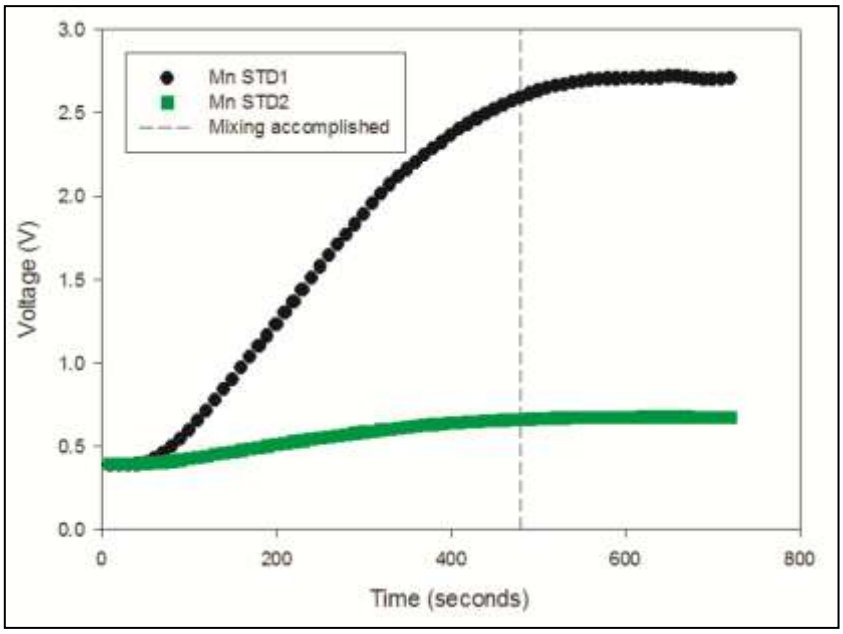

Figure 4-3 – Mn and PAN diffusion time test for mixing across a 600 µm wide x 100 mm long cells under no-flow conditions. Temperature 20°C. Standards prepared in Milli-Q water matrix. The dashed line indicates when the analyte and reagent solutions are fully mixed and reacted. Mn standards 4.55 µM, 9.1 µM. Test was performed directly on Prototype 2. The voltage output of the sensor with time is shown.

The results of the diffusive mixing tests confirmed that complete colour formation could be achieved in the optofluidic cell, provided a stop-flow step was integrated in the measurement routine. This new approach to mixing was the main feature of the Prototype 2 design. All further modifications were made to adapt the system's mechanical elements to the diffusive mixing step.

4.1.3 P2 Manifold

The removal of the serpentine mixer freed space on the microfluidic chip footprint, whose overall size was kept the same as in P1. The positions of the fluidic connectors and of the valves for fluid control were rearranged in order to limit even more the internal volume of the manifold and reduce dead volumes to a minimum. After the rearrangement, the new layout of the channels was compact enough to allow for a second, identical manifold to fit into the chip footprint. The two manifolds were totally independent from each other and were conceived to permit two simultaneous determinations of either the same, or two different analytes.

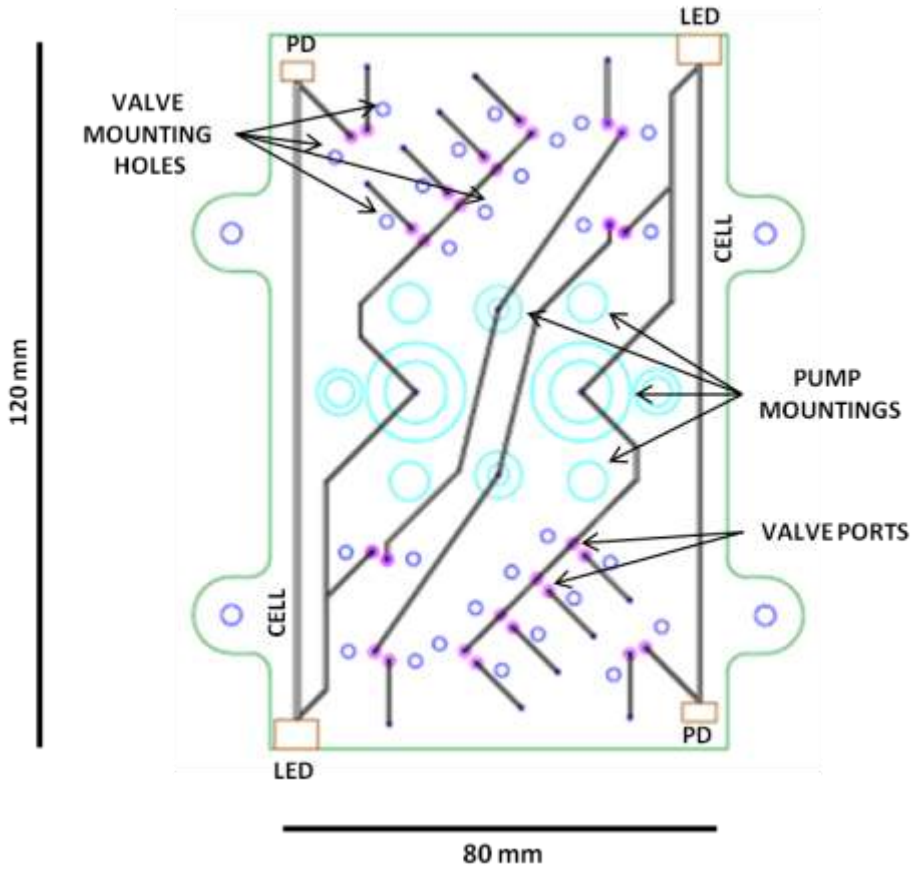

Figure 4-4 - CAD drawing of the microfluidic chip showing external shape (green), location of LEDs (large orange rectangles), photodiodes (small orange rectangles), recesses for pump mountings (turquoise), microfluidic channels (black), valve ports (pink), and mounting holes (indigo).

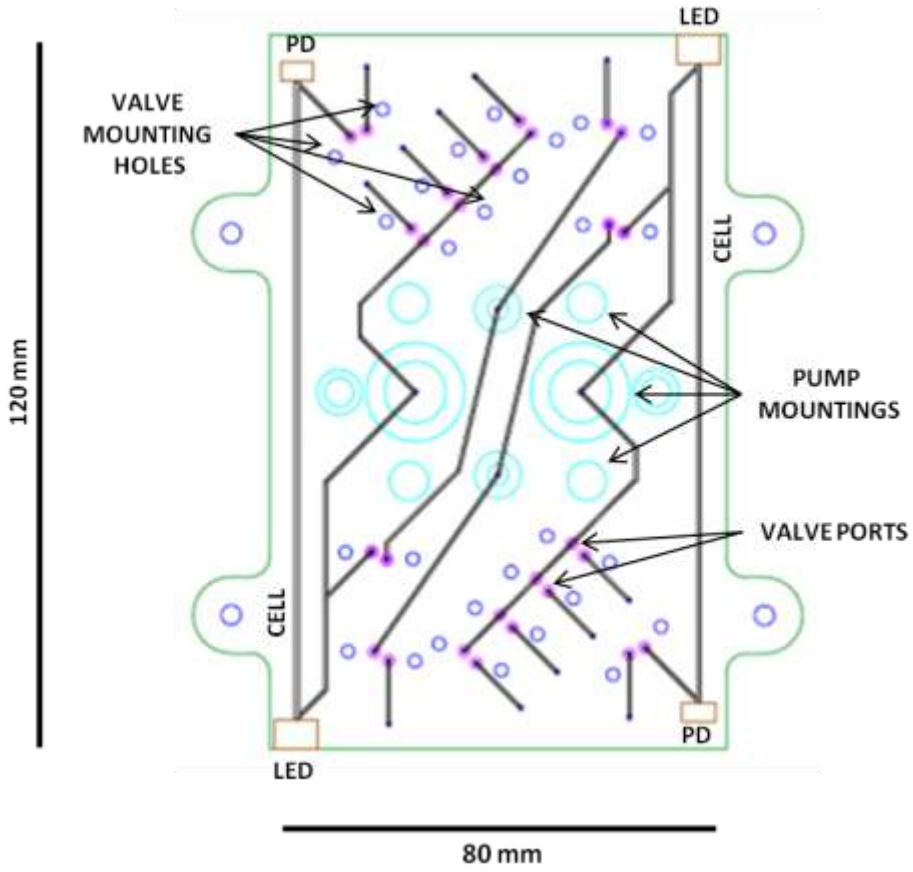

Figure 4-4 shows the CAD schematics of the P2 chip. The single manifold was mirrored along the diagonal of the chip. Each side of the chip included 4 connectors for fluidic inlets plus one for the waste output; 7 valves for fluidic control; one LED and one photodiode recessed at the extremes of a 100 mm opto-fluidic cell. The microchannels were 400 µm wide while the opto-fluidic cells were 600 µm wide x 100 mm long; all channels were micro-milled to a depth of 300 µm. These values limited the internal volume of the manifold to a total of 50 µL, against the internal volume of 190 µL of P1, thus leading to low reagent and sample consumption.

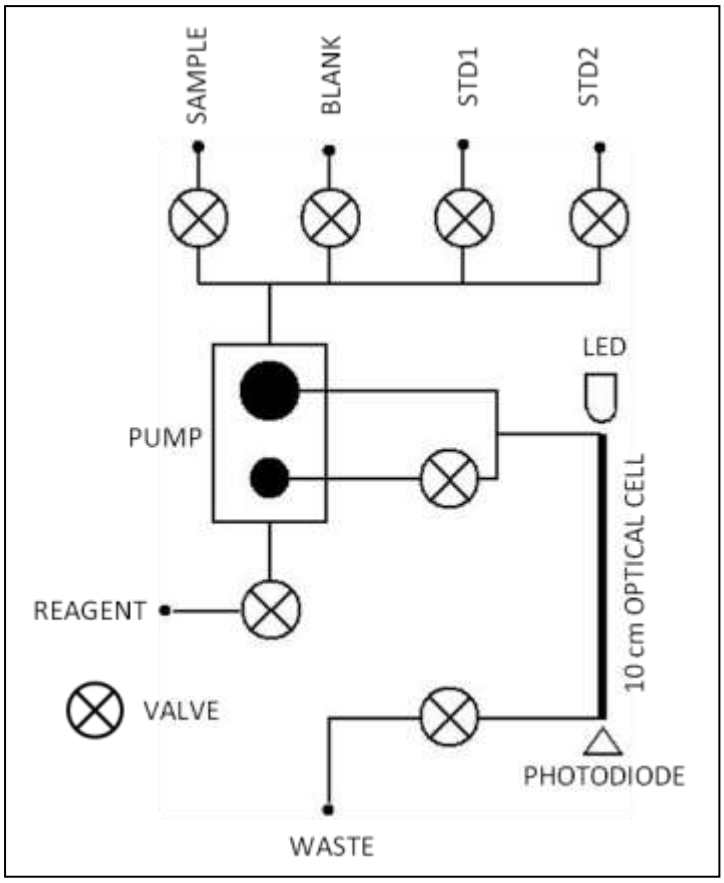

Figure 4-5 - Single manifold schematics.

The single manifold is detailed in the schematics in Figure 4-5. A first set of valves connected to the fluidic inlets allowed to choose between sample and standards.

The fluid is then withdrawn by the pump (see paragraph 4.2) together with the reagent. To obtain a procedural blank, during the injection stage the reagent is sent back to the reservoir, while the sample is contemporarily sent to the measuring cell. This allows the system to take a 100% transition measurement (no absorbing species in solution), which in the data processing stage is used to calculate the sample absorbances according to the equation presented in paragraph 2.1.1: $T = \frac{I}{I_0}$. Enabling the injection of both sample/standard and reagent into the opto-fluidic cell, allowed full measurement. A valve positioned after the opto-fluidic cell permitted the control of the fluid output. As in P1, standards, reagents and the waste were stored in gas-tight nutrition bags connected to the chip by PTFE tubing.

4.2 Prototype 2 Mechanical Elements

4.2.1 Pump configuration

The changes made to the microfluidic chip led to a modification of the pump. In P2 the elements of the pump had to be doubled to reflect the chip manifold. The pump materials, its footprint, the way it was connected to the PMMA chip body and the volumes of the plungers were not modified from what is described in paragraph 3.1.4, while the number of the plungers and cylinders had to be increased. A modification to the original sliding plate allowed it to drive 2 small plungers connected to the reagents inlets and 2 large plungers connected to the samples/standards inlets. This implied that the exact same operation (withdrawal or injection of fluid) was performed on both sides of the microfluidic chip at any given time. Figure 4-6 shows a front view of the new version of the syringe pump.

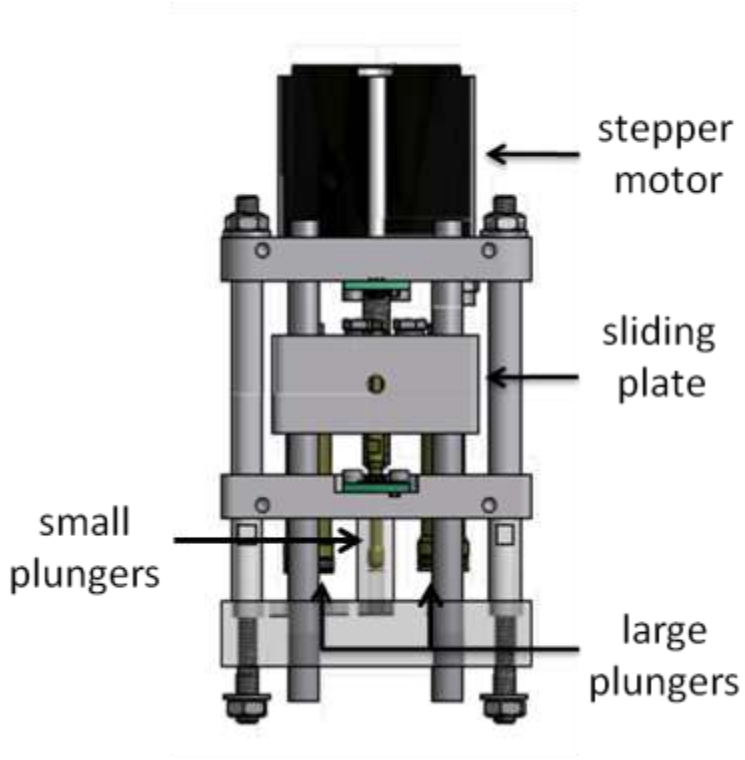

Figure 4-6 - CAD drawing of the second version of the custom-made syringe pump. Front view. The two large plungers are clearly shown, while the second small plunger is hidden behind the first one. Idea and drawings by Dr. Ed Waugh, Sensors Group, NOC, Southampton.

4.2.2 Fluidic connectors

The MINSTAC fluidic connectors were modified in order to avoid the potential contamination deriving from the fluid getting in contact with the stainless steel

compressor ring (see paragraph 3.4.6). The ring and the plastic nipple were removed and a flange was created at the end of each PTFE tubing, which acted as a gasket and sealed the interface between the PMMA chip body and the plastic nut of the fluidic connector (Figure 4-7).

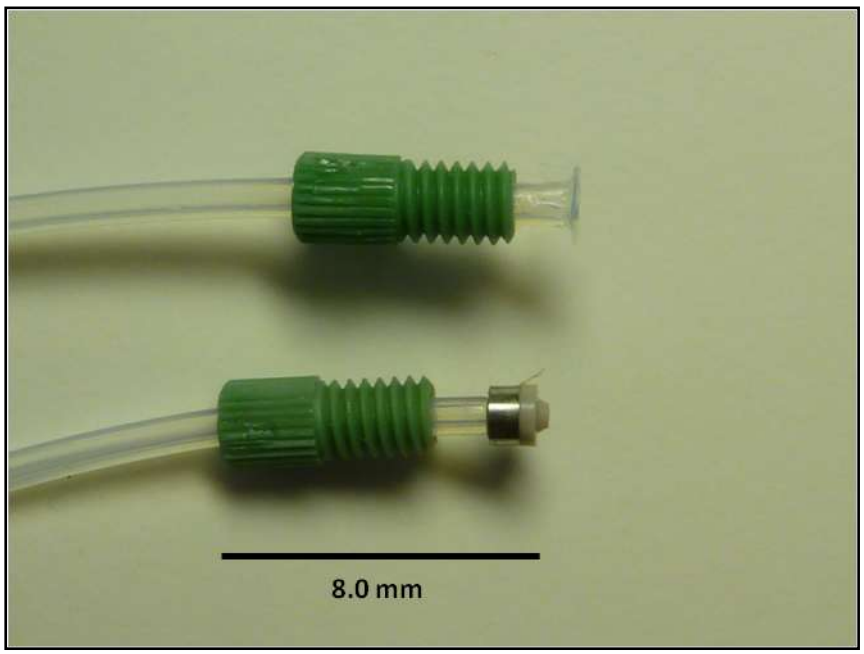

Figure 4-7 – Top: microfluidic connector with flanged tubing edge as gasket (used on P2). Bottom: microfluidic connector with stainless steel compressor ring and plastic nipple (used on P1). The green plastic nut sit against the flange or the ring.

4.2.3 LEDs

The alignment of the optical elements (LEDs and photodiodes) (paragraph 2.3.4) in P1 often proved to be a long process and did not always give the full saturation of the photodiodes. Although this was not a major issue, a small modification of the LEDs in P2 helped to minimise the problem: the dome shaped ends of the LEDs were cut off in order to create a flat surface. This flat surface was then polished and put in direct contact with the optical window at one extreme of the chip's opto-fluidic cell. The result was a much faster alignment process and an overall higher signal output (saturation of photodiodes with 5 V outputs, over a previous average output of 4.5 V) .

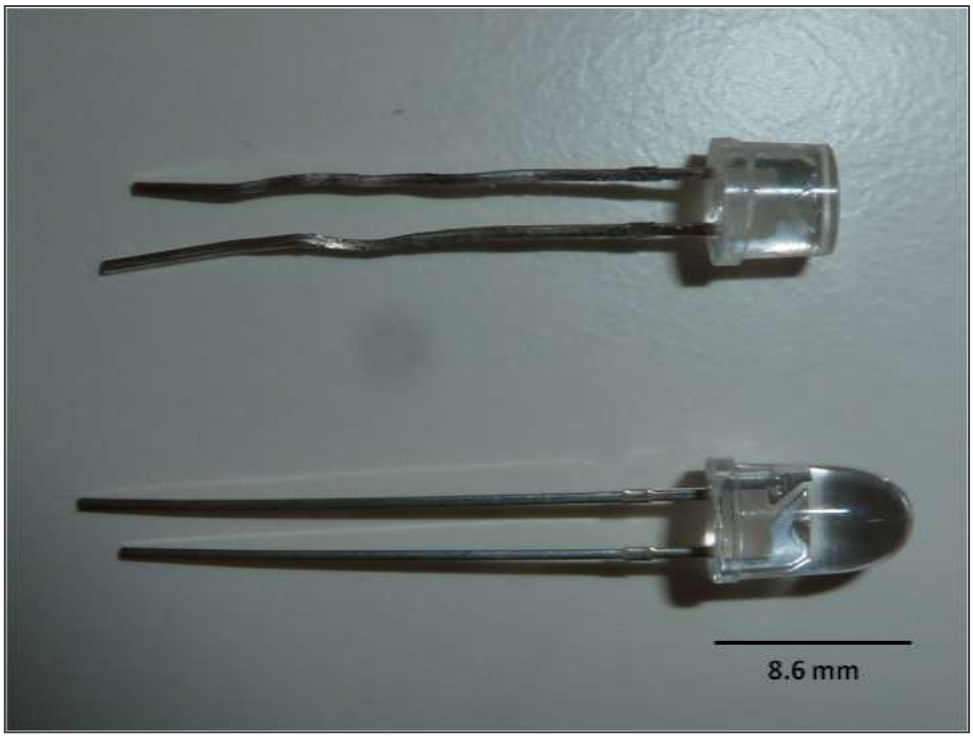

Figure 4-8 – A flattened LED and a dome shaped one. The flat surface allowed more light to reach the photodiode at the other extreme of the optical cell than the curved surface.

4.2.4 Housing

Since the overall size of the P2 fully integrated device was not different from that of P1, a housing similar in shape and size was chosen, but several improvements were made. To increase robustness, anodised aluminium was used for the housing body and end-caps instead of clear PMMA and Delrin. The length of the housing body was increased to accommodate a portable lithium ion battery (Lipo 11.1 V 10 Ah, #31207-01, Tenergy Corporation, USA) during deployments. Finally, the number of connectors on the top end-cap was increased from 6 to 12 to account for the double manifold of P2. A similar titanium frame as the one used on P1 was connected to the sides of the housing to support the fluids storage bags.

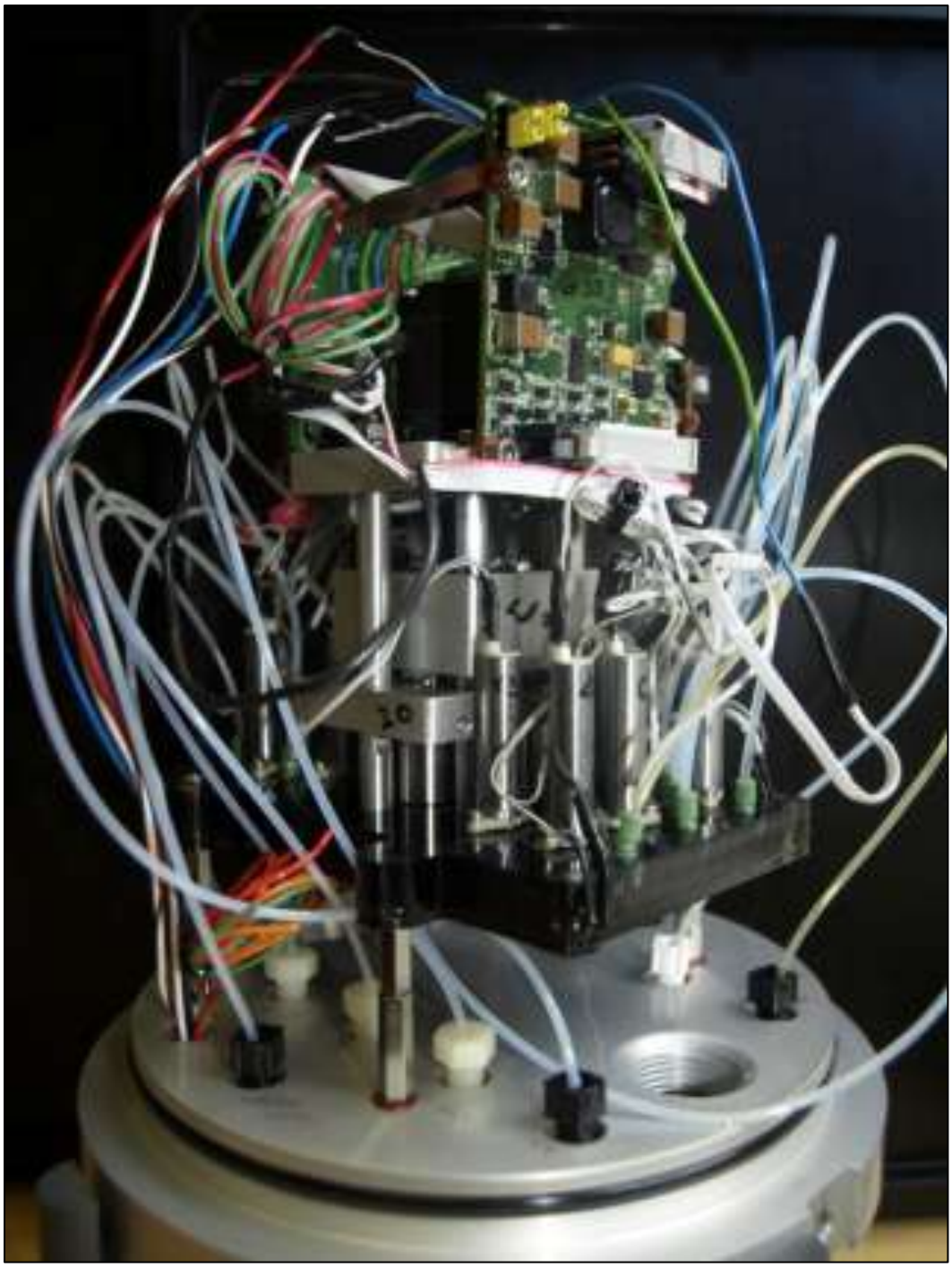

Figure 4-9 – PMMA microfluidic chip P2 with fluidic connectors, LEDs, photodiodes, valves, syringe pump, electronics boards and tubing, mounted on anodised aluminium housing end-cap, before being put into the cylindrical housing.

4.3 Tests of the integrated P2 system

P2's dual manifold allowed for the device to be used simultaneously as a dissolved Fe(II) and Mn analyser. The tests performed on it were therefore carried out for both the Fe(II)-Fz and Mn-PAN determination methods.

4.3.1 Flushing

To confirm the overcoming of the flushing and carry-over issue observed in P1, different flushing routines were tested on P2. The ASM (see paragraph 3.1.3) was programmed to withdraw a blank and a high concentration standard (1 µM for Fe(II) and 4 µM for Mn) in repetition. In between these operations an increasing number of 30 µL flushes (almost twice the volume of the optofluidic cell (18 µL)) were implemented to assess the minimum number of rinses needed to completely clear the channels. Figure 4-10 and Table 4-1 present the results obtained for Fe(II). After 5 x 30 µL flushes the carry over in the system was eliminated and the signal for MQ came back to the expected value (reference MQ measurement at time = 438 s). This figure was chosen for later deployments.

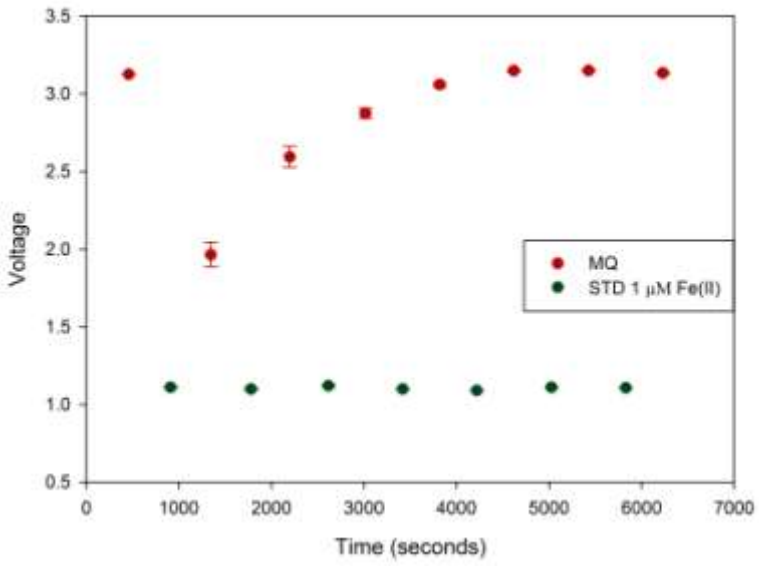

Figure 4-10 - Flushing test. Every point averages 50 measurements of MQ and 1 µM Fe(II) standard. Errorbars on graph.

	average of 50	stdev of 50	time
MQ	**3.1256**	0.0004	438
STD 1 uM	1.1102	0.0035	909
MQ x 1	1.9648	0.0794	1345
STD 1uM	1.0988	0.0053	1779
MQ x 2	2.5938	0.0680	2197
STD 1 uM	1.1199	0.0065	2615
MQ x 3	2.8746	0.0329	3015
STD 1uM	1.0993	0.0019	3417
MQ x 4	3.0589	0.0147	3818
STD 1 uM	1.0893	0.0013	4220
MQ x 5	**3.1489**	0.0057	4620
STD 1uM	1.1103	0.0012	5026
MQ x 6	**3.1499**	0.0036	5427
STD 1uM	1.1069	0.0017	5830
MQ x 7	**3.1335**	0.0049	6230

Table 4-1– Flushing test. Raw voltage data reported on Figure 4-10.

4.3.2 Power consumption

The average power consumption of the analyser during measurements was assessed, and found to be below 3.8 Watts, while its peak consumption never exceeded 6 Watts.

4.3.3 Bench-top calibrations for Fe(II) and Mn

Calibrations of the instrument were initially performed in the laboratory using Fe(II) standards and Mn atomic absorption standards diluted from fresh stock solutions with Milli-Q water as described in paragraphs 2.1.2.2 and 2.1.3.2. The resulting curves were compared to those obtained with a HITACHI-2800 dual beam spectrophotometer. Figure 4-11 shows the response of the sensor to different concentrations of Fe(II) (0, 250, 500, 1000, 2000 nM) and Mn (0, 2.28, 4.55, 6 µM). For each point different replicate samples were measured (in particular: n = 3 for Fe(II) calibration, n = 6 for Mn calibration). Milli-Q water was introduced into the measurement cell with no reagents at the beginning of each calibration to give a 100% transmission signal, against which all other blank, standard and sample transmissions were compared. The bench top data were collected using a 10 cm path length glass cell for Fe(II) and a 2 cm length glass cell for Mn. Both bench and microfluidic systems had linear responses. However, the sensitivity (slope) was lower than expected from theory. It is most likely that this reflects the peak wavelength output of the LEDs not coinciding with the maximum absorbance wavelength for the Fe(II)-Fz and Mn-PAN complexes. Thus this calibration did not yield the theoretical molar absorption coefficients (ε) of 27900 $l.mol^{-1}.cm^{-1}$ for Fe(II)-Fz and of 44000 $l.mol^{-1}.cm^{-1}$ for Mn-PAN.

Nonetheless, the calibrations demonstrated the ability of the microfluidic system to provide high sensitivity and to be effectively calibrated.

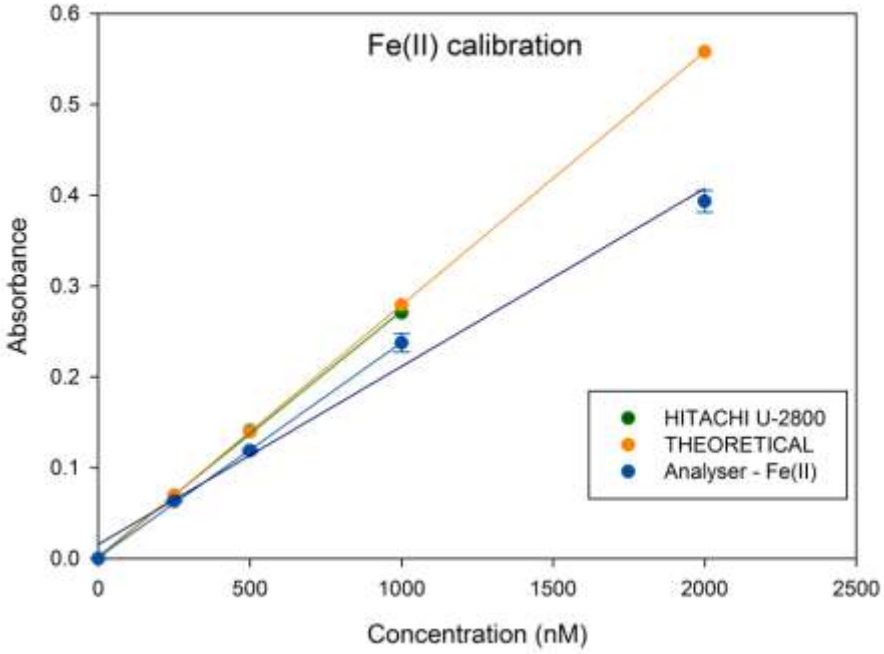

a)

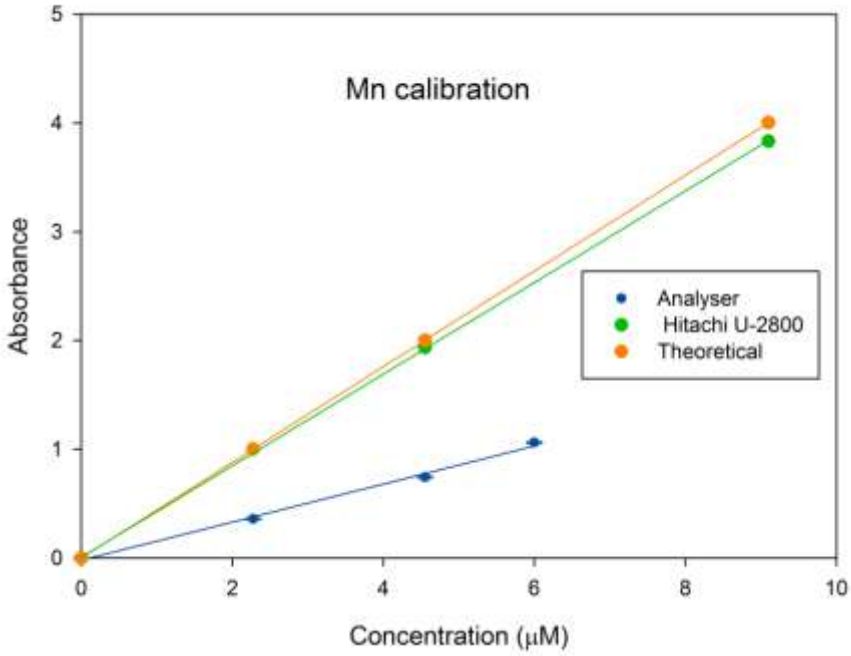

b)

Figure 4-11 – Analyser calibrations curves compared to calibrations obtained with a HITACHI U-2800 spectrometer and to the theoretical values. Error bars are within the symbol used for the analyte. a) Fe(II) calibration curve. b) Mn calibration curve. Laboratory absorption values were collected with a 2 cm cell; data in the graph were multiplied by 5 to make them comparable to the 10 cm cell values of the microfluidic analyser.

4.3.4 Limits of detection

The limits of detection (LOD) of the analyser were calculated as 3 times the standard deviation of the blank, with n = 3. For Fe(II) the LOD was 27 nM and for Mn it was 28.4 nM. The calibrations for Fe(II) and Mn were linear up to 2 and 6 μM respectively as shown in Figure 4-11. Closer to 2000 nM the calibration curve for Fe(II) started to bend. We did not investigate the behaviour of the analyser above such value of concentration as the range of linearity achieved was already satisfactory for the purpose of our work. For the same reason we did not test the analyser for concentrations of Mn above 6 μM.

4.3.5 Accuracy

Because of the instability of dissolved Fe(II) in oxic environments there are no specific Certified Reference Materials (CRMs) to check the accuracy of an independent measurement of this parameter. Therefore the accuracy of the Fe(II) measurements taken with P2 was assessed against freshly made and stabilised standards measured on bench-top analysers.

Accuracy for the Mn method was assessed against CASS-5 CRM (47.7 ± 3.6 nM) and was found to be 48.2 ± 12.6 nM, with n = 19. Although good accuracy was achieved in this test, the reason of its poor precision could be attributed to not else but a few small bubbles having entered the system during the analysis, thus creating noise in the signal. Later precision tests with prepared standards attained much better results: precision for a 1μM standard was found to be 2.4 %, with n = 19.

4.3.6 Bench-top calibration for P1 used as a total iron analyser

The double manifold of P2 potentially extended its use as a simultaneous total Fe and Fe(II) analyser. By adding a reduction step, while maintaining the same measurement routine, P2 could provide information on dissolved Fe redox speciation in the water sample. Ascorbic acid solution was prepared as described in paragraph 2.1.2.3 and added to the Ferrozine reagent (50:50) in the reagents reservoir. Once set up for total Fe analysis, the analyser would withdraw Ferrozine and ascorbic acid –together- from the reagent reservoir and inject them into the optofluidic channel, where -once in contact with the sample- the reduction step would take place.

Total Fe calibration tests on the bench were performed with the aim of achieving results similar to those obtained for Fe(II) calibrations. A double, simultaneous calibration with total Fe and Fe(II) standards was performed and compared to the absorbances measured by a Shimadzu UV-mini 1240 bench top spectrometer used with a 10 cm path-length cell.

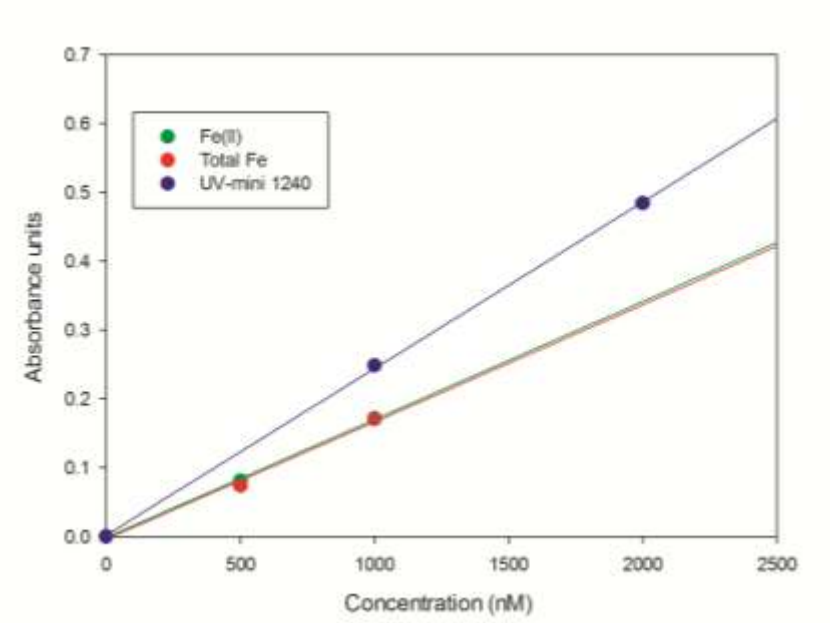

Figure 4-12 – Fe(II) and Total Fe calibration curves compared to calibrations obtained with a Shimadzu UV-Mini 1240 Spectrometer. Fe(II) standards: 0 nM, 500 nM, 1000 nM, for the analyser; 0 nM, 1000 nM, 2000 nM, for the bench top spectrometer.

The calibration curve showed good linearity and the matching values of the Fe(II) and total Fe standards lines confirmed that the reduction step added to the measurement routine was successful in reducing all Fe(III) in the prepared standards to Fe(II). The lower values than the ones obtained with the bench-top spectrometer are explained in paragraph 4.3.3. The limit of detection for the Total Fe analysis, calculated as described in paragraph 4.3.3, was found to be 130 nM.

4.4 Summary

This chapter presented the modifications made to device Prototype 1 in order to improve its reliability as a dissolved Fe(II) analyser and to increase its robustness.

The modifications mainly originated from a change in the basic concept upon which P1 was based: while P1 was designed to be a continuous flow analyser, P2 was re-designed in order to be a stop-flow measuring system. This conceptual difference led to a change in the mixing requirements of the device, and an in-cell diffusive -mixing method was applied to P2. The significant reduction in complexity of the technology was accompanied with the removal of 2 of the 3 opto-fluidic cells present in P1 chip, and the removal of the long serpentine mixer. Reducing the microfluidic channels allowed the design to be a more compact chip manifold which, once fitted into the same footprint of P1, left enough free

space to add a second manifold, identical to the first one. The double manifold allowed the simultaneous analysis of up to two analytes and was tested for Fe(II), Mn and finally total Fe analysis.

The range of improvements led to an increase of the signal output and reduced the contamination potential.

Calibration curves were obtained on the bench for Fe(II), Mn and total Fe, with good linearity and LODs favourable to a wide range of environmental applications. Accuracy tests were successfully run for Mn against CRM.

The validity of Prototype 2 was demonstrated on the bench, and it was considered ready to be applied in natural waters. Chapter 5 describes the application of the analyser to marine and fresh water environments.

Chapter 5

Environmental applications

The results of the tests performed on P2 in the laboratory (see chapter 4) characterized the performance of the device when used as an Fe(II), Mn and total Fe analyser. This confirmed it was suitable for making measurements in the ranges of concentrations expected in particular field deployments. Two deployments were thus planned to test the applicability of P2 to natural environments: one in the Baltic Sea, and a second one in the River Beaulieu, UK.

This chapter is based on two manuscripts in preparation: *First colorimetric LOC device, applied to Fe(II) and Mn determination at depth*, Milani A., Statham P.J., Connelly D., Mowlem M. – PLOS one; and *The behavior and speciation of Fe(II) in a high DOM river and estuarine system*. Hopwood M. J., Milani A., Statham P.J. – Estuarine and Coastal Shelf Science.

5.1 Baltic Sea deployment

The analyser was taken to sea during the Elisabeth Mann-Borgese cruise (06EZ1215) in August 2012 on the Baltic Sea, in collaboration with the Leibniz Institute for Baltic Sea Research (IOW, Warnemünde, Germany).

5.1.1 Baltic Sea

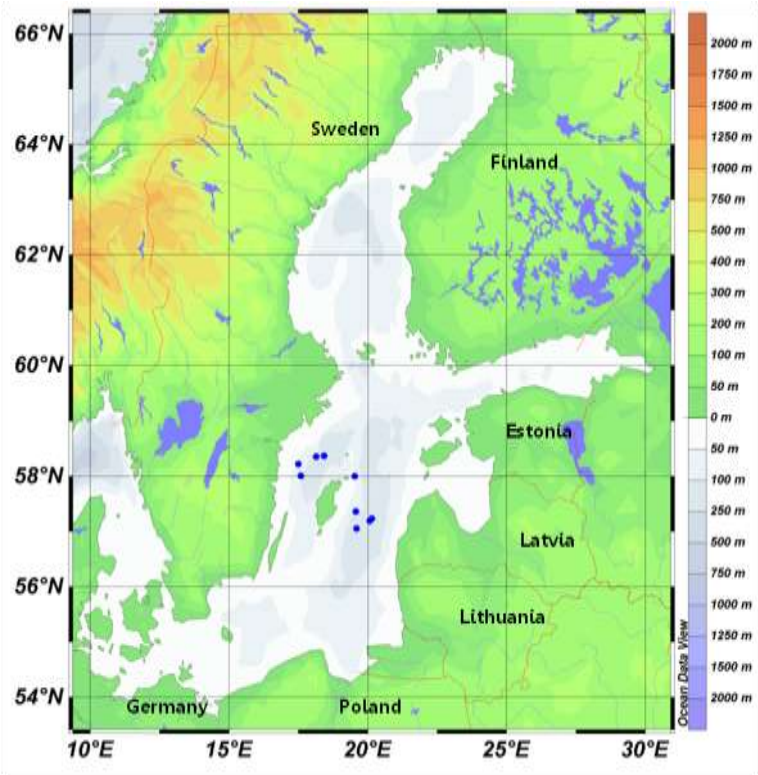

Figure 5-1 - Baltic Sea map with indicated CTD profile stations.

The Baltic Sea is the second-largest brackish water system in the world: it has a mean depth of 52 m (max. 460 m), an area of ~ 413 000 km2 and a volume of ~ 22 000 km3 (Feistel et al. 2008). The Baltic Sea consists of several deep basins (Arkona Basin, Bornholm Basin, Eastern and Western Gotland Basin, Gulf of Finland, Gulf of Bothnia, Bothnian Bay) which are separated by shallow sills (e.g., Drodgen Sill and Darss Sill). These sills restrict the propagation of saline North Sea waters at depth, and also restrict deep-water exchange between the basins. The largest basin (Gotland Basin) in particular is thus naturally prone to permanent haline stratification, long residence times, and oxygen deficiency in the deeper water layers. In the basins of the Baltic Sea, hypoxia has been occurring repeatedly for natural reasons ever since the Baltic Sea was formed at about 8000 yr BP. Such natural hypoxia occurred during several periods in the Holocene, including the medieval warm period (Leipe et al. 2008), but anthropogenic eutrophication has increased the spatial extent and intensity of oxygen depletion (Conley et al. 2009b). This situation is exacerbated by the large drainage basin of the Baltic and by its anthropogenic nutrient surplus (Feistel et al., 2008). The Baltic Sea is surrounded by industrialized countries with intensive agricultural activity and, with a catchment area of

> 1 700 000 km^2, experiences significant freshwater runoff over the entire basin. The Baltic Sea is thus affected by both natural and anthropogenic drivers and pressures, and is very sensitive to eutrophication (HELCOM 2009). Nutrient concentrations peaked during the 1980s and have since declined as a result of the success of efforts to reduce nutrient loading from the land. However, only 13 areas (2 open basins and 11 coastal sites) in the Baltic Sea are classified as "areas not affected by eutrophication", whereas 176 areas (15 open basins and 161 coastal sites) remain "areas affected by eutrophication" (HELCOM, 2009). Nutrient input from the sediments is also a serious problem and more significant than terrestrial inputs to the Gulf of Finland (Pitkanen et al. 2001) and the Baltic proper (Viktorsson et al. 2013). In addition, projected climatic changes, which are stronger for the Baltic Sea than the global average (BACC 2008), will affect both the freshwater balance and the seasonal extent of ice cover in the northern part of the Baltic.

Bottom waters in the central part of the Gotland Basin have been hypoxic or anoxic for more than half of the past 50 yr. Since the late 1970s, the frequency of major inflow events of oxygenated saline water from the North Sea has declined, with only two short ventilation episodes occurring, in 1993 and 2003. Yet, the resupply of saline water leads to a stabilization of the permanent stratification and slight uplift of the halocline, which results in an extension of the area exposed to hypoxic conditions (Conley et al., 2009). Some of the shallower, yet mostly stratified basins of the Baltic Sea (i.e., the Bornholm and Arkona Basins) experience hypoxic or anoxic conditions on shorter time-scales with a clear seasonality (Feistel et al., 2008). The Baltic Sea thus provides an ideal natural laboratory to study the impact of intermittent oxygen deficiency on different time-scales.

Strong stratification of the deep Baltic Sea water column results in the formation of a pelagic redoxcline – a transition zone with strong vertical redox gradients. Similar situations are observed in the Black Sea and in other stratified marine systems (e.g., in many fjords). Oxygen and other major electron acceptors (e.g., nitrate) that are abundant in the upper water layer oxidize reduced species (e.g., sulfide and reduced metal species) that accumulate in deeper waters. Consequently, pelagic redoxclines are prime locations of biogeochemical redox transformations that depend on the vertical transport of reduced and oxidized species across this layer.

[From: Friedrich et al. (2013)]

These peculiar redox conditions make the Gotland Deep and the Landsort Deep Basins ideal environments for testing a fast profiling Fe and Mn detection device such as P2 (Dellwig et al. 2010, Kremling 1983, Pohl and Hennings 2005b, Schnetger and Dellwig

2012). The expected high concentrations of reduced Fe and Mn should facilitate the testing of the device in order to demonstrate its ability to provide valuable data for metals biogeochemistry studies.

5.1.2 Objectives of the cruise

The main objective of the cruise was to test the reliability of the analyser in a marine system with substantial gradients in concentrations of dissolved Fe(II) and Mn. It was planned to deploy one P2 device attached to a CTD-carousel to obtain in-situ water column profiles of Fe(II) and Mn, whilst a second P2 would collect data on the same profiles from water pumped directly on board of the ship by a pump mounted on the CTD frame (more details on the pump-CTD in paragraph 5.1.4). This double measurement would give the opportunity to observe if any difference in measurements would occur due to pressure and temperature differences.

A secondary target was to use the device as a total Fe analyser and possibly combine the results from the Fe(II) and total Fe analysis to study the speciation of Fe in the water column.

Finally, a similar device for the in-situ measurement of Fe(II) and Mn in use at IOW (Meyer et al. 2012) was on board of the ship and it was planned to be deployed next to P2 on the CTD carousel. The inter-comparison of the results obtained with the two devices would have provided information on the accuracy of both analysers.

5.1.3 Cruise plan

The EMB ship set sails from Rostock, Germany, on the 20th of August 2012. She circled the Swedish Island of Gotland anticlockwise stopping in 10 stations for CTD water column profiles and sediment core sampling (Figure 5-2). The stations were distributed along the major basins of the Baltic Proper (see Table 5-1 for exact location). The cruise ended on the 6th of September 2012, when the ship returned to Rostock.

Figure 5-2 – EMB cruise route. August-September 2012.

Position	Station	GPS location	Date
Gotland Deep	Redox_01	57° 05’ 01’’ - 19° 59’ 50’’	23.08.12
	Redox_02	57° 19’ 04’’ - 20° 07’ 01’’	24.08.12
	Redox_03	57° 23’ 26’’ - 20° 15’ 34’’	27.08.12
	Redox_04	57° 35’ 98’’ - 19° 56’ 79’’	27.08.12
Farö Deep	Redox_05	58° 00’ 16’’ - 19° 53’ 00’’	28.08.12
	Redox_06	58° 00’ 02’’ - 19° 53’ 53’’	29.09.12
Landsort Deep	Redox_07	58° 36’ 51’’ - 18° 42’ 81’’	30.08.12
	Redox_08	58° 35’ 02’’ - 18° 14’ 17’’	31.08.12
	Redox_09	58° 21’ 88’’ - 17° 49’ 91’’	01.09.12
Norköping Deep	Redox_10	58° 00’ 77’’ - 17° 58’ 46’’	03.09.12

Table 5-1 – Summary of deployment stations during EMB cruise to the Baltic Proper, August-September 2012.

5.1.4 Deployment set up

On board of the EMB, the analyser was attached to the CTD frame of the IOW Pump-CTD system (Strady et al. 2008) (Figure 5-3). P2 was secured to the CTD frame with quick release cable ties and snap-hooks, which allowed for fast assembly and disassembly of the system. Each deployment needed only a 10 minutes preparation on the deck.

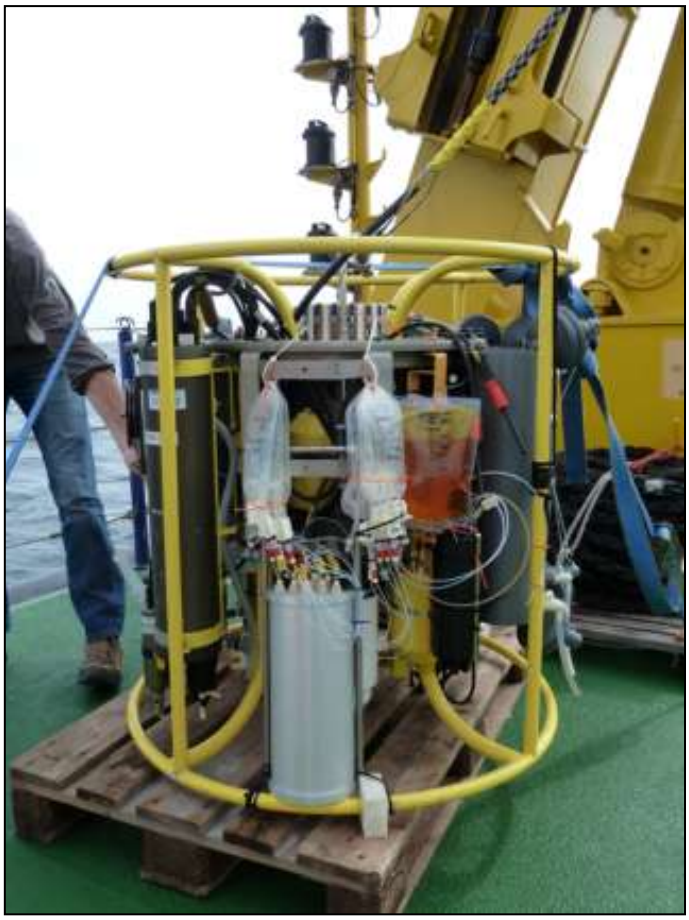

Figure 5-3 -Analyser attached to the IOW-Pump-CTD

The inlets of the two independent manifolds, with attached Millex 0.45 µm filters (see paragraph 2.2.2), were placed adjacent to each other to collect samples from the same water body.

A data system was fitted that allowed direct communication with the Fe/Mn analyser in real time via an RS232 port. It permitted the initiation of measurement cycles when the system was at a suitable depth and streamed live the data recorded to an on-board receiving station. The data were also logged on the SD card on board of the analyser and were later downloaded to a laptop for data processing.

Once in the water, the CTD carousel stopped at pre-planned depths that were decided daily after looking at the oxygen, turbidity, temperature and salinity profiles collected at each deployment site. These parameters gave information about the position of the redoxcline in the water column. They thus permitted the identification of the most interesting depths for dissolved Fe and Mn analysis and for methane and nutrient analysis performed by other scientists on-board. The sampling depths typically corresponded to several in the upper water column (where the expected concentrations of Fe and Mn were

low), several measuring depths immediately around the redoxcline (to follow the change in the analytes concentration due to redox processes), and several stations closer to the sea floor in order to record any concentration change due to sediment re-suspension.

As these tests were primarily carried out to demonstrate the robustness of the analyser in-situ, and given the nature of the deployment, the longevity of the reagents was not a major concern. Hence new standards and reagents for Fe(II) and Mn detection were prepared on a daily basis in the ship laboratory. Seawater Fe(II) and Mn concentrations were calculated from the measured absorbances by comparison with the known standard concentrations. Three point calibrations were performed at depth. The analyser ASM (paragraph 3.1.3) was set up to perform one measurement of seawater, followed by a measurement with just Milli-Q water (the 100% transmission value - see paragraph 4.3.3), at each sampling depth through the water column.

The IOW Pump-CTD accommodated a Rosette with 9 Niskin bottles Teflon coated for clean water sampling at depth. These were fired at the planned stations along the water column to collect samples that were later manually analysed on-board (paragraph 2.2.2).

The Pump-CTD also had a 350 m nylon hose, which continuously pumped water from depth directly to the ship laboratory (Strady et al. 2008). Although we had planned to use this water supply to provide samples for a second P2 device placed in the ship laboratory, a problem with the electronics of the analyser forced us to set aside this opportunity and focus on the in-situ measuring P2 device.

For the same reason we decided not to investigate Total Fe, but to concentrate our efforts towards the demonstration of the validity of the analyser as an Fe(II) and Mn detector.

The IOW dissolved Fe(II) and Mn analyser (Meyer et al. 2012) in this occasion was set up to perform just Mn measurements. It was placed on the Pump-CTD carousel next to P2 and sample inlets of the two devices were collocated as close as possible to one another. Unfortunately a problem with the pumping system in the IOW analyser prevented it from collecting reliable data, thus no comparison with P2 was possible.

5.1.5 Results

Over 16 days in the Baltic Proper, ten deployments of the analyser attached to the IOW-Pump-CTD system were done. To check the accuracy of the analyser, at most stations water sampling bottles were fired at depths corresponding to the in-situ measurements. The water samples were then analysed on-board as described in paragraph 2.2.2.

Several trial deployments were made to confirm the robustness of the mechanical components of the P2 device and the effectiveness of the ASM sampling routine. The pressure compensated housing showed no leaking and the stop-flow step of 10 minutes was long enough for the PAN-Mn diffusion across the cell even at depth.

Figure 5-4 shows some of the CTD profiles obtained during the cruise. They were used to assess the readiness of the analyser to be deployed on the CTD carousel (Figure 5-4 a and b) and to confirm the length of the waiting state for the Mn diffusion across the channel. Most of the test profiles failed to deliver reliable water column data because of the high blanks values, which did not allow to attain a proper calibration (hence some of the plots in Figure 5-4 show just absorbance data and not concentration data). However, they were extremely useful to identify potential issues with later deployments. This troubleshooting process eventually resulted in the data presented in Figure 5-5 and Figure 5-6.

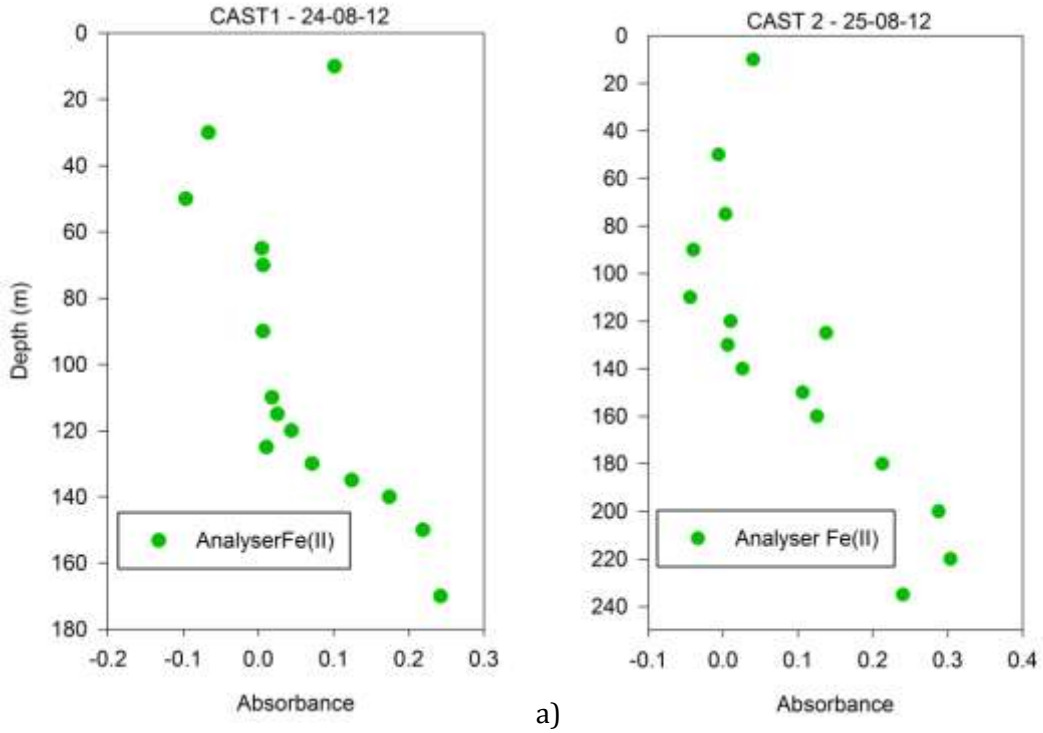

a) b)

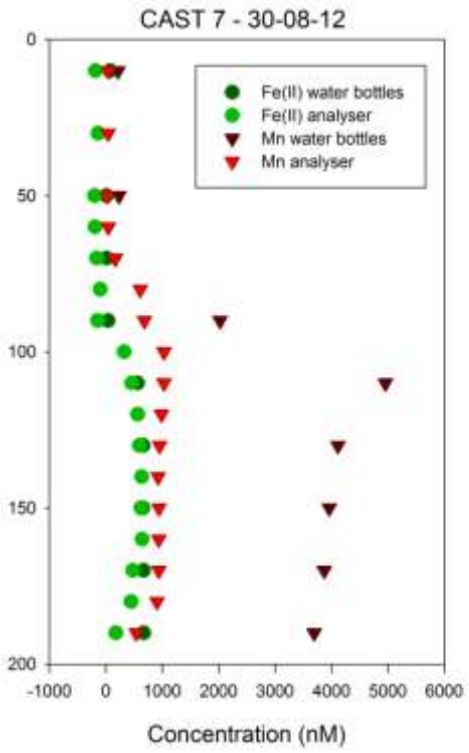

c)

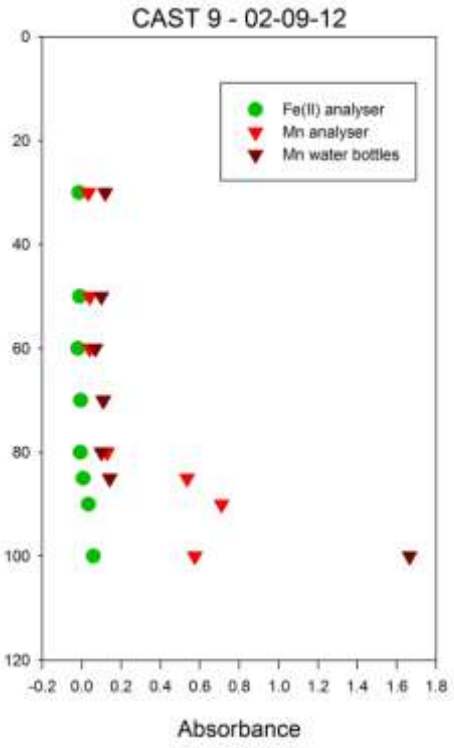

d)

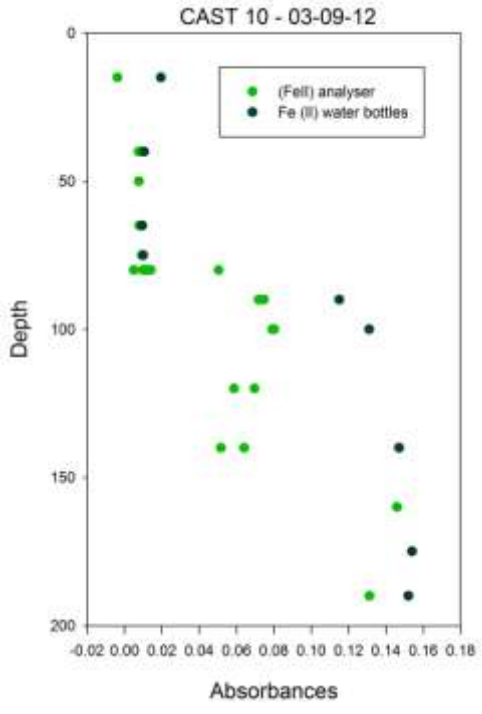

e)

Figure 5-4– CTD casts during EMB Baltic Sea cruise. Results from test-deployments.

Figure 5-5 shows a vertical profile obtained in the Gotland Deep basin for dissolved (<0.45 μm filtered) Fe(II) measured in-situ by the analyser and on-board from subsamples collected from the CTD Niskin bottles. The analyser was set up to measure Mn for the first time during this deployment. The waiting time for the PAN-Mn diffusion was too short (set to 5 minutes in this case) and the colour formation was not completed. Thus the Mn measurements are not shown.

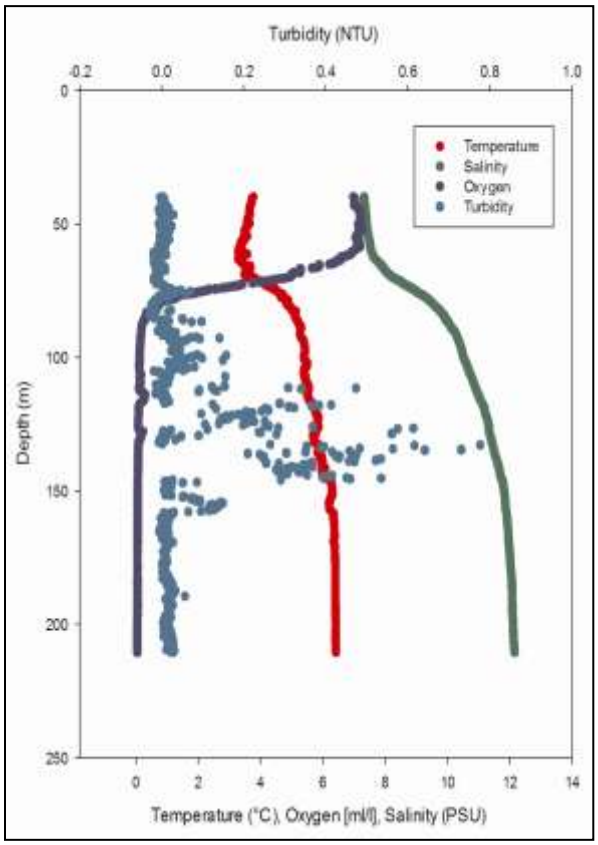

a)

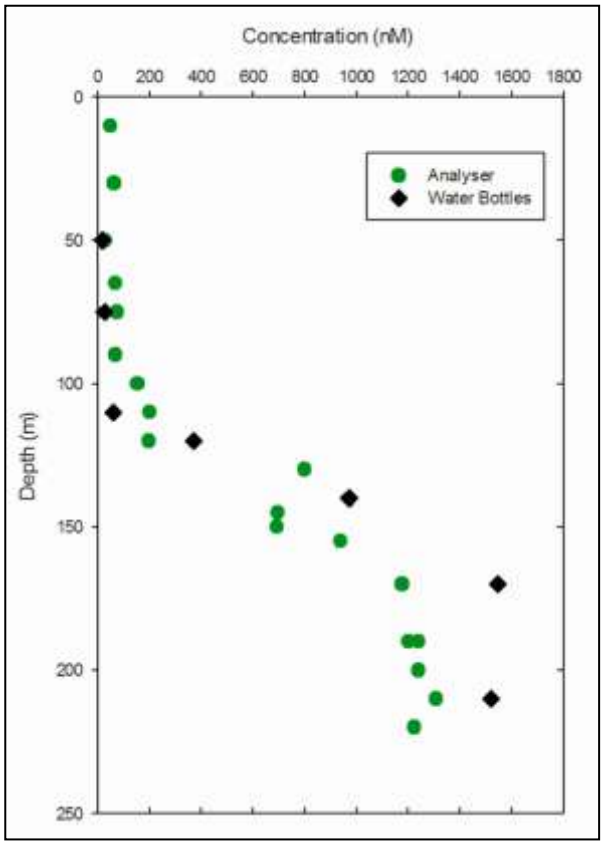

b)

Figure 5-5 - CTD profiles in Gotland Deep Basin. Cast 3, 26-08-2012. a) Temperature, Salinity, Oxygen, Turbidity. b) Fe(II) analyser and bottle water samples.

The concentrations of Fe(II) measured in individual water bottles samples match the data from the in-situ samples. The bottle samples were not filtered during sub-sampling and were directly added to a tube containing Ferrozine reagent in order to limit any oxidation of Fe(II) in solution prior to reaction with the reagent. We believe that the slightly higher values measured in samples taken directly from the water bottles closed below 120 m, compared to the data obtained in-situ, are consistent with the hypothetical release of Fe(II) from particles suspended in the water column (the values for turbidity at depth are slightly higher than those just above the redoxcline); these particles were removed by filtration with the in-situ analyser. This is just a proposed explanation, as the equipment on-board of the ship did not allow us to perform further analysis on the particulate phase in order to confirm our hypothesis. Nonetheless, the overall profile drawn by the analyser confirmed its use as an in-situ detector for Fe(II) in areas of high concentrations such as the Baltic Proper.

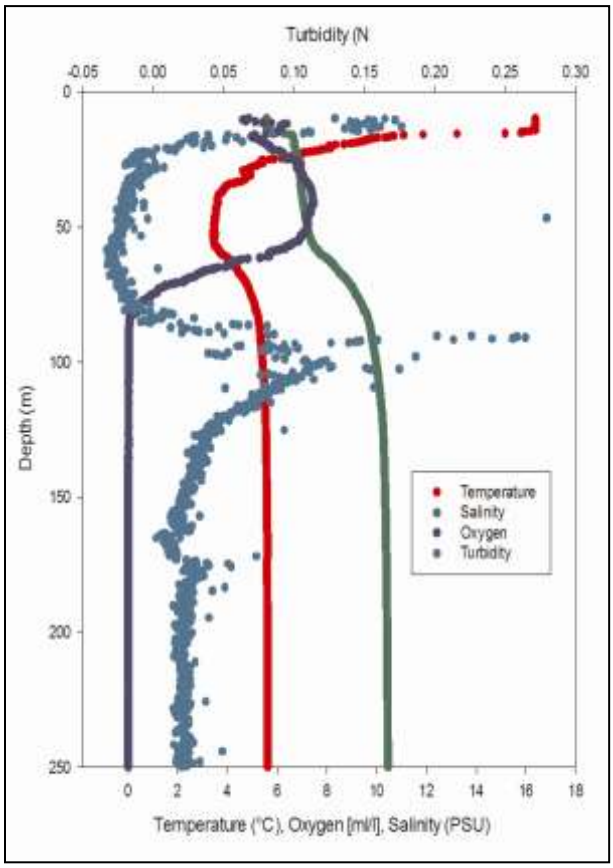

a)

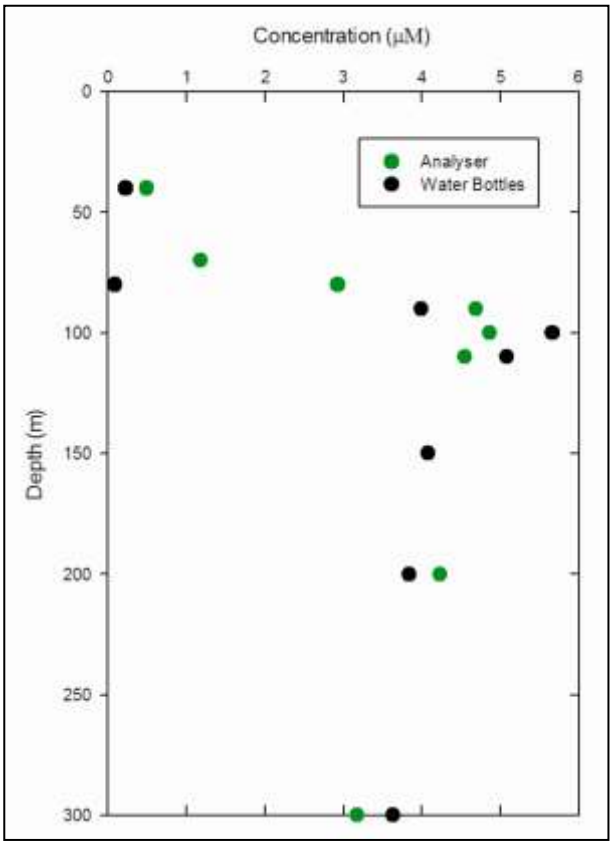

b)

Figure 5-6 - CTD profiles in Landsort Deep Basin. Cast 8, 01-09-2012 a) Temperature, Salinity, Oxygen, Turbidity. b) Mn analyser and bottle water samples.

A Mn profile done in the Landsort Deep is shown in Figure 5-6. For dissolved Mn, where oxidation is much slower than for Fe(II), there was time to filter the samples prior to analysis in the ship laboratory. Thus both manual shipboard and in-situ instrument measurements were done after filtration. The overall shape of the profiles measured in-situ and manually are similar and demonstrate the validity of the analyser as an in-situ Mn detector.

No Fe(II) data are shown in this profile because during the descent of the CTD carousel the inlet tubing became twisted together and the Fe(II) inlet was blocked. The live streaming of the ASM data to the ship allowed us to promptly recognise the problem and change the Fe(II) measurement routine so that the analyser could continue to measure Mn undisturbed.

For both deployments shown, in-situ calibrations (triplicate measurements of a high standard and a blank) were performed at depths corresponding to the two temperature extremes (65 m-3.4°C and 190 m-6.4°C for Fe; 40 m-3.6°C and 200 m-5.6°C for Mn) and used to compare with absorbances of the water samples collected close to those depths. No significant differences were found between the calibrations slopes, confirming that temperature and pressure effects were negligible under the environmental conditions experienced by the analyser during these deployments.

The in-situ analyser operated with a frequency of 5 minutes per sample for Fe(II) and 10 minutes per sample for Mn. The limit of detection (LOD) of the analyser were confirmed to be similar to what was previously measured in the Baltic: 35 nM Fe(II); 29 nM Mn.

Data collected by the in-situ analyser agree well with the general trend of Fe and Mn concentrations found by previous workers in the area (Conley et al. 2009a, Kremling 1983, Meyer et al. 2012, Pohl and Hennings 2005b). Figure 5-7 shows profiles of Fe(II) and Mn obtained in previous studies in the area. For Fe(II) data in the Baltic deep anoxic water, measurements from the present work should be comparable to total dissolved (0.45 μm) Fe data reported in previous studies in the area because in anoxic environments one would expect essentially all dissolved Fe to be in the reduced Fe(II) form (refer to oxygen profile in Figure 5-5 a)).

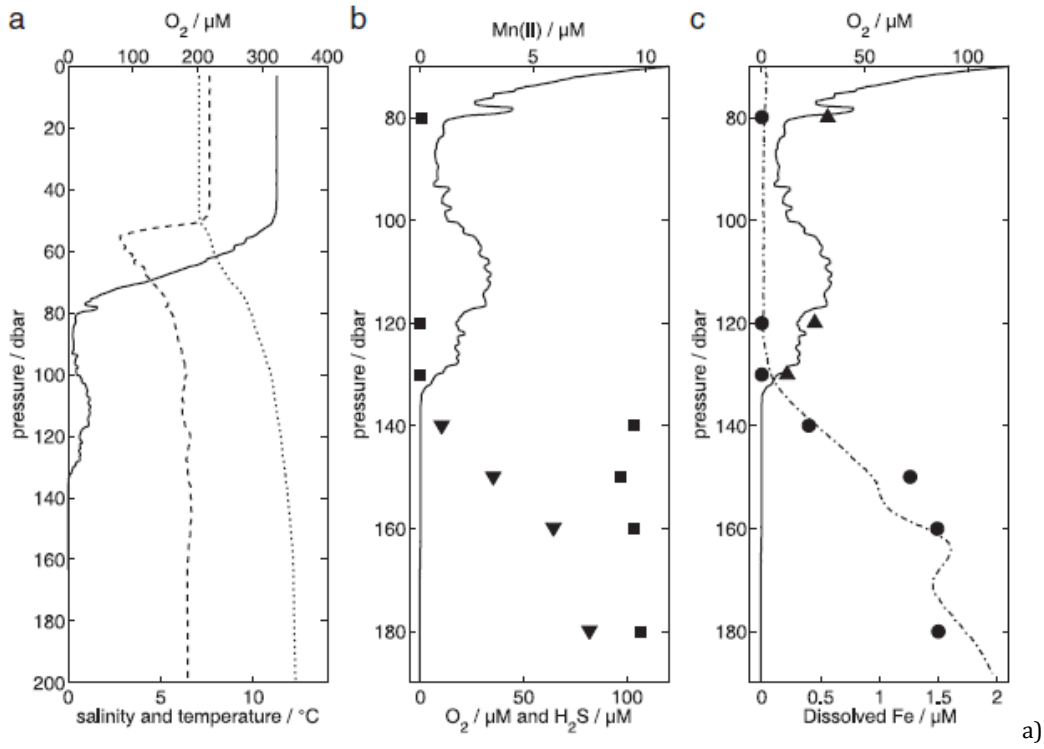

a)

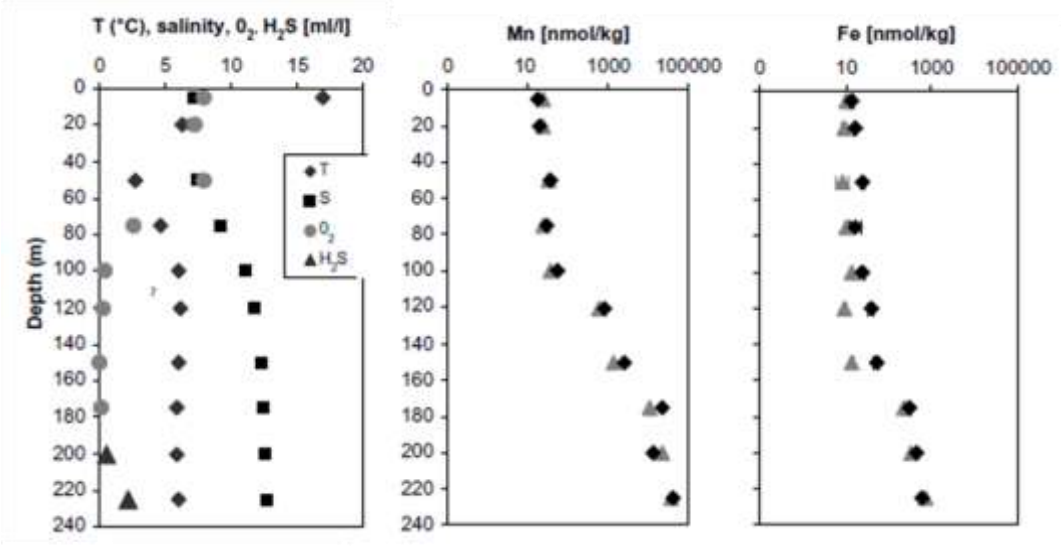

b)

Figure 5-7– Fe and Mn profiles in the Gotland Deep Basin. a) Meyer et al., 2012. b) Strady et al., 2008.

5.1.6 Conclusions of Baltic Sea deployment

The mechanical robustness of the instrument was proven by successful deployments to depths of over 300 m, even in rough weather conditions. Additionally the daily connection and disconnection to the pump-CTD frame for data downloading and standards/reagent re-fitting in the laboratory (which took no more than 10 minutes each day), further demonstrated its ability to provide routine measurements. The flexibility of the ASM allowed the streaming of live data during deployments, but it could be programmed to operate in complete autonomy, as well as being operated through remote connection.

The agreement of the bottle water and analyser data suggested good accuracy for the prototype analyser. This confirmed its potential use for investigating low oxygen areas such as the Baltic Sea.

Studies of redox interfaces are often difficult because in those dynamics system reactions take place on small time and space scales (Pohl and Hennings 2005a). The scope for our efforts is then widely justified: deploying an autonomous in situ fast profiler would improve significantly the amount of data on hand to characterize the biogeochemical behaviour of these environments. Having redox data available would allow better understanding of the low-oxygen/anoxic zones of the water bodies studied allowing for more synoptic interpretation of their evolution.

5.2 River Beaulieu deployment

P2 was used in combination with a recently developed reverse titration approach (Statham et al. 2012) to study changes in Fe(II) speciation in the River Beaulieu (Southampton, UK), a high dissolved organic matter (DOM) river. The study was planned and carried out with Mark Hopwood and Professor Peter J. Statham (NOC, Southampton).

The following work is an extract from the paper: Hopwood, M. J., Statham, P.J., Milani, A., *The behaviour and speciation of Fe(II) in a high DOM river and estuarine system*, submitted to *Estuarine, Coastal and Shelf Science*, under revision at the time of writing.

5.2.1 River Beaulieu

The River Beaulieu drains the New Forest (Hampshire, England) and thus contains water primarily from exposed heathland and some mixed coniferous/deciduous forest. The river water has a near neutral pH (6.5-7.8), high DOC (3-22 mgl^{-1}) and high dissolved (0.40 μm filtered) Fe (1-8 μM) content (Fang 1995, Holliday and Liss 1976, Jones 1993, Moore et al. 1979, Smith 1995).

River water samples were collected from Kings Hat footbridge on the Beaulieu River (50° 50’ 46” N 001° 27’ 17” W) approximately 3 km upstream from the top of the estuary, on the 17th of December 2012.

5.2.2 Objectives of the deployment

The wider aim of the study was to investigate temporal and spatial variations in the fraction of dissolved Fe present as Fe(II) in the river waters, and to assess if the Fe(II)-humic interactions play a significant role in the riverine and estuarine Fe biogeochemistry.

This study provided an opportunity to compare data obtained by manual sampling and via in-situ measurement in a freshwater environment, and thus was a relevant test for the P2 system.

5.2.3 Deployment set up

To investigate short term (hourly to diurnal) trends in riverine Fe chemistry the in-situ sensor was deployed over a full day from 1 hour before sunrise until 1 hour after sunset at King's Hat. Samples of water were also collected by hand every 10 minutes for manual Fe measurement.

The analyser was deployed near the river shore (Figure 5-8), submerged by 30-40 cm of water. The inlets of the two manifolds were positioned as close as possible to each other. 0.20 µm Millex filters were attached to the samples inlets (0.20 µm rather than 0.45 µm filters were chosen because of the expected high particulate matter in the river water).

An external battery was connected to the device and an RS232 cable for power and communication was attached to the bulk-head connector on the top end-cap of the housing. This set up provided constant access to the analyser ASM and allowed P2 to stream live data on a laptop set up on the river shore.

The analyser was set up to detect Fe(II) and total Fe (see paragraph 2.1.2.3). A FZ reagent storage bag was connected to the first manifold (Fe(II)), while a reagent bag filled with FZ and 0.1 M Ascorbic acid in equal amounts was attached to the second manifold (Total Fe).

All manual sampling apparatus was rigorously cleaned in 10 % HCl, rinsed three times with Milli-Q water and stored in airtight plastic bags until required. River water samples were collected by hand with a 2 m long Teflon coated pole. All water sample filtration (0.20 µm) was conducted in-situ and then samples for Fe(II) analysis were shaken immediately into aluminium wrapped vials containing ferrozine (1:10 ratio).

Salinity and temperature were also measured in-situ, as was luminosity. This latter parameter was recorded to demonstrate the influence of natural light on the diurnal reduction pattern of Fe(II) (photochemical reduction), whose concentration is expected to increase in the hours of stronger sunlight (around noon) to then decrease down to a minimum during night time.

Figure 5-8 – P2 device in housing on the River Beaulieu shore, before deployment. Reagents and waste storage bags are shown attached to the external frame of the device.

5.2.4 Results

Total dissolved (<0.20 μm) Fe and Fe(II) concentrations determined manually throughout the day had mean values (and standard deviations) of 20.1 μM (0.40) and 3.96 μM (0.87) respectively. As shown in Figure 5-9, a small decrease on the order of 1 μM over the eight-hour sampling period is evident for TFe. The concentration of Fe(II) decreases more significantly with a decrease of greater than 3 μM over the sampling period. A similar trend is evident in the analyser data, though the concentrations of dissolved Fe reported by the sensor are much lower.

Sensor analysis of Fe(II) and Fe(III) standards in the laboratory produced values for the sensor within ± 5.0% of the values reported via the Liquid Waveguide Capillary Cell (LWCC) high sensitivity technique so the difference between sensor values and manually collected samples is not attributable to a malfunction or contamination. Mixing time is the

crucial difference between the two datasets. In the sensor there was sufficient time for ferrozine to mix with the river water (a stop-flow step of 300 seconds was set) but apparently insufficient time for kinetic equilibrium to be achieved with strongly complexed or small colloidal Fe(II). The manual measurements were allowed to develop overnight. Both Fe(II) and Fe(III) are strongly organically complexed in this organic rich river system, and this strong bonding seems to impact colour development.

This result is similar in direction to that observed for the Fe(II) measurements taken in the Baltic Sea in suboxic waters with high particle concentrations (although the differences between the manually collected and in-situ measured values there was not as great, which is consistent with a much lower expected ligand concentrations in higher salinity waters allowing kinetic equilibrium to be achieved much faster).

The fraction of Fe(II) measured by the sensor can, in this case, be considered kinetically labile Fe(II); the fraction of total Fe(II) that is either free Fe(II), or only weakly complexed by DOM.

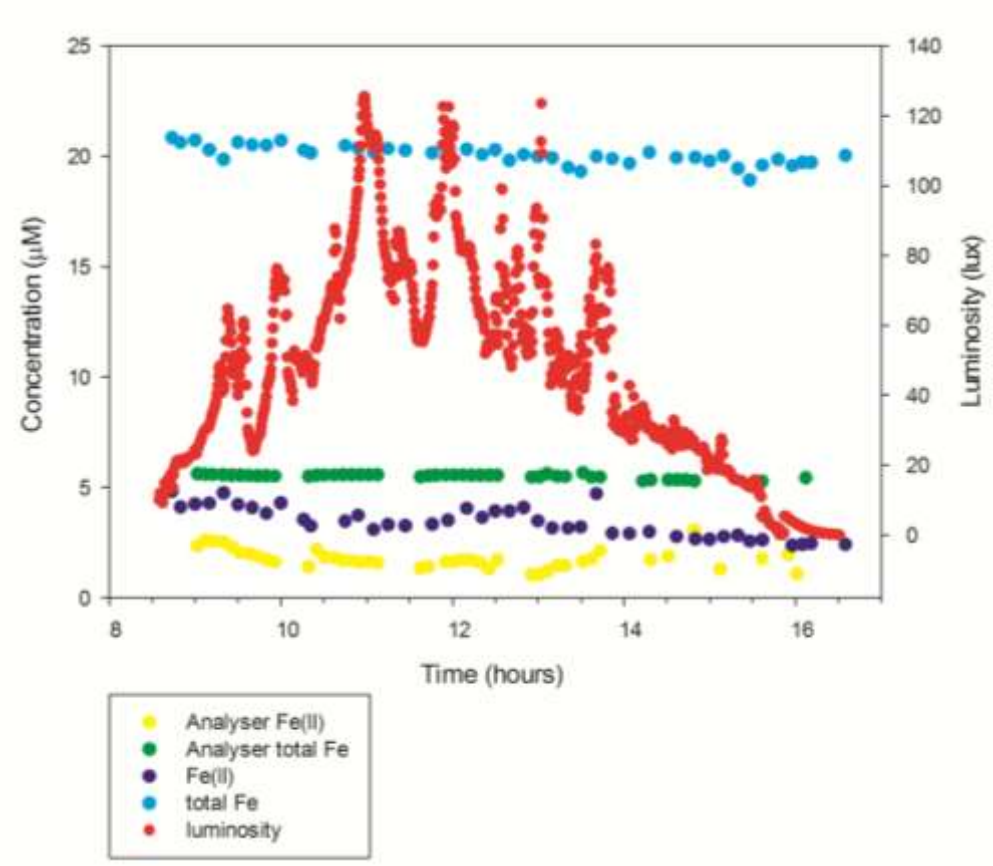

Figure 5-9 – 17-12-12 - King's Hat footbridge, River Beaulieu, Southampton, UK. Luminosity data; Total Fe and Fe(II) data obtained from in-situ measurements and manual sampling. Data recorded from 1 hour prior to sunrise until 1 hour after sunset.

Overall the Beaulieau River work did not confirm the starting hypothesis, as the diurnal cycle of Fe(II) concentration did not follow the light cycle as it was expected. Luminosity peaked around midday but was irregular due to the shaded location. The expected midday maximum in Fe(II) as part of a diurnal cycle is not distinguishable from the dataset. This suggests that either 1) photochemistry is not a dominant net source of Fe(II) in the river, 2) variations in Fe(II) concentration in the different water masses being sampled throughout the day are much greater than the natural daily variation in Fe(II) concentration that would be observed in a standing water mass, or 3) that the half life of Fe(II) in the river is sufficiently long (greater 12 hours) such that there is no observable decay in Fe(II) concentration overnight. Further work will be required to assess which of these hypotheses is the most likely.

5.2.5 Conclusions of Beaulieu River deployment

Prototype 2 was shown to be robust enough for longer deployments than CTD profiles as it provided reliable data for 11 hours without signs of failure, and it was stopped only because of logistic impediments in continuing the deployment. In-situ measurements of total Fe provided a stable trend over time.

However, while the River Beaulieu deployment confirmed the robustness of the mechanical elements and the longevity of the reagents used in P2, the differences in the Fe(II) and total Fe concentrations measured manually and by the analyser, highlighted an issue with the Fe species that the sensor was able to detect.

In the presented prototype (P2) for rapid in situ determination of Fe concentration, strongly complexed Fe(II) (or similarly Fe(III)) may lead to underestimation of total Fe(II) (or Fe(III)) unless mixing times are adequate to allow equilibrium with ferrozine to be reached. This is especially the case where Fe and DOM concentrations are high (eg in fresh water systems) or where the ligands present are particularly strong.

In order to use P2 for more detailed investigations on Fe speciation in natural waters, further tests on the stop-flow step implemented in the ASM routine of the analyser are needed. The comparison with an independent laboratory method such as the LWCC used in this study by M. Hopwood would be a good starting point to characterise the analyser's analytical capabilities.

5.3 Summary

P2 was deployed in natural environments to test its robustness and reliability in natural waters.

In August-September 2012 the device was successfully deployed in the Baltic Sea Proper as part of the Elizabeth Mann-Borgese cruise (06EZ1215). Attached to a CTD-frame, it provided water column profiles of both Fe(II) and Mn over a number of deployments. The validity of the diffusive mixing technique was thus proven under natural ambient conditions. The analyser operated with a frequency of 12 (Fe(II)) and 6 (Mn) samples per hour, with a LOD of 35 nM for Fe(II) and 29 nM Mn..

In December 2012 P2 was set up to measure total Fe and Fe(II) and deployed in the River Beaulieu for a full day as part of a joint laboratory investigation of the behaviour and speciation of Fe(II) in a high DOM river system. The analyser measurements were paired with laboratory measurements of samples manually collected on the same site. The comparison showed much lower values recorded by the analyser than by the manual measurements. This gap was ascribed to a difference in the development time between the in-situ and manual samples and gave insights into the analytical capacities of the device P2. At present, the current set up of the system allows the detection of total Fe(II) that is either free Fe(II), or only weakly complexed by DOM.

The two environmental applications of P2 confirmed its robustness as a prototype of an in-situ microfluidic analyser for Fe and Mn in natural waters. Weak points were identified, which should be the starting point for further optimisation of the technology.

The next chapter summarises what has been achieved during the course of this project and suggests possible ways ahead to improve the performance of P2.

Chapter 6

Conclusions

In this final chapter the main outcomes of the work are summarized, and the progress towards the objectives set in the introduction is reviewed. Suggestions on future general directions and specific improvements to the present version of the analyser are then provided.

6.1 Key outcomes from the research and development process

An automated microfluidic in-situ wet chemical system for the detection of Fe and Mn in natural water has been developed and optimized for sea water and fresh water deployments.

The objectives set at the beginning of the project (paragraph 1.5) were met as follows:

1. Colorimetry was chosen as the determination technique for Fe(II) and Mn and the Ferrozine and PAN method were used respectively. These methods proved to be reliable over 10 weeks for Fe-FZ and over 6 days for Mn-PAN.
2. Prototype chips were manufactured in-house by micro-milling the manifold channels in tinted PMMA, bonding the chip body to a lid via exposure to solvent vapours, and finally by aligning and cementing in place the optical components (LEDs and photodiodes) on the opto-fluidic measuring cell.
3. A first prototype (P1) of the device was manufactured and mechanical and electronic elements were integrated in the system. As it was a flow-through device, it featured a long serpentine channel as the mixer for samples/standards and the Ferrozine reagent.
4. Two identical analysers were deployed on the Lucky Strike hydrothermal vent field as part of the MoMAR-D mission, October 2010 to detect Fe(II). Although the deployment was unsuccessful it highlighted issues which led to a better understanding of how the system worked and how it could be improved for better performance
5. The analysis of the performance of the prototype during deployment, combined with additional issues such as length of flushing time, wear of the pump seals, cross-talk between detectors and light sources, and redundancy of the first optical cell pointed us in the direction of a new version of the microfluidic chip.
6. A second prototype (P2) was designed as a stop-flow measurement system. The major difference between P1 and P2 was the mixing method: P2 applied a simpler in-cell diffusive -mixing method, with no need for a long serpentine mixer. The more compact manifold of P2 left enough free space to add a second manifold, identical to the first one on the same sized chip as P1. The double manifold allowed the simultaneous analysis of up to two analytes.
7. P2 was manufactured and tested. The improvements implemented in the new design led to an increase of the signal output and reduced the contamination potential. It was lab-tested with successful results.
8. Two deployments of P2 tested its robustness and reliability in natural waters. In August-September 2012 the device was successfully deployed in the Baltic Sea Proper, where water column profiles of Fe(II) and Mn were recorded. In December 2012 P2 was set up to measure total Fe and Fe(II) in the River Beaulieu for a full day. Data recorded were compared to data obtained by manual sampling and results showed a consistent negative offset relative to the manual data. The difference was ascribed to the kinetics of reaction in high organic waters.

The final P2 system specifications are summarized in Table 6-1.

Device elements	Specifics
Pump	Custom-designed syringe pump
Valves	Lee Products 300 Series Solenoid Valves
Light source	LEDs, B5b-433-20, Roithner Laser Technik, Austria) output centered on 572 nm, FWHM ~30 nm
Detector	Photodetector, TSL257, TAOS Inc., USA
Electronics package	Custom-designed stand-alone electronics package (data logging; control of valves and pumps; led and photodiodes power; communications)
Sensor-user interface	Programmable Autonomous State Machine (ASM)
Housing	Anodised aluminium cylindrical housing,
Environmental conditions tested	170 bars and 4°C in lab 300 m and 3.4°C in environment
Chemical methods	Colorimetry: Fe-Ferrozine; Mn-PAN
Sampling frequency	Fe: 12 samples/hour Mn: 6 samples/hour
Typical LOD **3 times SD of blank**	Total Fe: 35 nM Fe(II): 27 nM Mn: 28 nM
Accuracy and precision	Mn: Tested against CASS-5 CRM (47.7 ± 3.6 nM): 48.2 ± 12.6 nM; 2.4 %, with n = 19 for a 1µM standard

Table 6-1 – Specifications of the dissolved Fe and Mn system

The overall expected outcome of a device able to operate at depths and at low temperature was demonstrated in the laboratory (successful tests of the device to up to 170 bars and 4°C) and in the environment (successful deployments to up to 300 m and 3.4°C). Although we were not able to plan any long-term deployments, laboratory tests on the reagents suggested that the analyser could be deployed for longer periods of time (see point 1 above). The LOD obtained are in the order of tens of nM, allowing the use of the device in different natural environments with nM to µM concentrations of dissolved Fe

and Mn. The sample frequency is appropriate for deployments on CTD-profilers and on mooring stations. The low power consumption, the compact shape and the low reagent consumption make P2 a reasonably easy-to-use device. At present an estimated cost per analyser if mass produced is on the order of £3000, making it an affordable measuring tool for most academic and industrial institutions.

Further work could be made on different elements of the prototype to improve its performances as a dissolved Fe and Mn analyser.

6.2 Future work

6.2.1 Chemical methods

In order to obtain a device deployable over long periods of time, the lifetime of the reagents must be extended. Although the Ferrozine reagent is already suitable for most type of deployments, the current Mn-PAN method does not allow deployments longer than a week due to the short lifetime of the Fe chelating agent Desferrioxamine B. This is a clear drawback when planning mooring type deployments or long-term observatories deployments. Further studies are thus needed to find a better Fe chelating agent for the Mn-PAN method, or different techniques should be explored.

A possible way to overcome the drawback of the Mn-PAN technique is to add an on-chip resin pre-concentration step, which will also extend the range of concentrations detectable by the analyser. Studies of this technique are already underway with the Toyopearl resin within the Sensors Group, NOC, Southampton (Milne et al. 2010). Mn is a good candidate for resin pre-concentration techniques, because of its simple speciation in natural waters. On the contrary, Fe speciation behavior poses higher challenges in finding pre-concentration treatments for its complexed species. On-chip UV oxidation methods could bypass these difficulties and improve the accuracy of the device by releasing Fe from organic complexes (DOC), allowing the measurement of total dissolved Fe, rather than just the labile fraction of the total Fe pool.

6.2.2 Mechanical elements

Improvements in the mixing technique would be worth investigating. Although there was no time to explore different mixer shapes during the course of this project, a range of passive micromixers could be tested to improve mixing time and reduce the flushings between samples in the device. Some of the passive mixers shapes worth investigating are

herringbone type mixers (Lee et al. 2011) and T-shaped mixers improved with parallel lamination (Capretto et al. 2011).

Mechanical improvements of the device could be directed toward an even simpler and more compact final system, both in terms of size and power consumption. Latching valves could be implemented on the chip to limit the power consumption. The custom made pump could be modified to work in a speed controlled way, while the pumping barrels could be included in the manufacture of the chip itself. Further versions of the analyser will see the miniaturization of these elements through the optimization of micro on-chip valves and pumps.

6.2.3 Software improvements

As a step towards the desirable commercialization of the device, the current user interface will need to be improved and simplified into a more user-friendly piece of software. Improvements in this direction are already underway in the Sensors Group at NOC, Southampton. A Windows user interface will soon allow the user to access the ASM through a GUI (graphic user interface), which will substitute the current script used to program the ASM. This will allow a smoother and faster assessment of the measurement routine and will guarantee easier access to the recorded data.

PUBLICATIONS

Milani A., Statham P. J., Mowlem M., Connelly D. – 2013 - *An in-situ microfluidic system for determination of FeII and Mn in natural waters* – Plos One - in preparation

Hopwood M. J., Milani A., Statham P.J. – 2013 - *The behavior and speciation of FeII in a high DOM* - Estuarine, Coastal and Shelf Science – in revision

Floquet C.F.A., Sieben V.J., Milani A., Joly E.P., Ogilvie I.R.G., Morgan H., Mowlem M.C. – 2011 - *Nanomolar detection with high sensitivity microfluidic absorption cells manufactured in tinted PMMA for chemical analysis* - Talanta 84(1): 235-239

PRESENTATIONS

Milani A., Floquet C.F.A., Sieben V.J., Bey S.K., Waugh E.M., Brown R., Fowler L., Statham P.J., Connelly D., Morgan H., Mowlem M.C. - *Micro-sensing technology for in-situ low level detection of Fe and Mn in seawater* – 2010 - Challenger conference, NOC, Southampton

POSTERS

Milani A., Statham P.J., Connelly D., Mowlem M. – 2013 - *Development and applications of an autonomous analyser for in-situ determination of iron and manganese in natural aquatic systems* – ASLO – New Orleans, USA

Milani A., Connelly D., Mowlem M., Statham P.J. – 2012 - *Micro-sensing technology for in-sity low level detection of iron in seawater* – EGU – Vienna, Austria

FIELDWORK

August 2012. EBM cruise to the Baltic Sea. Collaboration with IOW, Liebniz Institute for the Baltic Sea Research, Warnemunde, Germany.
October 2010. MOMAR-D cruise to Mid Atlantic ridge, Lucky Strike hydrothermal vent site on the oceanographic ship Pourquoi pas?; collaboration with Ifremer, France

References

BACC. 2008. Assessment of climate change in the baltic sea basin: Springer.

Barbante C, Cairns W. 2002. The role and fate of trace elements in the environment. Journal De Physique Iv 12: 125-141.

Beaton AD, Cardwell CL, Thomas RS, Sieben VJ, Legiret F-E, Waugh EM, Statham PJ, Mowlem MC, Morgan H. 2012. Lab-on-chip measurement of nitrate and nitrite for in situ analysis of natural waters. Environmental Science & Technology 46: 9548-9556.

Bergquist BA, Wu J, Boyle EA. 2007. Variability in oceanic dissolved iron is dominated by the colloidal fraction. Geochimica Et Cosmochimica Acta 71: 2960-2974.

Betteridge D, Fernando Q, Freiser H. 1963. Solvent extraction of certain transition metal ions with 1-(2-pyridylazo)-2-naphthol. A study of complex formation and distribution equilibria. Analytical Chemistry 35: 294-298.

Blain S, Treguer P. 1995. Iron(ii) and iron(iii) determination in sea-water at the nanomolar level with selective online preconcentration and spectrophotometric determination. Analytica Chimica Acta 308: 425-432.

Blandin J, Rolin JF. 2005. An array of sensors for the seabed monitoring of geohazards - a versatile solution for the long-term real-time monitoring of distributed seabed parameters. Sea Technology 46: 33-+.

Boyd PW, Ellwood MJ. 2010. The biogeochemical cycle of iron in the ocean. Nature Geoscience 3: 675-682.

Boyd PW, et al. 2007. Mesoscale iron enrichment experiments 1993-2005: Synthesis and future directions. Science 315: 612-617.

Boyd PW, et al. 2000. A mesoscale phytoplankton bloom in the polar southern ocean stimulated by iron fertilization. Nature 407: 695-702.

Brand LE, Sunda WG, Guillard RRL. 1983. Limitation of marine-phytoplankton reproductive rates by zinc, manganese, and iron. Limnology and Oceanography 28: 1182-1198.

Breitbarth E, et al. Iron biogeochemistry across marine systems - progress from the past decade. Biogeosciences 7: 1075-1097.

Brett CMA. 2007. Novel sensor devices and monitoring strategies for green and sustainable chemistry processes. Pure and Applied Chemistry 79: 1969-1980.

Bruland KW, Rue el. 2001. Analytical methods for the determination of concentration and speciation of iron. Pages 255-289 in Turner DR, Hunter KA, eds. The biogeochemistry of iron in seawater, John Wiley & Sons.

Bruland KW, Donat JR, Hutchins DA. 1991. Interactive influences of bioactive trace-metals on biological production in oceanic waters. Limnology and Oceanography 36: 1555-1577.

Buffle J, Horvai G. 2000. General concepts. Pages 1-17 in Buffle J, Horvai G, eds. In situ monitoring of aquatic systems: Chemical analysis and speciation, John Wiley & Sons.

Burton JD, Statham PJ. 1988. Trace-metals as tracers in the ocean. Tracers in the Ocean: 127-145

236.

Capretto L, Cheng W, Hill M, Zhang X. 2011. Micromixing within microfluidic devices. Pages 27-68 in Lin BC, ed. Microfluidics: Technologies and applications, vol. 304.

Chapin TP, Jannasch HW, Johnson KS. 2002. In situ osmotic analyzer for the year-long continuous determination of fe in hydrothermal systems. Analytica Chimica Acta 463: 265-274.

Chin CS, Johnson KS, Coale KH. 1992. Spectrophotometric determination of dissolved manganese in natural-waters with 1-(2-pyridylazo)-2-naphthol - application to analysis in situ in hydrothermal plumes. Marine Chemistry 37: 65-82.

Chin CS, Coale KH, Elrod VA, Johnson KS, Massoth GJ, Baker ET. 1994. In-situ observations of dissolved iron and manganese in hydrothermal vent plumes, juan-de-fuca ridge. Journal of Geophysical Research-Solid Earth 99: 4969-4984.

Chiswell B, Ohalloran KR. 1991. Comparison of 3 colorimetric methods for the determination of manganese in fresh-waters. Talanta 38: 641-647.

Coale KH. 2001. Iron fertilization in Steele J, Thorpe S, Turekian K, eds. Encyclopedia of ocean science.

Coale KH, Chin CS, Massoth GJ, Johnson KS, Baker ET. 1991. Insitu chemical mapping of dissolved iron and manganese in hydrothermal plumes. Nature 352: 325-328.

Colaco A, et al. 2011. Momar-d: A technological challenge to monitor the dynamics of the lucky strike vent ecosystem. Ices Journal of Marine Science 68: 416-424.

Conley DJ, et al. 2009a. Hypoxia-related processes in the baltic sea. Environmental Science & Technology 43: 3412-3420.

Conley DJ, et al. 2009b. Hypoxia-related processes in the baltic sea. Environmental Science & Technology 43: 3412-3420.

Crevillen AG, Hervas M, Lopez MA, Gonzalez MC, Escarpa A. 2007. Real sample analysis on microfluidic devices. Talanta 74: 342-357.

Daly KL, Byrne RH, Dickson AG, Gallager SM, Perry MJ, Tivey MK. 2004. Chemical and biological sensors for time-series research: Current status and new directions. Marine Technology Society Journal 38: 121-143.

de Baar H, de Jong J. 2001. Distribution, sources and sinks of iron in seawater. Pages 125-255 in Turner DR, Hunter KA, eds. The biogeochemistry of iron in seawater, John Wiley & Sons.

Dellwig O, Leipe T, Marz C, Glockzin M, Pollehne F, Schnetger B, Yakushev EV, Bottcher ME, Brumsack HJ. 2010. A new particulate mn-fe-p-shuttle at the redoxcline of anoxic basins. Geochimica Et Cosmochimica Acta 74: 7100-7115.

Elrod VA, Johnson KS, Coale KH. 1991. Determination of subnanomolar levels of iron(ii) and total dissolved iron in seawater by flow-injection analysis with chemiluminescence detection. Analytical Chemistry 63: 893-898.

Fang. 1995. University of Southampton, Southampton.

Feistel R, G. N, Wasmund N. 2008. Tate and evolution of the baltic sea, 1952-2005: A detailed 50-year survey of meteorology and climate, physics, chemistry, biology, and marine environment. Hoboken, NJ, USA: Wiley Interscience.

Floquet CFA, Sieben VJ, Milani A, Joly EP, Ogilvie IRG, Morgan H, Mowlem MC. 2011. Nanomolar detection with high sensitivity microfluidic absorption cells manufactured in tinted pmma for chemical analysis. Talanta 84: 235-239.

Friedrich J, et al. 2013. Investigating hypoxia in aquatic environments: Diverse approaches to addressing a complex phenomenon. Biogeosciences Discuss. 10: 12655-12772.

Gallager SM, Whelan J. 2004. The next generation of in situ biological and chemical sensors in the ocean: A workshop report. WHOI. Report no.

Gammons CH, Nimick DA, Parker SR, Snyder DM, McCleskey RB, Amils R, Poulson SR. 2008. Photoreduction fuels biogeochemical cycling of iron in spain's acid rivers. Chemical Geology 252.

Gibbs CR. 1976. Characterization and application of ferrozine iron reagent as a ferrous iron indicator. Analytical Chemistry 48: 1197-1201.

Gledhill M, Vandenberg CMG. 1994. Measurement of the redox speciation of iron in seawater by catalytic cathodic stripping voltammetry. Marine Chemistry 50: 51-61.

Goto K, Taguchi S, Fukue Y, Ohta K, Watanabe H. 1977. Spectrophotometric determination of manganese with 1-(2-pyridylazo)-2-naphthol and a nonionic surfactant. Talanta 24: 752-753.

HELCOM. 2009. Eutrophication in the baltic sea – an integrated thematic assessment of the effects of nutrient enrichment and eutrophication in the baltic sea region in HELCOM, ed. Eutrophication in the Baltic Sea – An integrated thematic assessment of the effects of nutrient enrichment and eutrophication in the Baltic Sea region.

Henderson GM, et al. 2007. Geotraces - an international study of the global marine biogeochemical cycles of trace elements and their isotopes. Chemie Der Erde-Geochemistry 67: 85-131.

Holliday LM, Liss PS. 1976. Behavior of dissolved iron, manganese and zinc in beaulieu estuary, s england. Estuarine and Coastal Marine Science 4.

Huang YM, Yuan DX, Ma J, Zhang M, Chen GH. 2009. Rapid speciation of trace iron in rainwater by reverse flow injection analysis coupled to a long path length liquid waveguide capillary cell and spectrophotometric detection. Microchimica Acta 166: 221-228.

Huikko K, Kostiainen R, Kotiaho T. 2003. Introduction to micro-analytical systems: Bioanalytical and pharmaceutical applications. European Journal of Pharmaceutical Sciences 20: 149-171.

Hunter KA, Boyd PW. 2007. Iron-binding ligands and their role in the ocean biogeochemistry of iron. Environmental Chemistry 4: 221-232.

Janasek D, Franzke J, Manz A. 2006. Scaling and the design of miniaturized chemical-analysis systems. Nature 442: 374-380.

Jannasch HW, Johnson KS, Sakamoto CM. 1994. Submersible, osmotically pumped analyzers for continuous determination of nitrate in-situ. Analytical Chemistry 66: 3352-3361.

Johnson KS, Beehler CL, Sakamotoarnold CM. 1986a. A submersible flow-analysis system. Analytica Chimica Acta 179: 245-257.

Johnson KS, Gordon RM, Coale KH. 1997. What controls dissolved iron concentrations in the world ocean? Marine Chemistry 57: 137-161.

Johnson KS, Beehler CL, Sakamotoarnold CM, Childress JJ. 1986b. Insitu measurements of chemical-distributions in a deep-sea hydrothermal vent field. Science 231: 1139-1141.

Johnson KS, Needoba JA, Riser SC, Showers WJ. 2007. Chemical sensor networks for the aquatic environment. Chemical Reviews 107: 623-640.

Jones SLID. 1993. Studies of organic carbon in estuarine and coastal waters involving size fractionation and carbon isotope techniquesUniversity of Southampton, Southampton.

Klinkhammer G, Bender M, Weiss RF. 1977. Hydrothermal manganese in galapagos rift. Nature 269: 319-320.

Klinkhammer GP. 1994. Fiber optic spectrometers for in-situ measurements in the oceans - the zaps probe. Marine Chemistry 47: 13-20.

Konovalov S, Samodurov A, Oguz T, Ivanov L. 2004. Parameterization of iron and manganese cycling in the black sea suboxic and anoxic environment. Deep-Sea Research Part I-Oceanographic Research Papers 51: 2027-2045.

Krachler R, Jirsa F, Ayromlou S. 2005. Factors influencing the dissolved iron input by river water to the open ocean. Biogeosciences 2: 311-315.

Kremling K. 1983. The behavior of zn, cd, cu, ni, co, fe, and mn in anoxic baltic waters. Marine Chemistry 13: 87-108.

Kuma K, Nishioka J, Matsunaga K. 1996. Controls on iron(iii) hydroxide solubility in seawater: The influence of ph and natural organic chelators. Limnology and Oceanography 41: 396-407.

Laes A, Vuillemin R, Leilde B, Sarthou G, Bournot-Marec C, Blain S. 2005. Impact of environmental factors on in situ determination of iron in seawater by flow injection analysis. Marine Chemistry 97: 347-356.

Laglera LM, van den Berg CMG. 2009. Evidence for geochemical control of iron by humic substances in seawater. Limnology and Oceanography 54: 610-619.

Laglera LM, Battaglia G, van den Berg CMG. 2011. Effect of humic substances on the iron speciation in natural waters by cle/csv. Marine Chemistry 127: 134-143.

Landing WM, Bruland KW. 1987. The contrasting biogeochemistry of iron and manganese in the pacific-ocean. Geochimica Et Cosmochimica Acta 51: 29-43.

Le Bris N, Sarradin PM, Birot D, Alayse-Danet AM. 2000. A new chemical analyzer for in situ measurement of nitrate and total sulfide over hydrothermal vent biological communities. Marine Chemistry 72: 1-15.

Lee C-Y, Chang C-L, Wang Y-N, Fu L-M. 2011. Microfluidic mixing: A review. International Journal of Molecular Sciences 12: 3263-3287.

Legiret F-E, Sieben VJ, Woodward EMS, Abi Kaed Bey SK, Mowlem MC, Connelly DP, Achterberg EP. 2013. A high performance microfluidic analyser for phosphate measurements in marine waters using the vanadomolybdate method. Talanta 116: 382-387.

Leipe T, Dippner JW, Hille S, Voss M, Christiansen C, Bartholdy J. 2008. Environmental changes in the central baltic sea during the past 1000 years: Inferences from sedimentary records, hydrography and climate. Oceanologia 50: 23-41.

Liu XW, Millero FJ. 2002. The solubility of iron in seawater. Marine Chemistry 77: 43-54.

Mallini LJ, Shiller AM. 1993. Determination of dissolved manganese in seawater by flow-injection analysis with colorimetric detection. Limnology and Oceanography 38: 1290-1295.

Manz A, Graber N, Widmer HM. 1990. Miniaturized total chemical-analysis systems - a novel concept for chemical sensing. Sensors and Actuators B-Chemical 1: 244-248.

Marle L, Greenway GM. 2005. Microfluidic devices for environmental monitoring. Trac-Trends in Analytical Chemistry 24: 795-802.

Martin, Windom HL. 1991. Present and future roles of ocean margins in regulating marine biogeochemical cycles of trace-elements. Chichester: John Wiley & Sons Ltd.

Martin JH. 1990. Glacial-interglacial co/sub 2/ change: The iron hypothesis. Paleoceanography 5: 1-13.

Martin JH, Gordon RM, Fitzwater S, Broenkow WW. 1989. Vertex - phytoplankton iron studies in the gulf of alaska. Deep-Sea Research Part a-Oceanographic Research Papers 36: 649-&.

Martin JH, et al. 1994. Testing the iron hypothesis in ecosystems of the equatorial pacific-ocean. Nature 371: 123-129.

Massoth GJ, Milburn HB, Johnson KS, Coale KH, Stapp MF, Meinig C, Bake ET. 1991. A suave (submersible system used to assess vented emissions) approach to plume sensing: The buoyant plume experiment at cleft segment, juan de fuca ridge, and plume exploration along the epr 9-11°n. Eos 72: 234.

Massoth GJ, Baker ET, Feely RA, Butterfield DA, Embley RE, Lupton JE, Thomson RE, Cannon GA. 1995. Observations of manganese and iron at the coaxial sea-floor eruption site, juan-de-fuca ridge. Geophysical Research Letters 22: 151-154.

Massoth GJ, Baker ET, Feely RA, Lupton JE, Collier RW, Gendron JF, Roe KK, Maenner SM, Resing JA. 1998. Manganese and iron in hydrothermal plumes resulting from the 1996 gorda ridge event. Deep-Sea Research Part Ii-Topical Studies in Oceanography 45: 2683-2712.

Measures CI, Yuan J, Resing JA. 1995. Determination of iron in seawater by flow injection-analysis using in-line preconcentration and spectrophotometric detection. Marine Chemistry 50: 3-12.

Meyer D, Prien RD, Dellwig O, Connelly DP, Schulz-Bull DE. 2012. In situ determination of iron(ii) in the anoxic zone of the central baltic sea using ferene as spectrophotometric reagent. Marine Chemistry 130: 21-27.

Miller WL, King DW, Lin J, Kester DR. 1995. Photochemical redox cycling of iron in coastal seawater. Marine Chemistry 50: 63-77.

Millero FJ. 1998. Solubility of fe(iii) in seawater. Earth and Planetary Science Letters 154: 323-329.

Milne A, Landing W, Bizimis M, Morton P. 2010. Determination of mn, fe, co, ni, cu, zn, cd and pb in seawater using high resolution magnetic sector inductively coupled mass spectrometry (hr-icp-ms). Analytica Chimica Acta 665: 200-207.

Moore RM, Burton JD, Williams PJL, Young ML. 1979. Behavior of dissolved organic material, iron and manganese in estuarine mixing. Geochimica Et Cosmochimica Acta 43.

Moore TS, Mullaugh KM, Holyoke RR, Madison ANS, Yucel M, Luther GW. 2009. Marine chemical technology and sensors for marine waters: Potentials and limits. Annual Review of Marine Science 1: 91-115.

Morel FMM, Price NM. 2003. The biogeochemical cycles of trace metals in the oceans. Science 300: 944-947.

Mowlem M, Hartman S, Harrison S, Larkin KE. 2008. Intercomparison of biogeochemical sensors at ocean observatories. Southampton: NOCS. Report no. 44.

Ogilvie IRG. 2012. Novel fabrication techniques for microfluidic based in-situ oceanographic nutrient sensorsUniversity of Southampton, Southampton.

Ogilvie IRG, Sieben VJ, Floquet CFA, Zmijan R, Mowlem MC, Morgan H. 2010. Reduction of surface roughness for optical quality microfluidic devices in pmma and coc. Journal of Micromechanics and Microengineering 20.

Ohno K, Tachikawa K, Manz A. 2008. Microfluidics: Applications for analytical purposes in chemistry and biochemistry. Electrophoresis 29: 4443-4453.

Okamura K, Gamo T, Obata H, Nakayama E, Karatani H, Nozaki Y. 1998. Selective and sensitive determination of trace manganese in sea water by flow through technique using luminol hydrogen peroxide chemiluminescence detection. Analytica Chimica Acta 377: 125-131.

Okamura K, Hatanaka H, Kimoto H, Suzuki M, Sohrin Y, Nakayama E, Gamo T, Ishibashi J. 2004. Development of an in situ manganese analyzer using micro-diaphragm pumps and its application to time-series observations in a hydrothermal field at the suiyo seamount. Geochemical Journal 38: 635-642.

Okamura K, Kimoto H, Saeki K, Ishibashi J, Obata H, Maruo M, Gamo T, Nakayama E, Nozaki Y. 2001. Development of a deep-sea in situ mn analyzer and its application for hydrothermal plume observation. Marine Chemistry 76: 17-26.

Ong SE, Zhang S, Du HJ, Fu YQ. 2008. Fundamental principles and applications of microfluidic systems. Frontiers in Bioscience 13: 2757-2773.

Osullivan DW, Hanson AK, Kester DR. 1995. Stopped-flow luminol chemiluminescence determination of fe(ii) and reducible iron in seawater at subnanomolar levels. Marine Chemistry 49: 65-77.

Pascoa R, Toth IV, Rangel A. 2009. Sequential injection trace determination of iron in natural waters using a long-pathlength liquid core waveguide and different spectrophotometric chemistries. Limnology and Oceanography-Methods 7: 795-802.

PascualReguera MI, OrtegaCarmona I, MolinaDiaz A. 1997. Spectrophotometric determination of iron with ferrozine by flow-injection analysis. Talanta 44: 1793-1801.

Pehkonen S. 1995. Determination of the oxidation-states of iron in natural-waters - a review. Analyst 120: 2655-2663.

Pitkanen H, Lehtoranta J, Raike A. 2001. Internal nutrient fluxes counteract decreases in external load: The case of the estuarial eastern gulf of finland, baltic sea. Ambio 30: 195-201.

Pohl C, Hennings U. 2005a. The coupling of long-term trace metal trends to internal trace metal fluxes at the oxic–anoxic interface in the gotland basin (57819,20vn; 20803,00ve) baltic sea. Journal of Marine Systems 56.

Pohl C, Hennings U. 2005b. The coupling of long-term trace metal trends to internal trace metal fluxes at the oxic-anoxic interface in the gotland basin (57 degrees 19,20 ' n; 20 degrees 03,00 ' e) baltic sea. Journal of Marine Systems 56: 207-225.

Prien RD. 2007. The future of chemical in situ sensors. Marine Chemistry 107: 422-432.

Provin C, Fukuba T, Okamura K, Fujii T. 2013. An integrated microfluidic system for manganese anomaly detection based on chemiluminescence: Description and practical use to discover hydrothermal plumes near the okinawa trough. Ieee Journal of Oceanic Engineering 38: 178-185.

Pullin MJ, Cabaniss SE. 2001. Colorimetric flow-injection analysis of dissolved iron in high doc waters. Water Research 35: 363-372.

Resing JA, Mottl MJ. 1992. Determination of manganese in seawater using flow-injection analysis with online preconcentration and spectrophotometric detection. Analytical Chemistry 64: 2682-2687.

Rios A, Escarpa A, Gonzalez MC, Crevillen AG. 2006. Challenges of analytical microsysterns. Trac-Trends in Analytical Chemistry 25: 467-479.

Roitz JS, Flegal AR, Bruland KW. 2002. The biogeochemical cycling of manganese in san francisco bay: Temporal and spatial variations in surface water concentrations. Estuarine Coastal and Shelf Science 54: 227-239.

Rue EL, Bruland KW. 1995. Complexation of iron(iii) by natural organic-ligands in the central north pacific as determined by a new competitive ligand equilibration adsorptive cathodic stripping voltammetric method. Marine Chemistry 50: 117-138.

Sarradin PM, Le Bris N, Le Gall C, Rodier P. 2005. Fe analysis by the ferrozine method: Adaptation to fia towards in situ analysis in hydrothermal environment. Talanta 66: 1131-1138.

Sayle RA, Milnerwhite EJ. 1995. Rasmol - biomolecular graphics for all. Trends in Biochemical Sciences 20: 374-376.

Schnetger B, Dellwig O. 2012. Dissolved reactive manganese at pelagic redoxclines (part i): A method for determination based on field experiments. Journal of Marine Systems 90: 23-30.

Shaked Y, Lis H. 2012. Disassembling iron availability to phytoplankton. Frontiers in Microbiology 3: 26.

Sieben VJ, Floquet CFA, Ogilvie IRG, Mowlem MC, Morgan H. 2010. Microfluidic colourimetric chemical analysis system: Application to nitrite detection. Analytical Methods 2: 484-491.

Smith J. 1995. Study of the composition of the river beaulieu with particular reference to the processes affecting trace element concentrationsUniversity of Southampton, Southampton.

Statham PJ, Jacobson Y, van den Berg CMG. 2012. The measurement of organically complexed fe-ii in natural waters using competitive ligand reverse titration. Analytica Chimica Acta 743.

Statham PJ, et al. 2003. Mapping the 3d spatial distribution of dissolved manganese in coastal waters using an in situ analyser and the autonomous underwater vehicle autosub. Underwater Technology 25: 129-134.

Statham PJ, et al. 2005. Spatially complex distribution of dissolved manganese in a fjord as revealed by high-resolution in situ sensing using the autonomous underwater vehicle autosub. Environmental Science & Technology 39: 9440-9445.

Stookey LL. 1970. Ferrozine - a new spectrophotometric reagent for iron. Analytical Chemistry 42: 779-&.

Strady E, Pohl C, Yakushev EV, Kruger S, Hennings U. 2008. Pump-ctd-system for trace metal sampling with a high vertical resolution. A test in the gotland basin, baltic sea. Chemosphere 70: 1309-1319.

Street JH, Paytan A. 2005. Iron, phytoplankton growth and the carbon cycle. Biogeochemical Cycles of Elements 43: 153-193.

Stumm W, Morgan J. 1995. Aquatic chemistry - chemical equilibria and rates in natural waters Wiley-Blackwell.

Sunda WG. 2001. Bioavailability and and bioaccumulation of iron in the sea. Pages 41-84 in Turner DR, Hunter KA, eds. The biogeochemistry of iron in seawater, John Wiley & Sons.

Tabeling P. 2010. Introduction to microfluidics. Pages 312. Oxford: OUP Oxford.

Tokar JM, Dickey TD. 2000. Chemical sensors technology: Current and future applications. Pages 303-329 in Varney MS, ed. Chemical sensors in oceanography, Gordon and Breach Science Publishers.

Toner BM, Fakra SC, Manganini SJ, Santelli CM, Marcus MA, Moffett J, Rouxel O, German CR, Edwards KJ. 2009. Preservation of iron(ii) by carbon-rich matrices in a hydrothermal plume. Nature Geoscience 2: 197-201.

Ussher SJ, Yaqoob M, Achterberg EP, Nabi A, Worsfold PJ. 2005. Effect of model ligands on iron redox speciation in natural waters using flow injection with luminol chemiluminescence detection. Analytical Chemistry 77: 1971-1978.

Ussher SJ, Milne A, Landing WM, Attiq-ur-Rehman K, Seguret MJM, Holland T, Achterberg EP, Nabi A, Worsfold PJ. 2009. Investigation of iron(iii) reduction and trace metal interferences in the determination of dissolved iron in seawater using flow

injection with luminol chemiluminescence detection. Analytica Chimica Acta 652: 259-265.

van den Berg A, Lammerink TSJ. 1998. Micro total analysis systems: Microfluidic aspects, integration concept and applications. Microsystem Technology in Chemistry and Life Science 194: 21-49.

Van den Berg CMG. 1995. Evidence for organic complexation of iron in seawater. Marine Chemistry 50: 139-157.

Viktorsson L, Ekeroth N, Nilsson M, Kononets M, Hall POJ. 2013. Phosphorus recycling in sediments of the central baltic sea. Biogeosciences 10: 3901-3916.

Viollier E, Inglett PW, Hunter K, Roychoudhury AN, Van Cappellen P. 2000. The ferrozine method revisited: Fe(ii)/fe(iii) determination in natural waters. Applied Geochemistry 15: 785-790.

Von Damm KL. 2000. Chemistry of hydrothermal vent fluids from 9 degrees-10 degrees n, east pacific rise: "Time zero," the immediate posteruptive period. Journal of Geophysical Research-Solid Earth 105: 11203-11222.

Vondamm KL. 1990. Seafloor hydrothermal activity - black smoker chemistry and chimneys. Annual Review of Earth and Planetary Sciences 18: 173-204.

Vuillemin R, Le Roux D, Dorval P, Bucas K, Sudreau JP, Hamon M, Le Gall C, Sarradin PM. 2009. Chemini: A new in situ chemical miniaturized analyzer. Deep-Sea Research Part I-Oceanographic Research Papers 56: 1391-1399.

Watson AJ. 2001. Iron limitation in the oceans. Pages 9-39 in Turner DR, Hunter KA, eds. The biogeochemistry of iron in seawater, John Wiley & Sons.

Watson AJ, Bakker DCE, Ridgwell AJ, Boyd PW, Law CS. 2000. Effect of iron supply on southern ocean co2 uptake and implications for glacial atmospheric co2. Nature 407: 730-733.

Willey JD, Whitehead RF, Kieber RJ, Hardison DR. 2005. Oxidation of fe(ii) in rainwater. Environmental Science & Technology 39: 2579-2585.

Xu X, Zhang S, Chen H, Kong J. 2009. Integration of electrochemistry in micro-total analysis systems for biochemical assays: Recent developments. Talanta 80: 8-18.

Yakushev EV, Pollehne F, Jost G, Kuznetso I, Schneider B, Urnlauf L. 2007. Analysis of the water column oxic/anoxic interface in the black and baltic seas with a numerical model. Marine Chemistry 107: 388-410.

Zhang JZ, Kelbe C, Millero FJ. 2001. Gas-segmented continuous flow analysis of iron in water with a long liquid waveguide capillary flow cell. Analytica Chimica Acta 438: 49-57.